A&A 532, A23 (2011)
DOI: 10.1051/0004-6361/201015399

Astronomy & Astrophysics

TIMASSS: the IRAS 16293-2422 millimeter and submillimeter spectral survey⋆,⋆⋆,⋆⋆⋆

I. Observations, calibration, and analysis of the line kinematics

E. Caux[1,2], C. Kahane[3], A. Castets[4,5,3], A. Coutens[1,2], C. Ceccarelli[3], A. Bacmann[4,5,3], S. Bisschop[6,7], S. Bottinelli[1,2], C. Comito[8], F. P. Helmich[9], B. Lefloch[3], B. Parise[8], P. Schilke[8,10], A. G. G. M. Tielens[6,9,11], E. van Dishoeck[6,12], C. Vastel[1,2], V. Wakelam[4,5], and A. Walters[1,2]

[1] Université de Toulouse, UPS-OMP, IRAP, Toulouse, France
e-mail: caux@cesr.fr
[2] CNRS, IRAP, 9 Av. colonel Roche, BP 44346, 31028 Toulouse Cedex 4, France
[3] Laboratoire d'Astrophysique de Grenoble, UMR 5571-CNRS, Université Joseph Fourier, Grenoble, France
[4] Université de Bordeaux, Laboratoire d'Astrophysique de Bordeaux, 33000 Bordeaux, France
[5] CNRS/INSU, UMR 5804, BP 89, 33271 Floirac Cedex, France
[6] Leiden Observatory, Leiden University, PO Box 9513, 2300 RA Leiden, The Netherlands
[7] Center for Star and Planet Formation, University of Copenhagen, Oster Voldgade 5-7, 1350 Copenhagen, Denmark
[8] Max-Planck-Institut für Radioastronomie, Auf dem Hürgel 69, 53121 Bonn, Germany
[9] SRON Netherlands Institute for Space Research, PO Box 800, 9700 AV, Groningen, The Netherlands
[10] I. Physikalisches Institut, Universität zu Kföln, Zülpicher Str. 77, 50937 Köln, Germany
[11] Kapteyn Astronomical Institute, University of Groningen, PO box 800, 9700 AV Groningen, The Netherlands
[12] Max-Planck Institute für Extraterrestrische Physik, Giessenbachstr. 1, 85748 Garching, Germany

Received 15 July 2010 / Accepted 22 March 2011

ABSTRACT

Context. Unbiased spectral surveys are powerful tools to study the chemistry and the physics of star forming regions, because they can provide a complete census of the molecular content and the observed lines probe the physical structure of the source.
Aims. While unbiased surveys at the millimeter and sub-millimeter wavelengths observable from ground-based telescopes have previously been performed towards several high mass protostars, very little exists on low mass protostars, which are believed to resemble our own Sun's progenitor. To help fill up this gap in our understanding, we carried out a complete spectral survey of the bands at 3, 2, 1, and 0.9 mm towards the solar type protostar IRAS 16293-2422.
Methods. The observations covered a range of about 200 GHz and were obtained with the IRAM-30 m and JCMT-15 m telescopes during about 300 h of observations. Particular attention was devoted to the inter-calibration of the acquired spectra with previous observations. All the lines detected with more than 3σ confidence-interval certainty and free from obvious blending effects were fitted with Gaussians to estimate their basic kinematic properties.
Results. More than 4000 lines were detected (with $\sigma \geq 3$) and identified, yielding a line density of approximatively 20 lines per GHz, comparable to previous surveys in massive hot cores. The vast majority (about two-thirds) of the lines are weak and produced by complex organic molecules. The analysis of the profiles of more than 1000 lines belonging to 70 species firmly establishes the presence of two distinct velocity components associated with the two objects, A and B, forming the IRAS 16293-2422 binary system. In the source A, the line widths of several species increase with the upper level energy of the transition, a behavior compatible with gas infalling towards a ~1 $M_\odot$ object. The source B, which does not show this effect, might have a much lower central mass of ~0.1 $M_\odot$. The difference in the rest velocities of both objects is consistent with the hypothesis that the source B rotates around the source A.
Conclusions. This spectral survey, although obtained with single-dish telescopes at a low spatial resolution, allows us to separate the emission from two different components, thanks to the large number of lines detected. The data of the survey are public and can be retrieved on the TIMASSS web site⋆⋆⋆⋆.

Key words. stars: protostars – molecular data – line: identification – astrochemistry

1. Introduction

The chemical composition of the gas from which the star forms is well known to influence the process of the star formation and be, in turn, influenced by the process itself. The first obvious example is that the Jeans mass depends on the gas temperature, which, in turn, is set by the molecular line cooling accross a large

⋆ Based on observations with the IRAM-30 m telescope (IRAM is supported by INSU/CNRS (France), MPG (Germany) and IGN (Spain)), and with the JCMT-15 m telescope (operated by the Joint Astronomy Centre on behalf of the Particle Physics and Astronomy Research Council of the United Kingdom, the Netherlands Organisation of Scientific Research, and the National Research Council of Canada).
⋆⋆ Tables 2–4 are available in electronic form at http://www.aanda.org
⋆⋆⋆ Survey data is available at the CDS via anonymous ftp to cdsarc.u-strasbg.fr (130.79.128.5) or via http://cdsarc.u-strasbg.fr/viz-bin/qcat?J/A+A/532/A23
⋆⋆⋆⋆ http://www-laog.obs.ujf-grenoble.fr/heberges/timasss

range of densities and temperatures. The chemical composition of the gas is of paramount importance because the cooling is dominated by different species as a function of the gas temperature and density and the elemental abundance (Goldsmith 2001). A second classical example is the slow contraction of the prestellar cores, which is governed by ambipolar diffusion. Since only ions feel the magnetic field that counteracts the gravitational force, the chemical composition of the gas, which determines the ion abundance, is crucial. In addition to this, since the gas chemical composition is largely affected by the star formation process, its study in star forming regions is a powerful diagnostic tool to identify the various processes at work. Finally, the study of the chemical composition in regions forming solar-type stars is of particular importance, as it helps us to understand the formation history of our own Solar System. For example, the comparison of the chemical composition of comets with that of solar-type protostars or protoplanetary disks is used to help ascertain the origin of the former (Crovisier et al. 2004). The same applies to the studies of the molecular content of meteorites. In particular, the claim that the amino acids found in carbonaceous meteorites may have formed during the first phases of the life of the Solar System is based on the measured large deuteration in the meteoritic amino acids and in the protostellar environment (Pizzarello & Huang 2005). In this context, unbiased spectral surveys at millimeter and submillimeter wavelengths are particularly relevant as they allow us to detect heavy and large molecules, and, specifically, complex organic molecules. In summary, unbiased spectral surveys at the millimeter to submillimeter wavelengths are a powerful method to characterize the molecular content of astrophysical objects, and the only way to obtain a complete census of the chemical species.

There are at least two other aspects that make unbiased spectral surveys precious tools for studying the star formation process. First, in general they provide multiple lines from the same molecule, allowing multi-frequency analysis and modeling. Since different lines from transitions with different upper level energies and Einstein coefficients are excited at different temperatures and densities, they probe different regions in the line of sight. A careful analysis can, therefore, distinguish between the various physical components in the beam. If one also adds the kinematic information provided by the line profiles, the method can be so powerful that it can identify sub-structures along the line of sight, even if the spatial resolution of the observations is inadequate. In the present article, we provide an example of this capability of unbiased spectral surveys.

Given their powerful diagnostic ability, several unbiased spectral surveys in the millimeter and sub-millimeter bands accessible from ground have been obtained in the past in the direction of star forming regions. A complete list of these surveys can be found in Herbst & van Dishoeck (2009). By far the most targeted sources are hot cores, the regions of high-mass protostar formation, where the dust temperature exceeds the sublimation temperature of the water-ice grain mantles, ~100 K. The combined effect of the mantle sublimation and the high gas temperature triggers a singular and rich chemistry. At the same time, the relatively high densities ($\geq 10^7$ cm^{-3}) and temperatures ($\geq$100 K) are favorable for the excitation of several high lying transitions. The result is that extremely rich spectra are observed towards the hot cores. About a dozen hot cores have been targeted in different bands (Schilke et al. 1997; Helmich & van Dishoeck 1997; Hatchell et al. 1998; Schilke et al. 2001; Tercero et al. 2010). One of the most studied hot cores is the Orion-KL source. Spectral surveys covering almost all the bands accessible from the ground have been obtained, from about 80 to 900 GHz, detecting thousands of lines from hundreds of species and relative isotopologues (see for instance Schilke et al. 1997; Lee et al. 2001; Comito et al. 2005; Olofsson et al. 2007; Demyk et al. 2007; Carvajal et al. 2009; Margulès et al. 2009; Tercero et al. 2010, and references therein). In addition, the 500–2000 GHz range is observed with the HIFI spectrometer (de Graauw et al. 2010) on board the recently launched *Herschel*[1] satellite (Pilbratt et al. 2010), in the Key Program HEXOS[2]. Similarly, the 500–2000 GHz range is observed in other hot cores, as part of the Key Program CHESS[3] (*Chemical Herschel Surveys of Star forming regions*). Preliminary results of the surveys performed in these two *Herschel* Key Programs can be found in Bergin et al. (2010) and Ceccarelli et al. (2010), respectively.

Although being both less massive and less luminous, solar-type protostars also possess regions where the dust mantles sublimate, yielding similar properties as those of hot cores (see Ceccarelli 2007, and references therein). These regions have been baptized hot corinos, to highlight that they share similarities with hot cores but are not just scaled-down versions of them (see also Bottinelli et al. 2007). The interest in observing hot corinos, whose sizes are comparable to the Solar System sizes, is amplified by there being likely to resemble the Solar Nebula. In other words, their study corresponds to an archeological study of the ancestor of our Solar System.

So far, only one (partial) spectral survey has been obtained towards a solar-type protostar (Blake et al. 1994; van Dishoeck et al. 1995). The targeted source was IRAS 16293-2422 (hereinafter IRAS 16293), in the L1689N cloud (d = 120 pc, Loinard et al. 2008). This survey partially covered the two windows in the 200 GHz and 350 GHz bands accessible from the ground, and was obtained with the JCMT and CSO telescopes. The sensitivity achieved (~40 mK) allowed the detection of 265 lines from 24 species, namely the most abundant molecules CO, H_2CO, CH_3OH, SO, SO_2 etc. Later, more sensitive observations have demonstrated that the IRAS 16293 line spectrum is rich in complex organic molecules (Ceccarelli et al. 2000b; Cazaux et al. 2003), and doubly (Ceccarelli et al. 1998) and triply (Parise et al. 2004) deuterated molecules. Additional support for an unbiased spectral survey towards IRAS 16293 is provided by the *Herschel*/HIFI data in the 555–636 GHz range which shows that, while IRAS 16293 has much fewer lines than the 2×10^6 $L_\odot$ source NGC 6334I, the same number of species is detected in both sources (Ceccarelli et al. 2010).

Several studies have been carried out towards IRAS 16293, with both single dish telescopes and interferometers. The emerging overall picture is that IRAS 16293 is a protobinary system (Wootten 1989; Mundy et al. 1992) surrounded by an envelope of about 2 $M_\odot$ (Crimier et al. 2010). The structure of the envelope has been the target of several studies (Ceccarelli et al. 2000a; Schöier et al. 2002; Jørgensen et al. 2005). Crimier et al. (2010) concludes that the envelope density follows a r^{-2} power law at distances larger than about 1300 AU and $r^{-3/2}$ innerwards. The grain mantles are predicted to sublimate at a distance of 75 AU, where the density is equal to 2×10^8 cm^{-3}. The envelope extends from about 25 AU to about 6000 AU from the center. Inside the envelope, the two sources, A (south-east) and B (north-west), of the binary system are separated by about 4″ (separation being measured from interferometer observations at

[1] *Herschel* is an ESA space observatory with science instruments provided by European-led principal Investigator consortia and with important participation from NASA.

[2] http://www.submm.caltech.edu/hexos/

[3] http://www-laog.obs.ujf-grenoble.fr/heberges/chess/

a spatial resolution of about 1″), which is equivalent to a linear distance of 480 AU. The source B is brighter than the source A in the millimeter continuum and in several "cold envelope" molecular lines, whereas the source A seems to be brighter in several hot-corino-like molecular lines (Kuan et al. 2004; Bottinelli et al. 2004; Chandler et al. 2005). Finally, Chandler et al. (2005) have claimed that source A might be a multiple system and the observations of Pech et al. (2010) suggest that A is itself a binary system of 0.5 $M_{\odot}$ and 1.5 $M_{\odot}$, respectively.

Despite its relatively complex structure at arcsec scales, IRAS 16293 remains the brightest and most appropriate source to carry out a detailed study of the gas chemical composition in the first phases of the formation of a solar-type star. As discussed above, the best way for that is to obtain unbiased spectral surveys, that are as sensitive as possible. In this paper, we present the results of the most sensitive unbiased spectral survey of the bands between 80 and 366 GHz observable from ground-based telescopes obtained so far in the direction of IRAS 16293. This study is part of a more general project to also observe the 500–2000 GHz frequency range with the spectrometer HIFI on board the *Herschel* satellite, in the context of the *Herschel* Key Program CHESS[4] (Ceccarelli et al. 2010).

2. Observations

The observations were obtained at the IRAM-30 m (frequency range 80–280 GHz) and JCMT-15 m (frequency range 328–366 GHz) telescopes during the period between January 2004 and August 2006. Overall, the observations required a total of about 300 h (~200 h at IRAM and ~100 h at JCMT) of observing time. The beam of the survey varied between 9″ and 33″, depending on the telescope used and the frequency, and the spectral resolution ranged between 0.3 and 1.25 MHz, corresponding to velocity resolutions between 0.51 and 2.25 km s^{-1}. The achieved rms varied between 4 and 14 mK in 1.5 km s^{-1} bins. The observations were centered on the B (north-west) component at $\alpha(2000.0) = 16^{h}32^{m}22.6^{m}$, $\delta(2000.0) = -24°28'33'$. The A and B components, separated by 4″, are both inside the beam of our observations at all frequencies. However, at the highest frequencies observed with the IRAM 30 m telescope (i.e. the 1 mm band), the attenuation of emission from source A is not negligible as we discuss in Sect. 5. All observations were performed in DBS (Double-Beam-Switch) observing mode, with a 90″ throw. The pointing and focus were checked every two hours on planets or on continuum radio sources (1741-038 or 1730-130). Table 1 summarizes the observed bands and the details of the observations. Because of the different weather conditions during the different runs, the system temperatures widely varied. However, during the data processing, scans with too high system temperatures were removed before averaging.

2.1. IRAM observations

The following three bands were almost fully covered by observations at the IRAM-30 m telescope: 3 mm band (80–115.5 GHz), 2 mm band (129–177.5 GHz), and 1 mm band (198–281.5 GHz).

In all IRAM-30 m observations, two frequency ranges were observed simultaneously, with two SIS receivers with orthogonal polarizations for each frequency range, in the following configuration: 3 mm receivers (A100 & B100) in parallel with 1 mm receivers (A230 & B230), and 2 mm receivers (C150 & D150) in parallel with 1 mm receivers (C270 & D270). Because of the limitation (at the time of the observations) of the IRAM-30 m backend capabilities in terms of instantaneous frequency bandwidth and spectral resolution, we chose the largest possible spectral bandwidth to cover the IRAM-30 m bands in the smallest observing time. For simultaneous observations in the 3 mm and 1 mm bands, the VESPA autocorrelator was split into four parts, two of them covering the whole IF band of the A&B100 receivers (0.5 GHz) with 320 kHz spectral resolution and the two others covering half of the IF band of the A&B230 receivers (1 GHz) with 1250 kHz spectral resolution. The second half of the IF band of the A&B230 receivers was covered with the 1 MHz filter banks (FB). For simultaneous observations in the 2 mm and upper 1 mm bands, the VESPA autocorrelator was split into four parts, two of them covering half of the IF band of the C&D150 receivers (0.5 GHz) with 320 kHz sampling and the two others covering half of the IF band of the C&D270 receivers (1 GHz) with 1250 kHz sampling. The second half of the IF band of the C&D150 receivers was covered with the 1 MHz FB.

The configuration for observations in the 2 mm band resulted in different spectral resolutions for each half of the IF band of the receivers (320 kHz ~ 0.65 km s^{-1} and 1 MHz ~ 2 km s^{-1}). Therefore, we shifted the tuning frequency of the receivers by only 0.5 GHz from one tuning to the next one to cover the entire 2 mm band at the highest and at the lowest spectral resolution, respectively. As a consequence, two different datasets were obtained, one at high resolution (generally used for studying brighter lines), and one at low resolution (for the faint lines).

2.2. JCMT observations

The JCMT-15 m observations covered the 328 to 366 GHz frequency range. They were obtained with a 345 GHz SIS receiver RxB3 used in dual-channel single-sideband (SSB) mode. Each polarization of the receiver was connected to a unit of the ACSIS autocorrelator providing a bandwidth of 0.5 GHz for a spectral resolution of 625 kHz. At 345 GHz, this yields a velocity resolution of about 0.5 km s^{-1}.

3. Calibration

3.1. Method

At the IRAM-30 m telescope, the calibration was performed with a cold and a warm absorbers, and the atmospheric opacity was obtained using the ATM program (Cernicharo 1985, IRAM internal report). At the JCMT-15 m, line strengths were calibrated via the chopper wheel method (Kutner & Ulich 1981).

Our spectral survey does not allow us to estimate the calibration uncertainties from line observation redundancy: each spectral range was observed only once and there is only negligible frequency overlap between adjacent spectra. From our simultaneous observations with two receivers in the 1 mm range, we may estimate the receiver contribution, but to derive the total calibration uncertainties of the survey, we performed a detailed comparison between our own and previous observations. As our comparisons rely only on observations obtained with the same telescopes towards the same position (namely source B), no bias is caused by the different source dilution in the beams and our results are unaffected by the underestimate of source A contribution at high frequency. The comparison includes virtually all the published data towards IRAS 16293 obtained with the IRAM-30 m and the JCMT-15 m telescopes, as well as unpublished data obtained with the IRAM-30 m telescope. The list of the

[4] http://www-laog.obs.ujf-grenoble.fr/heberges/chess/

Table 1. Parameters of the observations at IRAM-30 m and JCMT-15 m telescopes.

Telescope	Frequency (GHz)	Resolution (MHz)	Resolution (km s^{-1})	Backend[1]	rms[2] (mK)	T_{sys} (K)	HPBW (arcsec)	Beam efficiency	σ_{cal}[3] (%)	N_{cal}[4] lines	P_{cal}[5] (%)
IRAM	80–115.5	0.32	0.81–1.17	VESPA	4–8	90–400	30–21	0.80–0.78	11	28	15
IRAM	129–177	0.32	0.53–0.72	VESPA	5–14	200–1000	19–14	0.76–0.69	17	22	12
IRAM		1.0	1.65–2.25	1 MHz FB					10[(6)]	84[(6)]	95[(6)]
IRAM	197–265	1.0	1.13–1.52	1 MHz FB	7–13	180–1200	12–9	0.65–0.51	17	36	10
IRAM		1.25	1.41–1.90	VESPA							
IRAM	265–280	1.25	1.34–1.41	VESPA	9–17	470–4200	9	0.51–0.47			
JCMT	328–366	0.625	0.51–0.57	ACSIS	4–9	90–400	14	0.56–0.53	18	26	25

Notes. [(1)] In the 2 mm band, each frequency setting is observed twice, i.e. once at each of the two spectral resolutions (0.32 and 1 MHz), while in the 197–265 GHz band, each frequency setting is observed only one time, at a slightly different spectral resolution (1 or 1.25 MHz), [(2)] rms is given in 1.5 km s^{-1} bins, [(3)] σ_{Cal} is the calibration uncertainty, [(4)] N_{cal} is the number of compared lines for calibration purposes, [(5)] P_{cal} is the percentage of compared spectra for calibration purposes, [(6)] these values refer to the "internal" comparison between VESPA and 1 MHz FB spectra simultaneously observed; the other ones refer to "external" comparisons with published or previously obtained observations.

articles used for this comparison is the following: *a) IRAM-30 m bands:* Ceccarelli et al. (1998), Loinard et al. (2000), Cazaux et al. (2003), Wakelam et al. (2004), Parise et al. (2002), and Parise et al. (2005b); *b) JCMT-15 m band:* Blake et al. (1994), van Dishoeck et al. (1995), Loinard et al. (2000), Schöier et al. (2002), and Parise et al. (2004). Table 1 reports the percentage of the survey spectra that could be cross-checked and calibrated against previously published data for each band. In addition, we cross-checked the calibration in the 2 mm band by comparing the data obtained with 1 MHz and 320 kHz resolution. Finally, we estimated the calibration uncertainty produced by the receivers by comparing lines in the 1 mm band observed with the two receivers A230 and B230.

To quantify the differences, we obtained Gaussian fits of the lines and compared their characteristics (integrated intensity, peak intensity, and full width at half maximum *FWHM*), with the previously published values. The comparison was performed in the main beam brightness scale (T_{mb}) based on the T_A^*/T_{mb} beam efficiency factors given in Table1. This method provides two types of check: i) the average uncertainty for each band; and ii) possible specific calibration problems on single settings.

3.2. Calibration uncertainties

With the method described above to quantify the calibration uncertainty in the survey, we obtained the following results.

FWHM: In all the frequency ranges, except 1mm, the agreement between the survey and the published *FWHM* values is within 15–20% and no systematic trend is observed. In contrast, in the 1 mm band the *FWHM* of the survey lines appears to be systematically broader by ≃1 km s^{-1} than the published values. This is likely due to the relatively poorer spectral resolution of our survey in this range (0.8 to 1.9 km s^{-1}) compared to the linewidths (on average ≃4–5 km s^{-1}).

Integrated and peak intensity: The comparison of the integrated and peak intensity of the lines of the survey with published values yields the same results, when the difference due to the spectral resolution described above is taken into account. In addition, since the derivation of the integrated intensities does not depend on the line shape, we choose to quantify the calibration uncertainties by comparing the integrated line intensities.

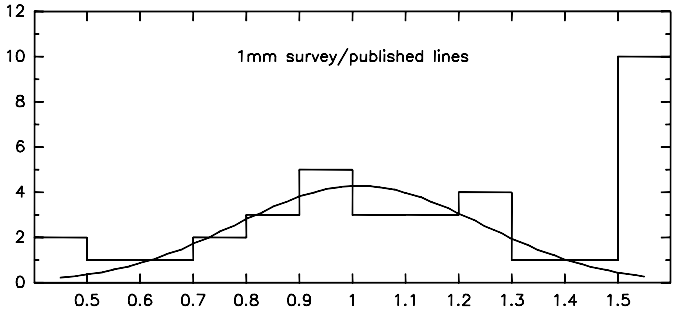

Fig. 1. Distribution of integrated intensity ratios of this survey's 1 mm lines compared to published observations obtained with the IRAM 30 m telescope. The curve is a Gaussian fit to the histogram ruling out the "anomalous" ratios (≤0.5 or ≥1.5). It can be noticed that the 12 "anomalous" ratios correspond to only 7 "anomalous spectra" among the 165 spectra observed in the 1 mm range.

Derived uncertainties: We can derive an estimate of the calibration uncertainty from the distribution of the integrated intensity ratios. Figure 1 shows the result for the 1 mm band. If one excludes the two extremes at ≤0.5 and ≥1.5, which correspond to spectra with "anomalous intensity", the ratio distribution can be fitted by a Gaussian with a mean value of R, very close to one and a standard deviation σ_{ratio}. On the basis of the assumption that the relative uncertainties in the published intensities, σ_{pub}, and on the survey line intensities, σ_{cal}, are independent variables, the error propagation formula implies that:

$$\sigma^2_{ratio} = R^2(\sigma^2_{cal} + \sigma^2_{pub}). \quad (1)$$

Most publications report calibration uncertainties of 15% (or do not report any estimate). Except in the 3 mm frequency range, where our comparisons suggest that the calibration uncertainty is probably somewhat smaller than 15%, we obtain consistent uncertainties assuming either that $\sigma_{pub} = 15\%$ for all the frequency ranges or that our observations are representative of average observation conditions in each frequency range, i.e., $\sigma_{pub} = \sigma_{cal}$ and thus $\sigma^2_{cal} \simeq \sigma^2_{ratio}/2$. Table 1 reports the resulting calibration uncertainties for each observed band.

We note that at 2 mm, the "external" comparisons with published spectra, which include all uncertainty factors, lead to higher values than "internal" comparisons between the VESPA and 1 MHz FB simultaneous observations, which take into account only the contribution of the backends. Similarly, at 1 mm, a comparison of the line intensities observed simultaneously with

the two receivers A230 and B230 shows that the receivers' contribution to the calibration uncertainties is approximately 10%, whereas the total calibration uncertainty is 17%.

Finally, the full list of lines used for the calibration comparison is reported in the on line material, in Table 2 for a comparison between the survey lines and previous observations obtained with the same telescopes and in Table 3 for a comparison between the survey lines observed simultaneously with VESPA and the 1 MHz filter bank at the IRAM-30 m telescope.

4. Data release

The data are made publicly available on the TIMASSS web site[5]. The site provides the files with the IRAM-30 m and JCMT-15 m data in CLASS format[6]. The intensities are in $T_A{}^*$. On the basis of the discussion of the previous section, the potential user is highly recommended to verify the calibration uncertainty in the data that she/he wants to use by looking at Tables 2 and 3. We emphasize that we did not apply any "rescaling" factor to the survey data because the difference may be caused by an incorrect calibration of the published rather than the survey data. Only a very careful scientific analysis can assess what is the most likely explanation. It is, therefore, the user's responsibility to verify that the data are correctly used, based on the information provided at the web site.

5. Results

5.1. Overall survey

Figure 2 shows the full survey in the four bands and the richness of the IRAS 16293 line spectrum. About 20 lines per GHz on average have been detected with a signal-to-noise ratio S/N higher than three in the 220 GHz frequency range covered by the survey. The line density seems to increase slightly with frequency: there are 17 lines/GHz in the 3 mm band, 19 and 23 lines/GHz in the 2 mm and 1 mm ranges respectively, and as many as 26 lines/GHz in the 0.9 mm range.

To quantify more rigorously the lines and species detected in the survey, we made Gaussian fits and line identification using the CASSIS[7] package. The spectroscopic data come from the CDMS and JPL databases (Müller et al. 2001, 2005; Pickett et al. 1998, and references quoted on the databases to data producers for each species). In a few cases (ortho and para H_2CO for instance), a specific database with each form separated has been used (see the CASSIS[7] web site). For the D-bearing isotopologues of methanol, only the lines reported by Parise et al. (2002, 2004) are included in this paper.

Hereinafter we only consider lines identified according to the following criteria: i) lines belonging to species included in the JPL and CDMS databases or to the D-bearing isotopologues of methanol, ii) lines detected with a certainty of more than 3σ in the integrated line intensity, iii) unblended lines, and iv) lines with upper level energies E_{up} lower than 250 K. This last condition only limits the number of methanol lines in this analysis, since lines of other molecules with E_{up} higher than 250 K are in any case too weak to be detected by our survey. When applying these criteria, we end up with ~1000 lines listed in Table 4. In the table, we report the line identification together with the result of the Gaussian fit of each line (see also Sect. 5.3).

Figure 3 shows the line densities, which are limited to the lines satisfying the above criteria, in each of the four survey frequency ranges, for various signal-to-noise ratios. In the 3 mm and 2 mm ranges, these densities are a factor of between two and three smaller than the estimates of the total densities including blended lines. This effect is even stronger in the 1 mm and 0.9 mm ranges, where the lack of weak lines ($3 \leqslant S/N < 10$) is particularly striking in Fig. 3. This is a bias due to our selection criterion of non-blended lines, as these frequency ranges are rich in lines from large molecules, which emit many weak lines, so that our unblended line criterion filters out a large fraction of these lines of moderate S/N. In contrast, the 2 mm range, which benefits from a better spectral resolution compared to the 3 mm and 1 mm ranges, is less affected by this selection effect.

Most of the lines retained in the 1 mm and 0.9 mm ranges and a large fraction (≃2/3) of the lines retained in the 3 mm and 2 mm ranges have a high S/N (⩾10). The density of lines with such high S/N is relatively constant in frequency and equal to ≃4−5 GHz.

When comparing with the line density quoted at the beginning of the section, namely about 20 lines per GHz, obtained considering lines with $S/N \geq 3$ but no other filter, clearly the introduction of the other criteria, unblended lines and, to a lesser degree, identified lines and $E_{up} \leq 250$ K, severely underestimates the line content.

The line intensity spans more than three orders of magnitude, from 10 mK to 24 K. The number of lines showing an integrated intensity higher than a given threshold is given in Fig. 4. For integrated intensity ranging between 1 and 30 K km s^{-1}, the distribution roughly follows a power law of slope –0.9. The power law breaks down in the high and low end of the distribution. This slope is identical to those observed by Schilke et al. (2001), White et al. (2003), and Comito et al. (2005), in their submillimeter surveys of Orion-KL. As found by these surveys, this slope does not provide a good fit for the brightest and the weakest lines.

5.2. Detected lines and species

Table 5 lists the species detected and identified in the survey, (see below).

In the framework of a survey analysis restricted to the four line criteria mentioned above, 69 different molecules (including ions) have been detected. They correspond to 32 distinct chemical species and include 37 rare isotopologues. They are listed in Table 5 which gives the number of lines detected for each species, the range of upper level energy of the lines and observational quantities. Among the ~1000 lines in Table 5, about half belong to only three species: CH_3HCO, $HCOOCH_3$, and CH_3OH.

Most of the 4000 lines detected in our survey belong to species already identified in this source (see Table 5), among which a few molecules display extremely rich spectra, including many weak and/or blended lines that are not included in the present study. Although we anticipate the presence of unidentified lines, their assignment will require a careful analysis and even probably modeling of these spectra. The $E_{up} \leq 250$ K selection criterion used in this work also prevent us from identifying any vibrationally excited lines. We postpone these considerations to a future article.

[5] http://www-laog.obs.ujf-grenoble.fr/heberges/timasss

[6] http://www.iram.fr/IRAMFR/GILDAS

[7] CASSIS has been developed by IRAP-UPS/CNRS, see http://cassis.cesr.fr.

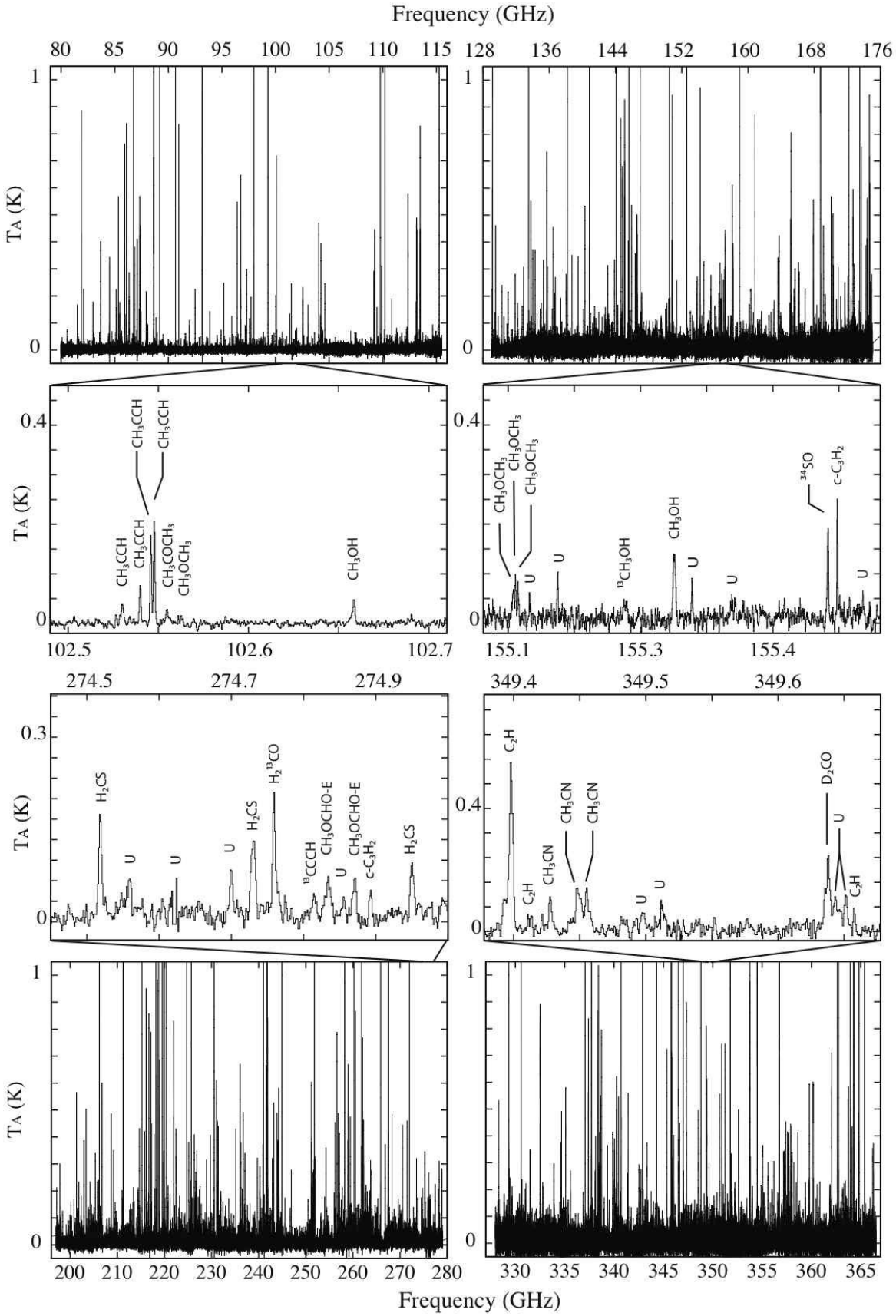

Fig. 2. The IRAS 16293 spectra in the four bands of the survey. *Upper panels*: IRAM-30 m 3 mm and 2 mm bands. *Lower panels*: IRAM-30 m 1 mm and JCMT-15 m 0.9 mm bands. The *middle panels* are zoomed views of sample frequency ranges in the four bands respectively. These panels include lines identification based on the publicly available spectral databases (see text for details).

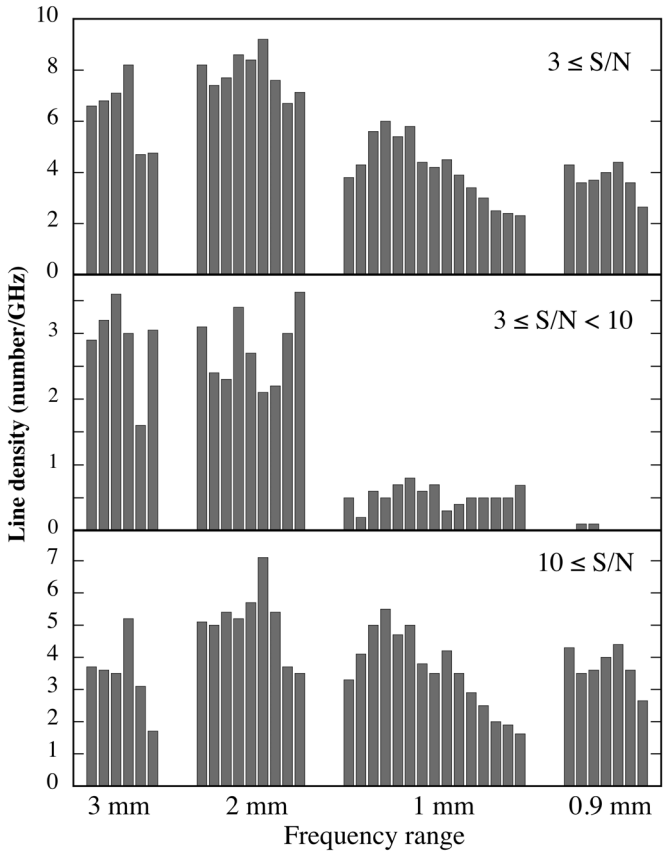

Fig. 3. Distribution of the density (averaged over 10 GHz intervals) of identified lines (see text) in each of the four frequency ranges. The *upper panel* corresponds to lines with $S/N \leqslant 3$, the *central panel* is restricted to lines with $3 \leqslant S/N < 10$ and the *lower panel* corresponds to lines with $S/N \geqslant 10$.

Table 5 also lists the sum of the line flux in each species. For species displaying rich and complex spectra and/or numerous lines with upper energy levels ≥250 K, this value is a lower limit because of the numerous weak and blended lines that are not included in the present analysis.

As noted by the previous studies (Blake et al. 1994; van Dishoeck et al. 1995), the millimeter and submillimeter spectrum of IRAS 16293 is dominated by simple O-rich species such as CO, SO, H_2CO, SO_2, and CH_3OH (the three first families alone constitute more than two-thirds of the total flux). In the frequency range covered by our survey, the total flux emitted in the CO main and isotopic lines is about 800 K km s^{-1}, ∼30% smaller than the flux emitted in the SO, H_2CO, SO_2, and CH_3OH lines together (∼1100 K km s^{-1}). Thus, CO is not the major cooling agent in this frequency range. In addition, our survey detects thousands of weaker lines from heavier and more complex molecules that had not been found in the previous surveys. The zoomed figures of Fig. 2 illustrate the situation, with several lines from CH_3CCH, CH_3CN, $HCOOCH_3$ etc. To roughly estimate the contribution of this "grass" of lines to the total cooling of the gas (in this range of frequencies), we consider a line density of about 15 lines per GHz (see above) and a line integrated intensity of ∼0.3 K km s^{-1}. This gives approximatively an integrated line intensity of 900 K km s^{-1}, which is comparable to the contribution of CO and its isotopologues.

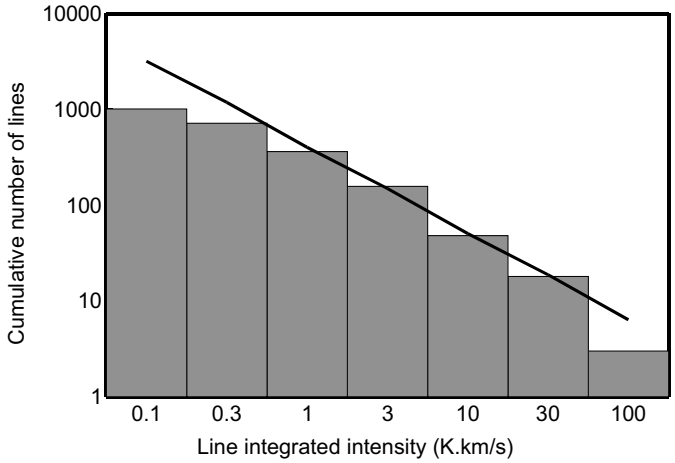

Fig. 4. Number of lines showing an integrated intensity larger than a given threshold. The solid line shows the single index power-law best fit to the distribution.

5.3. Line parameters

A Gaussian fit was performed for each of the lines of Table 4. The parameters of the fit (integrated intensity, line width *FWHM*, and rest velocity v_{LSR}) are reported in the same table. The uncertainties in the integrated line intensity are based on the spectra noise and the calibration uncertainties reported in Table 1. We verified that even when the line profile differs from a simple Gaussian (for example in self-absorbed lines, or lines with broad wings) the Gaussian fit area is very close to the true integrated line intensity and, therefore, reliable. The uncertainties in the line width *FWHM* and rest velocity v_{LSR} take into account the statistical errors (from the fit) and the uncertainty due to the limited spectral resolution, which indeed dominates the error. The cases where the line profiles are clearly not Gaussian are marked in Table 4. The average $\langle FWHM \rangle$ and $\langle v_{LSR} \rangle$ for each species and isotopologues are reported in Table 5, except for those that show severe blending caused by unresolved or partially resolved hyperfine structure (CH_3CN, HNCO, NH_2D, NS).

In the following, we analyze the information derived from the Gaussian *FWHM* and v_{LSR} of the lines.

Figure 5 shows the *FWHM* versus v_{LSR} for each species. In the plots, we have regrouped the isotopologues of the same species and, in a few cases, species with a small number of lines. In these cases, we verified that the species have similar *FWHM* and v_{LSR} to avoid introducing artificial trends in the plot. Figure 5 shows a remarkable and unexpected behavior: *the FWHM and v_{LSR} distributions are not the same but, in contrast depend on the species*.

On the basis of the different *FWHM* and v_{LSR} distributions, four types of "kinematical behaviors"t can be identified:

1. Type I (first row of Fig. 5): $\langle v_{LSR} \rangle \sim 4.0$ km s^{-1} and $\langle FWHM \rangle \sim 2.5$ km s^{-1}. The lines show very little dispersion in terms of both rest velocities and line widths. Small carbon chains and rings, and "small molecules" belong to this group.
2. Type II (second row): $\langle v_{LSR} \rangle \sim 3.7$ km s^{-1} with very little dispersion, *FWHM* from ∼2 km s^{-1} to ∼8 km s^{-1}. All species in this group are S- or N-bearing molecules. We note that HCO^+ and C_3H_2 (in the first row) have properties which are in-between type I and type II.

Table 5. Detected species ordered by decreasing fluxes of the main isotopologue.

TAG [1]	Species [3]	Nb[2] lines	E_{up} (K) min–max	$\langle V_{LSR}\rangle$ (km s^{-1})	$\langle FWHM\rangle$ (km s^{-1})	$\int T_{mb}dv$ (K km s^{-1})	TAG [1]	Species [3]	Nb[2] lines	E_{up} (K) min–max	$\langle V_{LSR}\rangle$ (km s^{-1})	$\langle FWHM\rangle$ (km s^{-1})	$\int T_{mb}dv$ (K km s^{-1})
28503	[aa] CO	3	5.5–33.2	5.93 ± 0.71	9.47 ± 1.77	605.8	41001	[bb] CH_3CN	>30	20.4–21.2			58.6
29501	[ab] ^{13}CO	3	5.3–31.7	3.94 ± 0.36	4.13 ± 1.16	116.0	46509	[bc] H_2CS	26	9.9–143.4	3.61 ± 0.35	4.53 ± 1.34	51.2
30502	[ac] $C^{18}O$	3	5.3–31.6	3.72 ± 0.18	2.90 ± 0.61	67.6	47505	[bd] $H_2^{13}CS$	4	22.5–97.1	4.09 ± 0.79	4.61 ± 2.29	2.9
29006	[ad] $C^{17}O$	3	5.4–32.4	3.84 ± 0.35	3.75 ± 0.66	25.5	47504	[be] HDCS	5	8.9–30.9	3.77 ± 0.12	2.81 ± 0.88	0.8
48501	[ae] SO	20	9.2–87.5	3.98 ± 0.20	4.18 ± 0.55	339.5	60503	[bf] OCS	12	16.3–134.8	3.13 ± 0.33	5.12 ± 0.77	38.6
50501	[af] ^{34}SO	13	15.6–86.1	3.81 ± 0.27	4.87 ± 0.84	28.0	62505	[bg] $OC^{34}S$	9	15.9–157.2	2.51 ± 0.26	3.98 ± 0.65	7.8
30591	[ag] o-H_2CO	10	6.8–143.3	3.45 ± 0.58	4.09 ± 0.58	163.3	61502	[bg] $O^{13}CS$	10	20.9–147.2	2.58 ± 0.51	4.49 ± 1.25	5.6
30581	[ag] p-H_2CO	7	10.5–99.7	3.67 ± 0.12	3.92 ± 0.65	93.6	60003	[bh] $HCOOCH_3$	182	17.9–145.0	2.52 ± 0.32	2.71 ± 0.77	51.6
31501	[ah] HDCO	10	17.6–102.6	3.39 ± 0.58	3.99 ± 1.06	26.7	44505	[bi] SiO	6	6.2–75.0	4.40 ± 0.46	5.57 ± 0.78	49.7
31503	[ak] $H_2^{13}CO$	12	10.2–157.5	2.96 ± 0.38	2.86 ± 1.29	12.7	27002	[bj] HNC	3	4.3–43.5	3.80 ± 0.56	2.81 ± 1.08	32.1
32592	[aj] o-D_2CO	6	16.8–81.2	3.51 ± 0.61	3.80 ± 0.84	11.7	28508	[bk] DNC	2	11.0–22.0	4.31 ± 0.02	2.47 ± 1.19	4.9
32582	[aj] p-D_2CO	8	5.3–99.5	3.38 ± 0.72	2.76 ± 1.24	5.5	28005	[as] $HN^{13}C$	4	4.2–41.8	3.74 ± 0.61	3.44 ± 1.76	4.8
32503	[ak] $H_2C^{18}O$	4	20.0–63.4	2.71 ± 0.16	2.67 ± 1.21	1.9	51501	[bl] HC_3N	17	19.6–203.0	3.53 ± 0.44	4.67 ± 1.97	35.4
64502	[al] SO_2	82	7.7–248.5	3.74 ± 0.32	5.30 ± 1.22	238.3	52005	[bm] DC_3N	6	22.3–77.0	4.29 ± 0.23	2.61 ± 0.41	1.0
66002	[am] $^{34}SO_2$	5	7.6–69.7	3.33 ± 0.72	4.20 ± 1.71	1.6	34502	[bn] H_2S	2	27.9–84.0	3.55 ± 0.52	4.90 ± 0.08	25.2
32504	[an] CH_3OH	99	7.0–233.6	3.42 ± 0.42	5.91 ± 1.35	217.6	35001	[bo] HDS	2	11.7–34.7	3.05 ± 0.55	2.41 ± 2.09	0.7
33502	[ao] $^{13}CH_3OH$	9	6.8–94.6	2.93 ± 0.47	3.92 ± 1.63	2.8	38082	[bp] o-c-C_3H_2	14	4.1–48.3	4.10 ± 0.27	2.73 ± 0.70	14.5
	[ap] CH_2DOH	12	4.5–40.8	2.74 ± 0.64	5.89 ± 0.91	6.4	38092	[bp] p-c-C_3H_2	9	6.4–47.5	4.27 ± 0.26	2.57 ± 1.29	4.5
	[ap] CHD_2OH	7	4.2–53.5	3.70 ± 0.88	4.76 ± 1.58	2.6	39003	[bq] c-C_3HD	5	17.4–25.34	4.44 ± 0.31	1.91 ± 0.88	1.5
	[ap] CH_3OD	4	6.0–26.8	2.55 ± 0.84	3.96 ± 1.29	2.3	46008	[br] CH_3OCH_3	82	11.1–169.8	2.53 ± 0.29	2.27 ± 0.69	18.8
	[aq] CD_3OH	3	12.2–42.0	2.43 ± 0.21	2.03 ± 0.49	0.5	40502	[bs] CH_3CCH	26	12.3–176.6	3.62 ± 0.32	3.03 ± 0.58	17.4
29507	[ar] HCO^+	3	4.3–42.8	3.29 ± 0.16	2.87 ± 1.39	144.2	41502	[bt] CH_2DCCH	4	16.3–38.1	4.34 ± 0.31	1.93 ± 0.40	0.2
30504	[ar] $H^{13}CO^+$	4	4.2–41.6	3.94 ± 0.46	2.43 ± 0.44	31.5	25501	[bu] CCH	13	4.2–25.1	3.83 ± 0.09	2.08 ± 0.20	14.7
30510	[as] DCO^+	3	10.4–51.9	4.19 ± 0.29	2.34 ± 0.83	14.3	26501	[bv] CCD	4	10.4–10.3	4.32 ± 0.52	2.54 ± 0.86	0.8
31506	[at] $HC^{18}O^+$	3	4.1–24.5	4.04 ± 0.37	2.15 ± 0.51	1.6	43002	[bw] HNCO	>8	10.5–143.5			13.8
31508	[ar] $D^{13}CO^+$	2	10.2–20.4	4.52 ± 0.16	2.34 ± 1.36	0.6	26504	[bx] CN	7	5.4–5.4	4.45 ± 0.10	1.82 ± 0.16	8.5
30505	[au] $HC^{17}O^+$	1	12.5–12.5	3.94 ± 0.22	4.03 ± 0.71	0.4	45506	[by] HCS^+	5	6.1–73.7	3.72 ± 0.20	3.32 ± 0.70	5.1
44501	[av] CS	4	7.0–65.8	3.70 ± 0.12	3.56 ± 0.43	126.5	42501	[bz] H_2CCO	13	9.7–66.9	3.00 ± 0.26	2.58 ± 0.44	4.8
46501	[av] $C^{34}S$	4	6.9–64.8	3.63 ± 0.16	3.60 ± 0.68	21.1	18501	[ca] NH_2D	>3	16.6–182.8			4.7
45501	[av] ^{13}CS	4	6.7–46.6	3.69 ± 0.22	4.06 ± 0.96	9.0	30008	[cb] NO	7	7.2–36.1	4.02 ± 0.12	2.25 ± 1.42	3.7
45502	[av] $C^{33}S$	4	7.0–65.3	3.68 ± 0.66	5.05 ± 1.67	7.2	56007	[cc] C_2S	12	15.4–53.8	4.10 ± 0.17	2.12 ± 0.62	2.6
27501	[aw] HCN	3	4.2–42.5	3.57 ± 0.78	7.06 ± 2.12	97.5	45013	[cd] PN	>3	13.5–63.1			2.1
28002	[ax] $H^{13}CN$	5	4.1–41.4	3.77 ± 0.26	4.05 ± 1.85	17.1	19002	[ce] HDO	1	95.2–95.2	2.87 ± 0.21	6.13 ± 0.58	2.1
28509	[ay] DCN	3	10.4–52.1	3.63 ± 0.46	4.09 ± 0.55	11.3	46010	[cf] NS	>6	9.9–17.8			1.3
28003	[az] $HC^{15}N$	4	4.1–41.3	3.60 ± 0.33	5.52 ± 1.47	6.4	49503	[cg] C_4H	6	20.5–30.2	4.00 ± 0.08	1.58 ± 0.28	0.7
44003	[ba] CH_3CHO	192	13.8–194.5	2.79 ± 0.39	2.68 ± 1.00	70.0	37003	[ch] c-C_3H	3	4.39–10.8	4.42 ± 0.22	1.79 ± 0.10	0.3

Notes. [(1)] In the CDMS as in the JPL catalog, the species are associated to a five digit number, called TAG; the first two digits correspond to their molecular weight in atomic mass units, and the third digit is a 5 in the CDMS catalog, and a 0 in the JPL catalog. Our identification of the ortho and para forms of H_2CO, D_2CO and c-C_3H_2 relies on the VASTEL Spectroscopic database (http://www.astro.caltech.edu/~vastel/CHIPPENDALES) so that these species are associated with specific TAG. The deuterated isotopologues of methanol, not yet included in the CDMS and JPL databases, do not have a TAG. Our identification of their lines is based on the data given in Parise et al. (2002) and Parise et al. (2004) and references therein. [(2)] For most N-bearing species, due to unresolved hyperfine structure, this number is a lower limit corresponding to groups of blended lines. [(3)] For each species, the spectroscopic references given here are the most recent cited in the CDMS and JPL databases. All of them should be read as reference and references therein: [(aa)] Winnewisser et al. (1997); [(ab)] Cazzoli et al. (2004); [(ac)] Klapper et al. (2001); [(ad)] Klapper et al. (2003); [(ae)] Bogey et al. (1997); [(af)] Klaus et al. (1996); [(ag)] Müller et al. (2000d); [(ah)] Bocquet et al. (1999); [(ai)] Müller et al. (2000c); [(aj)] Lohilahti & Horneman (2004); [(ak)] Müller et al. (2000b); [(al)] Müller et al. (2000a); [(am)] Belov et al. (1998); [(an)] Müller et al. (2004); [(ao)] Xu & Lovas (1997); [(ap)] Parise et al. (2002); [(aq)] Parise et al. (2004); [(ar)] Lattanzi et al. (2007); [(as)] van der Tak et al. (2009); [(at)] Schmid-Burgk et al. (2004); [(au)] Dore et al. (2001); [(av)] Kim & Yamamoto (2003); [(aw)] Thorwirth et al. (2003); [(ax)] Cazzoli & Puzzarini (2005); [(ay)] Brünken et al. (2004); [(az)] Cazzoli et al. (2005); [(ba)] Kleiner et al. (1996); [(bb)] Müller et al. (2009); [(bc)] Clouthier et al. (1994); [(bd)] Brown et al. (1987); [(be)] Minowa et al. (1997); [(bf)] Golubiatnikov et al. (2005); [(bg)] Lovas & Suenram (1987); [(bh)] Maeda et al. (2008); [(bi)] Cho & Saito (1998); [(bj)] Thorwirth et al. (2000a); [(bk)] Brünken et al. (2006); [(bl)] Thorwirth et al. (2000b); [(bm)] Spahn et al. (2008); [(bn)] Belov (1995); [(bo)] Camy-Peyret et al. (1985); [(bp)] Mollaaghababa et al. (1993); [(bq)] Bogey et al. (1987); [(br)] Neustock et al. (1990); [(bs)] Cazzoli & Puzzarini (2008); [(bt)] Leguennec et al. (1993); [(bu)] Padovani et al. (2009); [(bv)] Bogey et al. (1985); [(bw)] Lapinov et al. (2007); [(bx)] Klisch et al. (1995); [(by)] Margulès et al. (2003); [(bz)] Guarnieri & Huckauf (2003); [(ca)] Fusina et al. (1988); [(cb)] Meerts & Dymanus (1972); [(cc)] Lovas et al. (1992); [(cd)] Cazzoli et al. (2006); [(ce)] Johns (1985); [(cf)] Lovas & Suenram (1982); [(cg)] Chen et al. (1995); [(ch)] Yamamoto & Saito (1994).

3. Type III (third row): $\langle v_{LSR}\rangle \sim 2.5$–$3.0$ km s^{-1}, $\langle FWHM\rangle \leq 4.0$ km s^{-1}. Four complex organic molecules display this behavior.
4. Type IV (fourth row): v_{LSR} and *FWHM* have mixed behaviors, with characteristics belonging to the two last groups. CH_3OH lines have v_{LSR} and *FWHM* ranging from 2 to 9 km s^{-1}; H_2CO and CH_3CCH lines have moderate *FWHM* (4–5 km s^{-1}) and v_{LSR} ranging from 2.5 to 4 km s^{-1}; lines from the rare isotopes of OCS have $v_{LSR} \sim 2.5$ km s^{-1} and $FWHM \leq 4$ km s^{-1}.

We note that the FWHM averaged over each of the four frequency bands of the survey is similar, between 2 and 5 km s^{-1}, there being a slight increase in the 1 mm band caused by the poorer spectral resolution. We verified that none of the four kinematical behaviors are produced by this instrumental effect. Table 6 summarizes the situation. To more clearly understand the

Table 6. Distribution of the detected species in four kinematical types.

Type (Source)	v_{LSR} (km s^{-1})	*FWHM* (km s^{-1})	E_{up} (K)	*FWHM* behavior	Species
Type I (Envelope)	~4	≤2.5	0–50	constant	CN, NO, C_2S, C_2H, C_3H, C_4H, HCO^+, C_3H_2
Type II (Source A)	~3.7	2–8	0–250	increases	HCN, HC_3N, HNC, SO, SO_2, CS, HCS^+, H_2CS
Type III (Source B)	2.5–3	≤ 4	0–200	constant	CH_3CHO, $HCOOCH_3$, CH_3OCH_3, H_2CCO
Type IV (mixed)	2.5–4	2–8	0–250	increases	CH_3OH, H_2CO, CH_3CCH, OCS

Notes. First column reports the associated component (see Sect. 6), second, third and fourth columns report the typical velocities, *FWHM* and upper level energy E_{up} ranges of the detected lines. Fifth column describes the behavior of *FWHM* with increasing E_{up} and last column lists the species belonging to each type.

physical meaning of the plots in Fig. 5 (and the four identified types), we plotted in Fig. 6 the values of the *FWHM* as function of the upper level energy E_{up} of the transition. The species were grouped as in Fig. 5; it is striking that the distinction between the four types defined by the (*FWHM*, v_{LSR}) distribution is also visible in this plot.

Type I species have lines with E_{up} lower than 50 K. We note that this is not an observational bias: except for a few very light molecules, such as C_2H, the species associated with type I have high energy transitions in the survey frequency range, but the line intensities decrease abruptly when E_{up} becomes higher than 50 K. In contrast, type II, III, and IV species have lines with E_{up} up to 200 K but different behaviors. For type II species, the *FWHM* increases with E_{up}, whereas for type III and IV the *FWHM* is constant and does not depend on E_{up}. In contrast, analogous plots of v_{LSR} versus E_{up} indicate that the lines' velocity does not depend on E_{up} in any species. A related effect was discovered by Schöier et al. (2002), who noted a correlation between the linewidths and the excitation temperatures derived by Blake et al. (1994) and van Dishoeck et al. (1995). These properties are used to give a physical meaning to the four types in Sect. 6. Finally, we note that when detected, the deuterated species show the same behavior as the main isotopomers, except the D-isotopomers of type III species that have too weak lines to be detected in our survey.

6. Discussion

6.1. Comparison with previous surveys

When compared to the previous survey toward IRAS 16293 (Blake et al. 1994; van Dishoeck et al. 1995), the present one not only enlarges the covered frequency range (~200 GHz versus ~40 GHz) but also the number of detected species, thanks to the higher sensitivity (~10 mK versus ~40 mK). The average line density of the previous unbiased survey of IRAS 16293 was 7 lines per GHz, which should be compared with 20 lines per GHz for the present one. Several species detected in our survey were not detected in the previous one: complex organic molecules ($HCOOCH_3$, $HCOOCH_3$ and CH_3OCH_3), carbon chains and rings (C_2S, C_4H, c-C_3H), N-bearing species (NO, PN, NS), and several D-bearing molecules.

Towards hot cores, numerous surveys have been performed. They have covered the whole range of frequencies reachable from the ground, from the 3 mm range observed with IRAM, SEST, NRAO, or JCMT to the submillimeter windows observable with the CSO and JCMT (MacDonald et al. 1996; Schilke et al. 1997; Helmich & van Dishoeck 1997; Nummelin et al. 1998; Thompson & MacDonald 1999; Kim et al. 2000; Nummelin et al. 2000; Lee et al. 2001; Schilke et al. 2001; White et al. 2003; Comito et al. 2005; Kim et al. 2006; Belloche et al. 2007; Olofsson et al. 2007; Tercero et al. 2010). The line densities usually range from 10 to 20 lines per GHz, i.e. have value comparable to the present survey. SgrB2 appears as a noticeable exception, displaying significantly higher line densities, as high as 100 lines per GHz in the 3 mm range observed with IRAM (Belloche et al. 2007) or 40 lines per GHz in the 1 mm range observed with SEST (Nummelin et al. 1998, 2000). Interestingly, the slope of –0.9 that we observe for the cumulative number of lines versus flux threshold is identical to the slopes observed by Schilke et al. (2001), White et al. (2003), and Comito et al. (2005) in their submillimeter surveys of Orion-KL.

In conclusion, our survey in terms of molecular content has a richness comparable to that of hot cores and confirms that the high abundance of deuterated isotopologues, which are easily detected for a number of species, is a distinctive characteristic of low mass protostars.

6.2. Kinematical types and associated components

As mentioned in the Introduction, IRAS 16293 is formed by a proto-binary system surrounded by an infalling envelope. In addition, multiple outflows originate in the system (e.g. Castets et al. 2001). Before attempting to interpret the observations of Sect. 5.3 and, specifically, the meaning of the four kinematical types of Table 6, based on the line rest velocities and widths, we review what is known so far about the envelope and the proto-binary system.

6.2.1. Envelope

The envelope extends for 6000–7000 AU in radius, equivalent to about 100″ in diameter, and is relatively massive (~2 $M_\odot$) (Crimier et al. 2010). At the border of the envelope, the dust temperature is ~13 K and the density is ~10^5 cm^{-3}. The dust temperature reaches 100 K at a radius 75–86 AU, where the density is (2–3) × 10^8 cm^{-3}, creating the region called hot corino. The rest velocity of the cold envelope has been measured in several studies and is ~3.9 km s^{-1} (Mizuno et al. 1990; Bottinelli et al. 2004; Takakuwa et al. 2007). Molecules probing the cold envelope have ~2 km s^{-1} line widths.

6.2.2. Proto-binary system

Several interferometric studies have been carried out in the past to characterize the nature of the two sources, A (south-east) and B (north-west), forming the binary system (Kuan et al. 2004; Bottinelli et al. 2004; Chandler et al. 2005; Bisschop et al. 2008; see also references in Table 7). Some species are associated only or predominantly with one of the two sources A and B, and others are observed in both sources. All studies

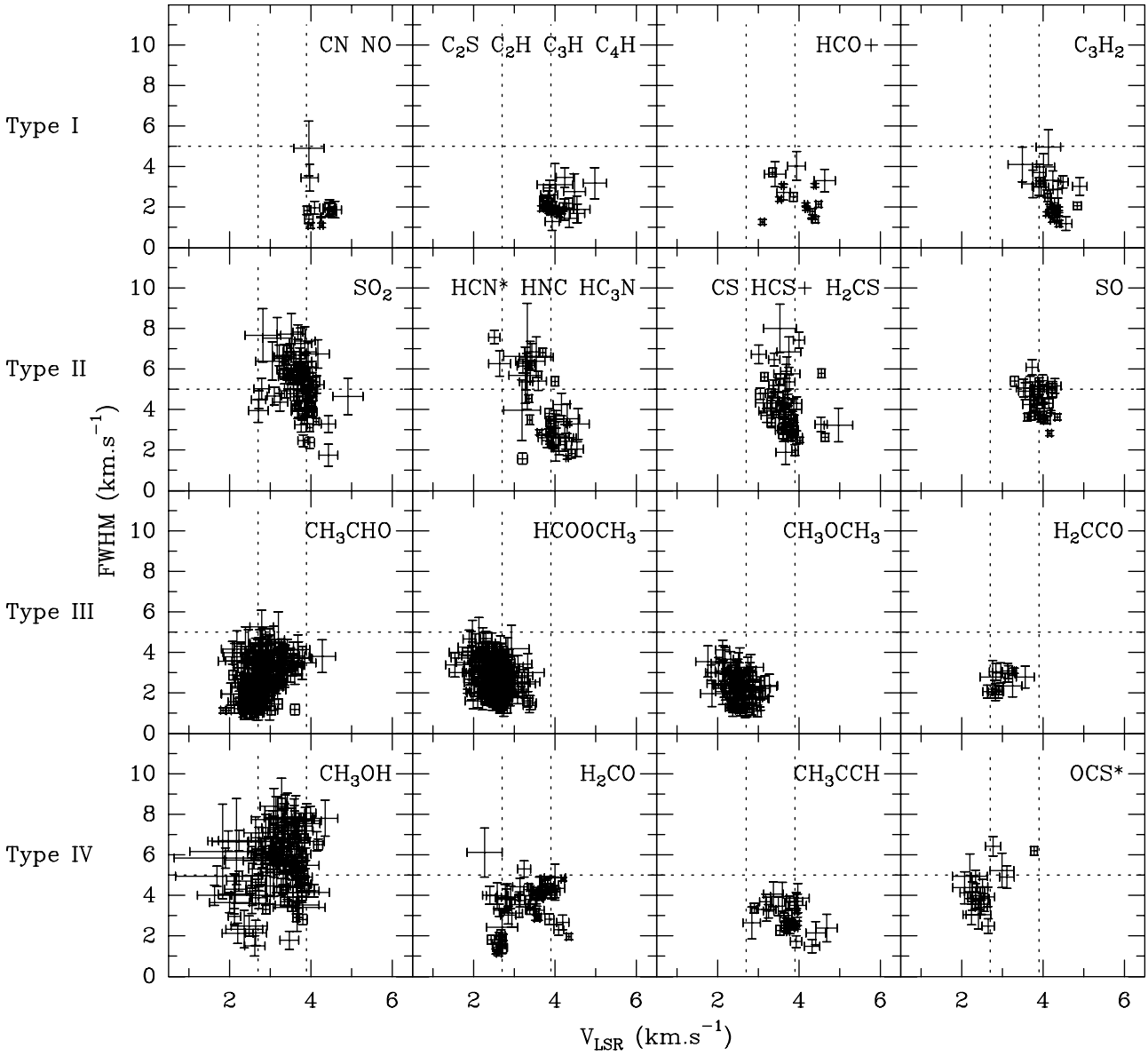

Fig. 5. Plots of the rest velocity $v_{\rm LSR}$ versus the *FWHM*, derived from the Gaussian fits of the lines (Table 4). All the detected species and the relevant isotopologues of Table 5 are plotted, except those in which the lines have obviously non-Gaussian profiles (see text). In particular, the labels HCN* and OCS* mean that the main isotopologues of these species are not included, because of their non-Gaussian profiles. The one-σ error bars include fit and spectral resolution uncertainties. The vertical lines at $v_{\rm LSR} = 2.7$ and 3.9 km s^{-1} correspond to the velocity of the components B and A, respectively (see Sect. 6). The horizontal line at 5 km s^{-1} corresponds approximatively to the average of the line *FWHM* range.

agree in measuring broader lines towards A (~8 km s^{-1}) than B (~3 km s^{-1}). However, the rest velocity of the molecular emission in the two objects is more uncertain: there is some evidence that the two objects have different rest velocities (higher in source A than in source B), but this difference might also be due to absorption by the envelope according to Chandler et al. (2005) or self-absorption in optically thick lines from source B according to Bottinelli et al. (2004); Kuan et al. (2004) also report velocities that are somewhat higher in source A than source B, with a dispersion larger than 2.5 km s^{-1} in the values for all species. According to Bisschop et al. (2008), both sources A and B show emission at velocities between 1.5 and 2.5 km s^{-1}; Huang et al. (2005) mention two velocity components at 1.5 and 4.5 km s^{-1} for source A and show emission from B peaking at ~2 km s^{-1}. We note that all these studies use moderate spectral resolutions (~1 km s^{-1}), deal with a small number of lines (often only one) for each species and, in some cases, suffer from poor S/N for the weakest lines.

Table 7 summarizes, for each of the species classified according to their kinematical type in Table 6, the results of interferometric observations towards the three components of IRAS 16293 (sources A and B and the envelope).

6.2.3. Interpretation of the kinematical types

On the basis of published interferometric observations, each species is assigned to one or two of the three components (source A, B, and the envelope). For example, CN displays type I kinematical characteristics ($v_{\rm LSR} \sim 4$ km s^{-1} and $FWHM \sim 2$ km s^{-1}) and has only found to be associated with the envelope and was not detected in any of the two sources A and B.

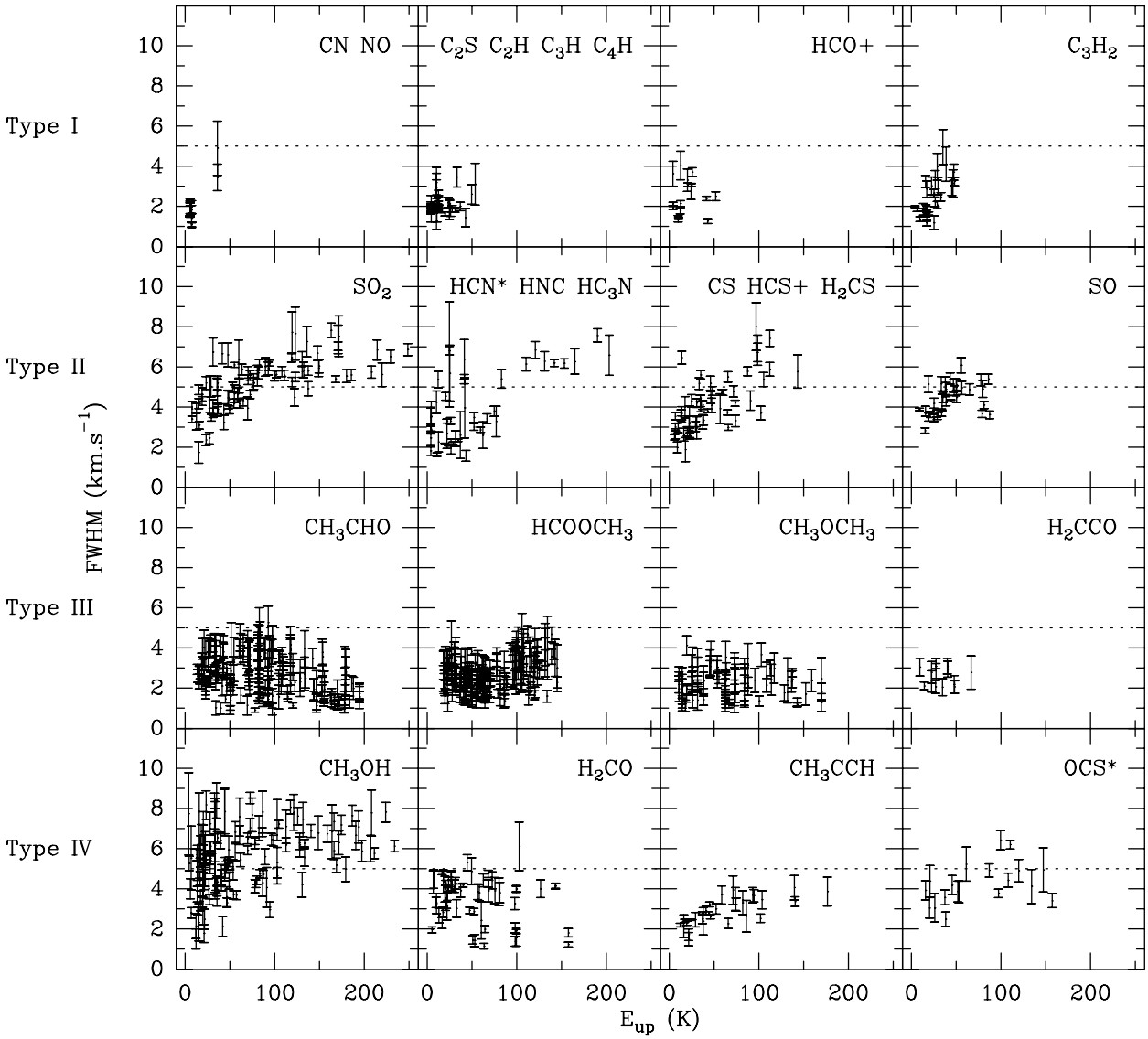

Fig. 6. Plots of the linewidth, *FWHM*, versus the energy of the upper level of the transition, E_{up}. The species are grouped as in Fig. 5. All the detected species and the relevant isotopologues of Table 5 are plotted, except those in which the lines obviously have non-Gaussian profiles (see text). In particular, the labels HCN* and OCS* mean that the main isotopologues of these species are not included, because of their non-Gaussian profiles. The one-σ error bars include fit and spectral resolution uncertainties. The horizontal line at 5 km s^{-1} corresponds approximatively to the average of the line *FWHM* range.

In contrast, CH_3CHO has the characteristics of the type III behavior (v_{LSR} = 2.5–3 km s^{-1} and $FWHM \leq 4$ km s^{-1}) and has only been detected in the direction of source B. Some species of Table 6 (C_2H, C_3H, C_4H, C_2S, NO, HNC, HCS^+, and CS) have not been observed with interferometers, to the best of our knowledge, so are not reported in Table 7. The correspondence between the four types of Table 6 and the interferometric observations presented in Table 7 suggests that the species belonging to the same kinematical type are associated with a spatially different source: envelope (type I), source A (type II), source B (type III), and a mix of the three previous components (type IV). We note that the distribution of molecules in four kinematical types is not an artifact or a bias caused by the survey pointing, which detects more emission from source B than source A at higher frequencies. Even excluding all lines observed at IRAM-30 m or JCMT-15 m telescopes with a HPBW larger than 14″, i.e. all lines with frequencies higher than 200 GHz, the v_{LSR} versus *FWHM* plots and the *FWHM* versus E_{up} plots show the same behavior.

1. Type I corresponds to molecules abundant in the cold envelope of IRAS 16293. We cannot exclude that these species also emit in the densest parts of sources A and B but that this emission is strongly absorbed by the gas in the envelope. NO, which shows two broad and relatively bright lines with E_{up} = 36 K, bright narrow lines with E_{up} = 7 K and barely detected lines with E_{up} = 19 K (not included in this paper), might be an example of this situation, which deserves a detailed excitation study to come. The 343.8 GHz line associated with source B was identified by Kuan et al. (2004) as the C_3H_2 $23_{13,10}$–$23_{12,11}$ transition(E_{low} = 790 K) but the CH_3CHO $18_{2,17}$–$17_{2,16}$ transition (with E_{up} = 166 K) seems a more reasonable identification.
2. Type II identifies molecules prevalently associated with source A. A few exceptions, for which emission from source B is mentioned in the literature, deserve some attention. The identification by Huang et al. (2005) of a line to $SO_2(v_2 = 1)$ associated with source B is also questionable given the very high upper energy level (E_{low} = 1800 K) of the transition, as

Table 7. Correspondence between kinematical types and spatial distributions derived from interferometric observations.

Type	Source A	Source B	Envelope	Refs.
Type I		(C_3H_2)	CN	B2004
	HCN	(HCN)		T2007
	HCN			H2005
	HC_3N			C2005
	SO	(SO)		C2005
Type II	SO			H2005
	SO_2			C2005
	SO_2	(SO_2)		H2005
	H_2CS	(H_2CS)		H2005
				K2004
		CH_3CHO		B2008
		CH_3OCH_3		C2005
	(CH_3OCH_3)	CH_3OCH_3		H2005
		H_2CCO		K2004
Type III	(H_2CCO)	H_2CCO		B2008
		$HCOOCH_3$		R2006
	$HCOOCH_3$	($HCOOCH_3$)		B2004
	$HCOOCH_3$	$HCOOCH_3$		K2004
	$HCOOCH_3$			C2005
	CH_3OH			C2005
	CH_3OH	CH_3OH		K2004
Type IV	H_2CO	H_2CO		S2004
	H_2CO	H_2CO		C2005
	OCS	OCS		H2005

Notes. The first column reports the kinematical type of the species according to the definition given in Table 6. Columns 2–4 report where the species has been detected: source A, B and envelope respectively. The species in parenthesis means that weaker emission has also been observed in the relevant component or that they are questionable identifications (see text). Last column reports the interferometric observations references; B2004: Bottinelli et al. (2004); B2008: Bisschop et al. (2008); C2005: Chandler et al. (2005); H2005: Huang et al. (2005); K2004: Kuan et al. (2004); R2006: Remijan & Hollis (2006); S2004: Schöier et al. (2004); T2007: Takakuwa et al. (2007).

is the attribution by Huang et al. (2005) of H_2CS emission to source B, as no map is shown for this species. Finally, SO emission is rather extended and associated with both sources A and B (Chandler et al. 2005). It is possible that part of the line broadening is due to wings associated with the outflow, whereas the bulk of the emission is associated with the cold envelope (which would instead make SO a species of type I). In addition, without detailed excitation models to be presented in subsequent studies, it is not possible to exclude that, for some type II species, the cold envelope contributes to the emission observed at low E_{up} and small *FWHM*.

3. Type III species have lines that are prevalently emitted by source B. $HCOOCH_3$, which has been observed in both source A and B appears as a notable exception. Excitation modeling of this species will be discussed in detail in a subsequent paper. Several qualitative arguments may already explain why no lines with type II characteristics are present in this study: (i) as the lines emitted by the source A are much broader than the lines emitted by the source B, whose lines display a higher percentage of blending with nearby lines excluding them from this study; (ii) in our large beam observations, emission from sources A and B are superposed; the narrow lines emitted from the source B appear "on top of the" broad lines emitted by the source A and are, thus, more easily detected; (iii) this second effect is enhanced by the pointing towards the source B.
4. Type IV species are a mixed bag. The species are present in both sources A and B and, sometimes, even in the envelope. Depending on the intensity contribution, the lines can have a low or high v_{LSR} and *FWHM*. Therefore, type IV species are not associated with any specific component.

Using the kinematic properties of the lines, we were able to identify general trends depending on whether the emission of the species originates in source A or B, although both sources are included in our single dish observations. Despite the kinematic differences being small, for example a difference in the v_{LSR} of not more than 1.5 km s^{-1}, we were able to draw a general picture thanks to the large number of detected lines.

6.3. The dynamics of sources A and B

Identified where the emission from the various species originates helps us to clarify the nature of sources A and B. As noted in several previous works, A and B have apparently different chemical compositions: source B is brighter in complex organic molecules, while source A is brighter in simpler S- and N-bearing molecules (see Table 7). Furthermore, the *FWHM* of the lines arising in source A are broader than in source B.

Our analysis established two additional properties that had previously not been recognized (see discussion in Sect. 6.1): i) the two sources have different velocities (v_{LSR}) and ii) in the source A, the *FWHM* of the lines increases with increasing upper level energy (Fig. 6) whereas it remains constant in the source B.

For the linewidth behavior, a related effect, the increase in *FWHM* with the excitation temperature, had already been observed by Schöier et al. (2002), but this represents a less direct probe of the gas kinematics, as it relied on modeling assumptions to derive the excitation temperatures. The increase in the line *FWHM* with increasing excitation has been interpreted in two ways: either it is caused by infalling gas onto the accreting protostellar object (Ceccarelli et al. 2003), or shocks caused by jet/wind interaction with the inner dense envelope (Schöier et al. 2002; Jørgensen et al. 2002). The two interpretations predict different molecular emission distributions. However, the existing maps do not allow us to distinguish these interpretations. In addition, to reliably differentiate between these two interpretations we would need to perform a detailed modeling of the source that is beyond the scope of this paper. At this stage, it can simply be said that the interpretation of the infalling gas (Ceccarelli et al. 2000b) would lead to reasonable estimates of source A and B central masses: for optically thin emission, the free-fall velocity may be estimated from the linewidth, assuming that the *FWHM* includes quadratically a turbulent width δ_{th} and the free-fall broadening; its analytic expression yields the following expression of the core mass, where the widths are expressed in km s^{-1} and the radius r in AU.

$$M(M_\odot) = 1.4 \times 10^{-4}(FWHM^2 - \delta_{th}^2)r. \quad (2)$$

Assuming that the turbulent width in the A and B core external layers is close to that of the envelope static gas, we derive $\delta_{th} \sim 2$ km s^{-1} from the type I species linewidths. According to the interferometric observations of type II and type III species reported in Table 7, both sources show a radius of ~1.5″ (i.e. 180 AU at a distance of 120 pc). For core A, typical *FWHM* larger than ~6 km s^{-1} lead to a central mass of at least 0.8 $M_\odot$, whereas for core B, where the *FWHM* is smaller than ~3 km s^{-1}, the central mass cannot exceed 0.1 $M_\odot$. This assumes that the

linewidths are due to collapsing envelopes rather than rotating disks. If they were, in contrast, due to rotating disks, one would have to take into account the (unknown) inclination angle. The available interferometer observations, which are barely able to spatially resolve the core A only (Bottinelli et al. 2004), do not allow us to distinguish between these two possibilities. In the following, we restrict the discussion to the infalling envelopes, for simplicity, but our conclusions are also largely applicable to the disk case.

The difference between the $v_{\rm LSR}$ of both sources can be interpreted in the following way: the source B rotates around its companion, source A; for a distance of 480 AU between cores A and B, and a core A mass of 0.8 $M_\odot$, the rotation velocity of core B is 1.2 km s^{-1}. The observed difference between A and B velocities ($v_{\rm LSR}$ of 3.9 and 2.7 km s^{-1} respectively) is thus perfectly consistent with this picture. Bottinelli et al. (2004) already discussed this possibility but did not have enough evidence to state that it was more likely than another hypothesis where the line kinematical properties reflect opacity effects. The large number of lines and species observed in our survey allows us to investigate the source dynamics.

7. Conclusions

We have presented an unbiased spectral survey of the 3, 2, 1, and 0.9 mm bands accessible from ground towards the class 0 source IRAS 16293. We used the IRAM-30 m and JCMT-15 m telescopes, performing about 300 h of observations. This is the most sensitive survey ever published in these bands towards a solar-type protostar.

The data have been released for public use in two CLASS files, which can be retrieved on the TIMASSS web site[8]. The site also contains two accompanying files (reported in the on line material) providing information about the calibration of the single receiver settings, obtained by comparing the survey lines with previously obtained observations.

The line density, ~20 lines/GHz, appears to be as high as in comparable surveys obtained towards high mass protostars (with the exception of SgrB2). More than one thousand unblended lines with $S/N \geq 3$ and upper energy levels lower than 250 K have been identified by comparing with the JPL and CDMS catalogs. They correspond to 32 chemically distinct species, a chemical richness comparable to those of hot cores. The identification of 37 additional rare isotopologues and, specifically, numerous D-bearing molecules confirm that IRAS 16293 has a remarkably high abundance of deuterated species. The 3 mm – 0.9 mm spectra are dominated by relatively simple molecules (CO, SO, H_2CO, SO_2, and CH_3OH). However, the numerous weaker lines emitted by larger molecules account to at least as much as the CO integrated line intensities.

The analysis of the profiles of this large set of identified lines, and specifically the central velocities and widths, provides clues to help us identify where each emission predominantly originates: cold envelope (narrow lines at $V_{\rm LSR} \simeq 3.9$ km s^{-1}), source A (broader lines at $V_{\rm LSR} \simeq 3.9$ km s^{-1}), and source B (narrow lines at $V_{\rm LSR} \simeq 2.7$ km s^{-1}). Furthermore, in source A, the line widths increase with the upper energy level of the transition. If this behavior is interpreted as being caused by gas infalling towards a central object, the core A mass is ~1 $M_\odot$ and the smaller line widths observed towards source B set an upper limit to the mass of this source, ≤0.1 $M_\odot$. The observed difference in the $V_{\rm LSR}$, ~1.2 km s^{-1}), is consistent with the source B rotating around the more massive source A. From a chemical point of view, the source B shows predominant emission from O-bearing complex molecules whereas N- and S-bearing molecules are strong emitters in the source A. To derive reliable estimates of the corresponding chemical abundances, it will be necessary to carry out careful radiative transfer modeling, which we intend to present in future articles.

[8] http://www-laog.obs.ujf-grenoble.fr/heberges/timasss/

Acknowledgements. We are deeply thankful to the IRAM staff and the successive TACs, and particularly to Clemens Thum, for his help in preparing and programming the observations at the IRAM-30 m telescope. We gracefully thank the JCMT staff, particularly Remo Tilanus and Jim Hogh, who were always able to quickly resolve problems. We thank Laurent Pagani for fruitful discussions about calibration problems. We are very thankful to the molecular databases JPL and CDMS, which were largely used for the work presented here as to the spectroscopic groups providing the data. This work has been supported by l'Agence Nationale pour la Recherche (ANR), France (contracts ANR-08-BLAN-022) and by the Ministère de la Recherche Scientifique et Université J. Fourier de Grenoble, France (PPF WAGOS). Finally, we warmly thanks the referee, Dr, J. Cernicharo, and the editor, Dr. M. Walmsley, who contributed to improve a lot this paper with numerous helpful comments.

References

Belloche, A., Comito, C., Hieret, C., et al. 2007, in Molecules in Space and Laboratory
Belov, S. 1995, J. Mol. Spect., 173, 380
Belov, S. P., Tretyakov, M. Y., Kozin, I. N., et al. 1998, J. Mol. Spect., 191, 17
Bergin, E. A., Phillips, T. G., Comito, C., et al. 2010, A&A, 521, L20
Bisschop, S. E., Jørgensen, J. K., Bourke, T. L., Bottinelli, S., & van Dishoeck, E. F. 2008, A&A, 488, 959
Blake, G. A., van Dishoek, E. F., Jansen, D. J., Groesbeck, T. D., & Mundy, L. G. 1994, ApJ, 428, 680
Bogey, M., Demuynck, C., & Destombes, J. L. 1985, A&A, 144, L15
Bogey, M., Demuynck, C., Destombes, J. L., & Dubus, H. 1987, J. Mol. Spect., 122, 313
Bocquet, R., Demaison, J., Cosléou, J., et al. 1999, J. Mol. Spect., 195, 345
Bogey, M., Civiš, S., Delcroix, B., et al. 1997, J. Mol. Spect., 182, 85
Bottinelli, S., Ceccarelli, C., Neri, R., et al. 2004, ApJ, 617, L69
Bottinelli, S., Ceccarelli, C., Williams, J. P., & Lefloch, B. 2007, A&A, 463, 601
Brown, R. D., Godfrey, P. D., McNaughton, D., & Yamanouchi, K. 1987, Mol. Phys., 62, 1429
Brünken, S., Fuchs, U., Lewen, F., et al. 2004, J. Mol. Spect., 225, 152
Brünken, S., Müller, H. S. P., Thorwirth, S., Lewen, F., & Winnewisser, G. 2006, J. Mol. Struct., 780, 3
Butner, H. M., Charnley, S. B., Ceccarelli, C., et al. 2007, ApJ, 659, L137
Camy-Peyret, C., Flaud, J., Lechuga-Fossat, L., & Johns, J. W. C. 1985, J. Mol. Spect., 109, 300
Carvajal, M., Margulès, L., Tercero, B., et al. 2009, A&A, 500, 1109
Castets, A., Ceccarelli, C., Loinard, L., Caux, E., & Lefloch, B. 2001, A&A, 375, 40
Cazaux, S., Tielens, A. G. G. M., Ceccarelli, C., et al. 2003, ApJ, 593, L51
Cazzoli, G., & Puzzarini, C. 2005, J. Mol. Spect., 233, 280
Cazzoli, G., & Puzzarini, C. 2008, A&A, 487, 1197
Cazzoli, G., Puzzarini, C., & Lapinov, A. V. 2004, ApJ, 611, 615
Cazzoli, G., Puzzarini, C., & Gauss, J. 2005, ApJS, 159, 181
Cazzoli, G., Cludi, L., & Puzzarini, C. 2006, J. Mol. Struct., 780, 260
Ceccarelli, C. 2007, in Molecules in Space and Laboratory
Ceccarelli, C., Castets, A., Loinard, L., Caux, E., & Tielens, A. G. G. M. 1998, A&A, 338, L43
Ceccarelli, C., Castets, A., Caux, E., et al. 2000a, A&A, 355, 1129
Ceccarelli, C., Loinard, L., Castets, A., Tielens, A. G. G. M., & Caux, E. 2000b, A&A, 357, L9
Ceccarelli, C., Maret, S., Tielens, A. G. G. M., Castets, A., & Caux, E. 2003, A&A, 410, 587
Ceccarelli, C., Bacmann, A., Boogert, A., et al. 2010, A&A, 521, L22
Chandler, C. J., Brogan, C. L., Shirley, Y. L., & Loinard, L. 2005, ApJ, 632, 371
Chen, W., Novick, S. E., McCarthy, M. C., Gottlieb, C. A., & Thaddeus, P. 1995, J. Chem. Phys., 103, 7828
Cho, S., & Saito, S. 1998, ApJ, 496, L51
Clouthier, D. J., Huang, G., Adam, A. G., & Merer, A. J. 1994, J. Chem. Phys., 101, 7300
Comito, C., Schilke, P., Phillips, T. G., et al. 2005, ApJS, 156, 127
Crimier, N., Ceccarelli, C., Maret, S., et al. 2010, A&A, 519, A65

Crovisier, J., Biver, N., Bockelée-Morvan, D., et al. 2004, in Planetary Systems in the Universe, ed. A. Penny, IAU Symp., 202, 178
de Graauw, T., Helmich, F. P., Phillips, T. G., et al. 2010, A&A, 518, L6
Demyk, K., Mäder, H., Tercero, B., et al. 2007, A&A, 466, 255
Dore, L., Puzzarini, C., & Cazzoli, G. 2001, Can. J. Phys., 79, 359
Fusina, L., di Lonardo, G., Johns, J. W. C., & Halonen, L. 1988, J. Mol. Spect., 127, 240
Goldsmith, P. F. 2001, ApJ, 557, 736
Golubiatnikov, G. Y., Lapinov, A. V., Guarnieri, A., & Knöchel, R. 2005, J. Mol. Spect., 234, 190
Guarnieri, A., & Huckauf, A. 2003, Z. Naturforsch, 58, 275
Hatchell, J., Thompson, M. A., Millar, T. J., & MacDonald, G. H. 1998, A&AS, 133, 29
Helmich, F. P., & van Dishoeck, E. F. 1997, A&AS, 124, 205
Herbst, E., & van Dishoeck, E. F. 2009, ARA&A, 47, 427
Huang, H., Kuan, Y., Charnley, S. B., et al. 2005, Adv. Space Res., 36, 146
Johns, J. W. C. 1985, J. Opt. Soc. Am. B Opt. Phys., 2, 1340
Jørgensen, J. K., Schöier, F. L., & van Dishoeck, E. F. 2002, A&A, 389, 908
Jørgensen, J. K., Lahuis, F., Schöier, F. L., et al. 2005, ApJ, 631, L77
Kim, E., & Yamamoto, S. 2003, J. Mol. Spect., 219, 296
Kim, H., Cho, S., Chung, H., et al. 2000, ApJS, 131, 483
Kim, S., Kim, H., Lee, Y., et al. 2006, ApJS, 162, 161
Klapper, G., Lewen, F., Gendriesch, R., Belov, S. P., & Winnewisser, G. 2001, Zeitschrift Naturforschung Teil A, 56, 329
Klapper, G., Surin, L., Lewen, F., et al. 2003, ApJ, 582, 262
Klaus, T., Saleck, A. H., Belov, S. P., et al. 1996, J. Mol. Spect., 180, 197
Kleiner, I., Lovas, F. J., & Godefroid, M. 1996, J. Phys. Chem. Ref. Data, 25, 1113
Klisch, E., Klaus, T., Belov, S. P., Winnewisser, G., & Herbst, E. 1995, A&A, 304, L5
Kuan, Y., Huang, H., Charnley, S. B., et al. 2004, ApJ, 616, L27
Kutner, M. L., & Ulich, B. L. 1981, ApJ, 250, 341
Lapinov, A. V., Golubiatnikov, G. Y., Markov, V. N., & Guarnieri, A. 2007, Astron. Lett., 33, 121
Lattanzi, V., Walters, A., Drouin, B. J., & Pearson, J. C. 2007, ApJ, 662, 771
Lee, C. W., Cho, S., & Lee, S. 2001, ApJ, 551, 333
Leguennec, M., Demaison, J., Wlodarczak, G., & Marsden, C. J. 1993, J. Mol. Spect., 160, 471
Lohilahti, J., & Horneman, V. 2004, J. Mol. Spect., 228, 1
Loinard, L., Castets, A., Ceccarelli, C., et al. 2000, A&A, 359, 1169
Loinard, L., Torres, R. M., Mioduszewski, A. J., & Rodríguez, L. F. 2008, ApJ, 675, L29
Lovas, F. J., & Suenram, R. D. 1982, J. Mol. Spect., 93, 416
Lovas, F. J., & Suenram, R. D. 1987, J. Chem. Phys., 87, 2010
Lovas, F. J., Suenram, R. D., Ogata, T., & Yamamoto, S. 1992, ApJ, 399, 325
MacDonald, G. H., Gibb, A. G., Habing, R. J., & Millar, T. J. 1996, A&AS, 119, 333
Maeda, A., De Lucia, F. C., & Herbst, E. 2008, J. Mol. Spect., 251, 293
Margulès, L., Lewen, F., Winnewisser, G., Botschwina, P., & Müller, H. S. P. 2003, Phys. Chem. Chem. Phys. (Incorporating Faraday Transactions), 5, 2770
Margulès, L., Motiyenko, R., Demyk, K., et al. 2009, A&A, 493, 565
Meerts, W. L., & Dymanus, A. 1972, J. Mol. Spect., 44, 320
Minowa, H., Satake, M., Hirota, T., et al. 1997, ApJ, 491, L63
Mizuno, A., Fukui, Y., Iwata, T., Nozawa, S., & Takano, T. 1990, ApJ, 356, 184
Mollaaghababa, R., Gottlieb, C. A., Vrtilek, J. M., & Thaddeus, P. 1993, J. Chem. Phys., 99, 890
Müller, H. S. P., Farhoomand, J., Cohen, E. A., et al. 2000a, J. Mol. Spect., 201, 1
Müller, H. S. P., Gendriesch, R., Lewen, F., & Winnewisser, G. 2000b, Zeitschrift Naturforschung Teil A, 55, 486
Müller, H. S. P., Gendriesch, R., Margulès, L., et al. 2000c, Phys. Chem. Chem. Phys. (Incorporating Faraday Transactions), 2, 3401
Müller, H. S. P., Winnewisser, G., Demaison, J., Perrin, A., & Valentin, A. 2000d, J. Mol. Spect., 200, 143
Müller, H. S. P., Thorwirth, S., Roth, D. A., & Winnewisser, G. 2001, A&A, 370, L49
Müller, H. S. P., Menten, K. M., & Mäder, H. 2004, A&A, 428, 1019
Müller, H. S. P., Schlöder, F., Stutzki, J., & Winnewisser, G. 2005, J. Mol. Struct., 742, 215
Müller, H. S. P., Drouin, B. J., & Pearson, J. C. 2009, A&A, 506, 1487
Mundy, L. G., Wootten, A., Wilking, B. A., Blake, G. A., & Sargent, A. I. 1992, ApJ, 385, 306
Neustock, W., Guarnieri, A., & Demaison, G. 1990, Z. Naturforsch, 45, 702
Nummelin, A., Bergman, P., Hjalmarson, A., et al. 1998, ApJS, 117, 427
Nummelin, A., Bergman, P., Hjalmarson, Å., et al. 2000, ApJS, 128, 213
Olofsson, A. O. H., Persson, C. M., Koning, N., et al. 2007, A&A, 476, 791
Padovani, M., Walmsley, C. M., Tafalla, M., Galli, D., & Müller, H. S. P. 2009, A&A, 505, 1199
Parise, B., Ceccarelli, C., Tielens, A. G. G. M., et al. 2002, A&A, 393, L49
Parise, B., Castets, A., Herbst, E., et al. 2004, A&A, 416, 159
Parise, B., Caux, E., Castets, A., et al. 2005a, A&A, 431, 547
Parise, B., Ceccarelli, C., & Maret, S. 2005b, A&A, 441, 171
Pech, G., Loinard, L., Chandler, C. J., et al. 2010, ApJ, 712, 1403
Pickett, H. M., Poynter, I. R. L., Cohen, E. A., et al. 1998, J. Quant. Spect. Rad. Transf., 60, 883
Pilbratt, G. L., Riedinger, J. R., Passvogel, T., et al. 2010, A&A, 518, L1
Pizzarello, S., & Huang, Y. 2005, Geochim. Cosmochim. Acta, 69, 599
Remijan, A. J., & Hollis, J. M. 2006, ApJ, 640, 842
Schilke, P., Groesbeck, T. D., Blake, G. A., & Phillips, T. G. 1997, ApJS, 108, 301
Schilke, P., Benford, D. J., Hunter, T. R., Lis, D. C., & Phillips, T. G. 2001, ApJS, 132, 281
Schmid-Burgk, J., Muders, D., Müller, H. S. P., & Brupbacher-Gatehouse, B. 2004, A&A, 419, 949
Schöier, F. L., Jørgensen, J. K., van Dishoeck, E. F., & Blake, G. A. 2002, A&A, 390, 1001
Schöier, F. L., Jørgensen, J. K., van Dishoeck, E. F., & Blake, G. A. 2004, A&A, 418, 185
Spahn, H., Müller, H. S. P., Giesen, T. F., et al. 2008, Chem. Phys., 346, 132
Takakuwa, S., Ohashi, N., Bourke, T. L., et al. 2007, ApJ, 662, 431
Tercero, B., Cernicharo, J., Pardo, J. R., & Goicoechea, J. R. 2010, A&A, 517, A96
Thompson, M. A., & MacDonald, G. H. 1999, A&AS, 135, 531
Thorwirth, S., Müller, H. S. P., Lewen, F., Gendriesch, R., & Winnewisser, G. 2000a, A&A, 363, L37
Thorwirth, S., Müller, H. S. P., & Winnewisser, G. 2000b, J. Mol. Spect., 204, 133
Thorwirth, S., Müller, H. S. P., Lewen, F., et al. 2003, ApJ, 585, L163
van der Tak, F. F. S., Müller, H. S. P., Harding, M. E., & Gauss, J. 2009, A&A, 507, 347
van Dishoeck, E. F., Blake, G. A., Jansen, D. J., & Groesbeck, T. D. 1995, ApJ, 447, 760
Wakelam, V., Castets, A., Ceccarelli, C., et al. 2004, A&A, 413, 609
White, G. J., Araki, M., Greaves, J. S., Ohishi, M., & Higginbottom, N. S. 2003, A&A, 407, 589
Winnewisser, G., Belov, S. P., Klaus, T., & Schieder, R. 1997, J. Mol. Spect., 184, 468
Wootten, A. 1989, ApJ, 337, 858
Xu, L., & Lovas, F. J. 1997, J. Phys. Chem. Ref. Data, 26, 17
Yamamoto, S., & Saito, S. 1994, J. Chem. Phys., 101, 5484

Pages 15 to 41 are available in the electronic edition of the journal at http://www.aanda.org

Table 2. Comparison of the spectral survey lines with previous observations.

Setting number	Species	Transition	Freq. (MHz)	$\int T_A^* dv$ (K km s^{-1})		Ref.
				survey	prev. obs.	
2	HDO	$1_{10} - 1_{11}$	80578	0.507	0.4	(6)
11*	CH_3CCH	$5_2 - 4_2$	85450	0.188	0.18	(3)
11*	CH_3CCH	$5_1 - 4_1$	85455	0.411	0.5	(3)
11*	CH_3CCH	$5_0 - 4_0$	85457	0.524	0.54	(3)
14*	$H^{13}CO^+$	1 – 0	86754	4.351	3.97	(12)
14*	$H^{13}CO^+$	1 – 0	86754	4.351	4.56	(13)
14*	SiO	2 – 1	86846	1.910	1.9	(4)
14*	SiO	2 – 1	86846	1.910	2.04	(12)
14*	SiO	2 – 1	86846	1.910	2.23	(14)
14*	SiO	2 – 1	86846	1.910	2.16	(15)
19	HCO^+	1 – 0	89188	15.195	13.93	(13)
19	CH_2DOH	$2_{02} - 1_{01}$ o_1	89251	0.182	0.19	(10)
19	CH_2DOH	$2_{02} - 1_{01}$ e_0	89407	0.262	0.31	(10)
21	CH_3OCHO-E	$8_{08} - 7_{07}$	90227	0.164	0.15	(3)
21	CH_3OCHO-A	$8_{08} - 7_{07}$	90229	0.144	0.11	(3)
36	^{34}SO	$3_2 - 2_1$	97715	0.791	1	(4)
38	CH_3OCHO-A	$8_{45} - 7_{44}$	98682	0.248	0.22	(3)
38	CH_3OCHO-E	$8_{45} - 7_{44}$	98711	0.118	0.14	(3)
60*	$C^{18}O$	1 – 0	109782	9.900	9.02	(16)
60*	$C^{18}O$	1 – 0	109782	9.900	7.35	(17)
60*	$C^{18}O$	1 – 0	109782	9.900	8.7	(13)
61*	CH_3CN	$6_{40} - 5_{40}$	110349	0.164	0.48	(3)
61*	CH_3CN	$6_{30} - 5_{30}$	110364	0.189	0.88	(3)
61*	CH_3CN	$6_{20} - 5_{20}$	110375	0.304	0.77	(3)
61*	CH_3CN	$6_{10} - 5_{10}$ / $6_{00} - 5_{00}$	110382	0.695	2.02	(3)
62	D_2CO	$2_{12} - 1_{11}$	110838	0.515	0.64	(15)
65	$C^{17}O$	1 – 0	112359	2.855	3.07	(16)
65	$C^{17}O$	1 – 0	112359	2.855	2.59	(17)
74	SiO	3 – 2	130268	1.361	4.86	(15)
74	SiO	3 – 2	130268	1.361	4.61	(14)
81	CH_3CHO-E	$7_{07} - 6_{06}$	133830	0.383	0.41	(3)
81	CH_3CHO-A	$7_{07} - 6_{06}$	133854	0.597	0.57	(3)
81	CH_2DOH	$3_{03} - 2_{02}$ o_1	133872	0.739	0.6	(10)
81	CH_2DOH	$3_{22} - 2_{21}$ o_1	133881	0.465	0.34	(10)
82	HDCO	$2_{11} - 1_{10}$	134284	1.466	1.8	(9)
82	HDCO	$2_{11} - 1_{10}$	134284	1.466	1.55	(15)
85	SO_2	$5_{15} - 4_{04}$	135696	3.115	4.6	(4)
85	SO_2	$5_{15} - 4_{04}$	135696	3.115	3.41	(12)
88	$H_2^{13}CO$	$2_{12} - 1_{11}$	137450	0.524	0.58	(9)
88	$H_2^{13}CO$	$2_{12} - 1_{11}$	137450	0.524	0.58	(15)
88	$H_2^{13}CO$	$2_{12} - 1_{11}$	137450	0.524	0.76	(15)
88	$H_2^{13}CO$	$2_{12} - 1_{11}$	137450	0.524	0.76	(15)
95	H_2CO	$2_{12} - 1_{11}$	140839	19.242	16.6	(9)
95	H_2CO	$2_{12} - 1_{11}$	140839	19.242	15.57	(15)
100	C_2H_5CN	$16_{5,12} - 15_{5,11}$ / $16_{5,11} - 15_{5,10}$	143406	0.256	0.55	(3)
101	CH_3OCH_3	$7_{3,4,2} - 7_{2,5,2}$	143600	0.107	0.42	(3)
101	CH_3OCH_3	$7_{3,4,1} - 7_{2,5,1}$	143603	0.414	0.31	(3)
101	CH_3OCH_3	$7_{3,4,0} - 7_{2,5,0}$	143606	0.189	0.28	(3)
146	CHD_2OH	$4_0 - 3_0$ e_0	166435	0.500	0.48	(10)
151	H_2S	$1_{10} - 1_{01}$	168762	17.511	17.5	(4)
282*	$H_2^{13}CO$	$3_{13} - 2_{12}$	206132	1.752	1.6	(9)
282*	$H_2^{13}CO$	$3_{13} - 2_{12}$	206132	1.752	1.97	(15)
282*	$H_2^{13}CO$	$3_{13} - 2_{12}$	206132	1.752	2.19	(15)
282*	$H_2^{13}CO$	$3_{13} - 2_{12}$	206132	1.752	2.48	(15)
282*	SO	$4_5 - 3_4$	206176	21.367	36	(15)
285*	CH_2DOH	$2_{12} - 3_{03}$ e_0	207780	0.690	1.01	(10)
292*	H_2CO	$3_{13} - 2_{12}$	211211	31.416	43.8	(9)
292*	H_2CO	$3_{13} - 2_{12}$	211211	31.416	33	(15)
292*	H_2CO	$3_{13} - 2_{12}$	211211	31.416	26.4	(16)
296	$H_2^{13}CO$	$3_{22} - 2_{21}$	213037	0.711	0.45	(15)
296	$H_2^{13}CO$	$3_{21} - 2_{20}$	213294	0.593	0.46	(15)
303	H_2S	$2_{20} - 2_{11}$	216710	7.436	3	(4)

Table 2. continued.

Setting number	Species	Transition	Freq. (MHz)	$\int T_A^* dv$ (K km s^{-1}) survey	prev. obs.	Ref.
304	SiO	5 – 4	217104	4.524	4.83	(14)
312	D_2CO	$4_{14} - 3_{13}$	221191	1.274	1.6	(9)
316	CH_2DOH	$5_{23} - 4_{14}$ e_1	223071	0.972	1.13	(10)
316	CH_2DOH	$5_{33} - 4_{32}$ o_1	223153	1.204	0.58	(10)
316	CH_2DOH	$5_{23} - 4_{22}$ e_1	223315	0.717	0.38	(10)
321	HDO	$3_{12} - 2_{21}$	225897	2.089	1.7	(6)
322	CH_3OCH_3	1413	226346	1.685	0.89	(3)
323	CH_3CHO-E	$12_{0,12} - 11_{0,11}$	226551	0.809	0.49	(3)
323	CH_3OCHO-E	$20_{2,18} - 19_{2,18}$	226713	1.540	1.19	(3)
323	CH_3OCHO-A	$20_{2,19} - 19_{2,18}$	226718	0.707	0.49	(3)
323	CH_3OCHO-A	$20_{1,19} - 19_{1,18}$	226778	1.324	0.84	(3)
332	D_2CO	$4_{04} - 3_{03}$	231410	3.334	2.43	(15)
332	D_2CO	$4_{04} - 3_{03}$	231410	3.334	2.01	(16)
332	D_2CO	$4_{04} - 3_{03}$	231410	3.334	1.92	(17)
332	D_2CO	$4_{04} - 3_{03}$	231410	3.334	2.69	(13)
332	D_2CO	$4_{04} - 3_{03}$	231410	3.340	3	(9)
332	CH_3CHO-A	$12_{48} - 11_{47}$	231457	0.520	0.51	(3)
342	D_2CO	$4_{22} - 3_{21}$	236102	1.718	1.86	(8)
342	D_2CO	$4_{22} - 3_{21}$	236102	1.718	1.9	(9)
342	D_2CO	$4_{22} - 3_{21}$	236102	1.710	1.9	(15)
353	HDO	$2_{11} - 2_{12}$	241561	2.268	2	(6)
363*	HDCO	$4_{14} - 3_{13}$	246925	2.067	8.43	(15)
363*	HDCO	$4_{14} - 3_{13}$	246925	2.067	7.6	(9)
401	HDO	$2_{20} - 3_{13}$	266161	0.214	0.21	(6)
434	$C^{18}O$	3 – 2	329335	55.768	33.6	(11)
436	$^{13}CH_3OH$	$7_{17} - 6_{16}$	330194	0.458	0.51	(5)
436	$^{13}CH_3OH$	$7_{34} - 6_{33}$	330408	1.123	0.91	(5)
437	^{13}CO	3 – 2	330588	55.854	67.2	(11)
446	HDCO	$5_{14} - 4_{13}$	335096	4.550	3.95	(2)
446	HDCO	$5_{14} - 4_{13}$	335097	4.550	4.5	(9)
450	$C^{17}O$	3 – 2	337061	12.481	11	(1)
450	CH_3OH	$3_3 - 4_2$ E^+	337136	0.826	1.05	(2)
452	H_2CS	$21_{1,10} - 9_{1,9}$	338081	1.723	2.4	(1)
455	^{34}SO	$8_9 - 7_8$	339858	3.863	2.98	(1)
461	D_2CO	$6_{06} - 5_{05}$	342522	1.875	1.9	(9)
461	CS	7 – 6	342883	38.535	51.4	(11)
462	$H_2^{13}CO$	$5_{15} - 4_{14}$	343325	3.181	1.37	(9)
464	SO	$8_8 - 7_7$	344311	18.647	18.1	(1)
470	SiO	8 – 7	347331	8.546	5.79	(1)
475	D_2CO	$6_{25} - 5_{24}$	349631	1.506	1	(9)
479	H_2CO	$5_{15} - 4_{14}$	351768	35.945	38.3	(9)
483	$H_2^{13}CO$	$5_{05} - 4_{04}$	353812	0.869	0.6	(9)
484	HCN	4 – 3	354505	41.068	63.4	11)
485	$H_2^{13}CO$	$5_{24} - 4_{23}$	354899	0.557	0.3	(9)
490	SO_2	$15_{4,12} - 15_{3,13}$	357241	3.603	3.29	(1)
490	SO_2	$11_{48} - 11_{39}$	357388	4.201	2.25	(1)
496	DCO^+	5 – 4	360170	3.135	4.02	(2)
501	HNC	4 – 3	362630	8.264	11.9	(11)
501	H_2CO	$5_{05} - 4_{04}$	362736	18.394	28.9	(9)
503	H_2CO	$5_{24} - 4_{23}$	363946	11.728	11.9	(9)

Notes. All observations are obtained with the same telescopes: IRAM 30 m from 80 to 280 GHz, JCMT from 328 to 366 GHz. The coordinates of the observed position are $\alpha(2000.0) = 16^h32^m22.6^m$, $\delta(2000.0) = -24°28'33''$; except for the settings numbers tagged with an asterisk that correspond to a slightly different position: $\alpha(2000.0) = 16^h32^m22.7^m$, $\delta(2000.0) = -24°22'13''$.

References. (1) Blake et al. (1994); (2) van Dishoeck et al. (1995); (3) Cazaux et al. (2003); (4) Wakelam et al. (2004); (5) Parise et al. (2004); (6) Parise et al. (2005a); (7) Butner et al. (2007); (8) Ceccarelli et al. (1998); (9) Loinard et al. (2000); (10) Parise et al. (2002); (11) Schöier et al. (2002), unpublished IRAM 30 m observations: (12) June 1997, (13) September 2000, (14) April 1998, (15) January 1999, (16) March 2000, (17) August 2000, (18) March 1998.

Table 3. Comparison of the strong spectral survey lines simultaneously observed with different backends.

Setting number	Frequency (MHz)	$\int T_A^* dv$ (K km s^{-1})		Setting number	Frequency (MHz)	$\int T_A^* dv$ (K km s^{-1})		Setting number	Frequency (MHz)	$\int T_A^* dv$ (K km s^{-1})	
		VESPA	FB			VESPA	FB			VESPA	FB
73	129515	2.436	3.091	105	145603	11.325	11.266	136	161172	0.501	0.367
74	130268	1.361	5.378	106	146368	2.447	1.604	137	161603	0.462	0.713
75	130892	0.506	0.290	107	146968	28.254	27.119	138	162186	0.340	0.302
76	131015	1.432	2.062	108	147174	3.356	3.312	139	162530	0.779	0.900
77	131885	1.103	1.042	109	147944	0.600	0.904	140	163119	1.409	1.142
78	132246	0.510	0.948	110	148112	1.802	1.816	140	163162	0.610	0.617
79	132891	1.429	2.186	111	148807	0.327	0.304	141	163753	2.187	2.047
80	133355	0.226	0.337	112	149022	0.764	0.563	142	164138	0.432	0.448
81	133786	3.012	1.995	113	149533	1.211	1.282	144	165048	1.493	1.987
82	134284	1.499	2.367	114	150142	1.232	1.140	144	165369	1.444	1.939
83	134897	1.358	0.798	115	150852	2.651	2.765	145	165677	2.606	1.283
84	135298	1.361	2.372	116	151378	1.399	1.898	146	166167	2.838	2.476
85	135696	3.131	4.058	117	151861	0.627	1.278	147	166896	2.483	2.226
86	136464	1.975	1.792	119	152609	2.889	2.860	149	167909	3.481	3.193
87	136635	1.459	1.313	120	153282	1.263	1.175	150	168087	0.622	0.636
88	137450	0.512	0.868	121	153865	1.525	1.792	150	168092	0.576	0.584
89	137903	0.769	0.821	122	154426	1.347	1.227	151	168762	17.648	18.619
90	138178	16.594	18.887	123	154657	1.652	1.948	152	169114	2.601	2.574
91	138739	1.716	1.647	124	155321	1.468	1.111	153	169743	0.399	0.561
92	139484	1.490	1.696	125	155507	1.066	1.048	154	170268	2.965	3.644
94	140306	2.451	2.967	126	156128	1.296	1.337	155	170691	0.737	0.726
95	140839	18.764	15.396	127	156602	2.266	1.967	156	171183	1.604	2.101
96	141244	0.451	0.569	128	157246	1.859	2.994	157	171688	1.454	1.553
97	141984	0.537	0.502	129	157599	0.517	0.417	158	172181	18.028	14.817
98	142379	0.594	0.711	130	158108	2.840	3.706	159	172678	5.176	5.507
99	142769	0.628	0.495	130	158200	2.105	2.313	160	173506	7.830	8.033
100	143057	2.545	2.622	131	158972	13.990	11.328	161	173687	6.316	7.010
101	143866	2.455	2.390	132	159439	0.695	0.719	162	174345	1.860	1.973
102	144077	5.405	6.935	133	159777	0.594	1.009	163	174663	2.927	2.708
103	144616	4.056	3.609	134	160343	2.371	2.091				
104	145103	3.614	5.050	135	160828	4.805	4.875				

Notes. The two backends used in the 129–175 GHz range were the VESPA autocorrelator (0.32 MHz resolution) and the 1 MHz resolution Filter Banks (FB).

Table 4. Identified non-blended lines. The line characteristics are derived from Gaussian fits.

TAG	Species & Transition	Frequency (MHz)	E_{up} (K)	A_{ij} s^{-1}	V_o (km s^{-1})	δ_{V_o}	$FWHM$ (km s^{-1})	δ_{FWHM}	Int (K)	δ_{Int}	Flux (K km s^{-1})	δ_{Flux}	Comments
28503	CO (1-0)	115271.20	5.53	7.20E-08	5.90	0.23	7.49	0.54	10.718	0.667	108.94	11.98	broad, wings
28503	CO (2-1)	230538.00	16.60	6.91E-07	5.23	0.39	10.00	0.92	10.405	0.826	189.77	32.26	broad, wings
28503	CO (3-2)	345795.99	33.19	2.50E-06	6.65	0.40	10.91	0.94	14.595	1.087	307.10	55.28	broad, wings
29501	^{13}CO (1-0)	110201.35	5.29	6.33E-08	4.34	0.06	2.82	0.14	3.148	0.135	11.92	1.31	small wings
29501	^{13}CO (2-1)	220398.68	15.87	6.07E-07	3.84	0.10	5.03	0.22	5.440	0.210	48.19	8.19	small wings
29501	^{13}CO (3-2)	330587.97	31.73	2.19E-06	3.63	0.47	4.55	1.13	6.493	1.377	55.92	10.07	wings
30502	C^{18}O (1-0)	109782.17	5.27	6.27E-08	3.92	0.03	2.19	0.06	3.362	0.081	9.88	1.09	
30502	C^{18}O (2-1)	219560.35	15.81	6.01E-07	3.57	0.04	3.28	0.10	4.842	0.131	27.88	4.74	
30502	C^{18}O (3-2)	329330.55	31.61	2.17E-06	3.67	0.13	3.22	0.30	4.891	0.396	29.79	5.36	self-abs
29006	C^{17}O (1-0)	112359.28	5.39	6.70E-08	4.24	0.25	4.45	0.60	0.511	0.059	3.07	0.34	self-abs
29006	C^{17}O (2-1)	224714.39	16.18	6.43E-07	3.62	0.02	3.66	0.05	1.576	0.020	10.32	1.75	
29006	C^{17}O (3-2)	337061.13	32.35	2.32E-06	3.66	0.09	3.15	0.22	2.010	0.121	12.07	2.17	self-abs
48501	SO (2_2-1_1)	86093.95	19.31	5.25E-06	4.03	0.09	3.50	0.20	0.804	0.041	3.63	0.4	small wings
48501	SO (2_3-1_2)	99299.87	9.23	1.13E-05	4.19	0.02	3.88	0.06	1.930	0.020	9.86	1.09	small wings
48501	SO (5_4-4_4)	100029.64	38.58	1.08E-06	4.14	0.10	4.30	0.23	0.191	0.009	1.09	0.12	wings
48501	SO (3_2-2_1)	109252.22	21.05	1.08E-05	4.35	0.06	3.63	0.15	0.449	0.016	2.19	0.24	
48501	SO (3_3-2_2)	129138.92	25.51	2.25E-05	4.09	0.08	3.46	0.18	2.361	0.108	11.39	1.94	
48501	SO (6_5-5_5)	136634.80	50.66	1.75E-06	4.23	0.11	5.11	0.27	0.200	0.009	1.44	0.25	
48501	SO (3_4-2_3)	138178.60	15.86	3.17E-05	3.92	0.11	3.79	0.25	3.069	0.174	16.50	2.81	
48501	SO (4_3-3_2)	158971.81	28.68	4.23E-05	3.96	0.08	3.57	0.18	2.594	0.113	13.74	2.34	
48501	SO (4_4-3_3)	172181.40	33.78	5.83E-05	4.00	0.08	3.72	0.18	3.161	0.131	18.00	3.06	
48501	SO (7_6-6_6)	174928.86	64.89	2.51E-06	3.78	0.11	4.89	0.28	0.257	0.012	1.94	0.33	
48501	SO (5_4-4_3)	206176.01	38.58	1.01E-04	3.99	0.12	4.89	0.33	2.489	0.098	20.49	3.48	
48501	SO (5_5-4_4)	215220.65	44.10	1.19E-04	4.00	0.02	4.31	0.05	2.919	0.024	21.76	3.70	
48501	SO (5_6-4_5)	219949.44	34.99	1.34E-04	3.86	0.10	4.48	0.26	4.467	0.210	35.18	5.98	
48501	SO (6_5-5_4)	251825.77	50.66	1.92E-04	3.80	0.10	4.49	0.27	3.066	0.144	27.27	4.64	
48501	SO (6_6-5_5)	258255.83	56.50	2.12E-04	4.21	0.12	4.96	0.33	2.139	0.093	21.58	3.67	
48501	SO (6_7-5_6)	261843.72	47.55	2.28E-04	4.23	0.10	4.83	0.24	4.960	0.202	49.49	8.41	
48501	SO (3_3-2_3)	339341.46	25.51	1.45E-05	3.77	0.09	4.19	0.25	3.391	0.149	27.20	4.92	
48501	SO (8_7-7_6)	340714.16	81.25	4.99E-04	3.78	0.07	4.10	0.18	3.886	0.133	30.54	5.50	wings
48501	SO (8_8-7_7)	344310.61	87.48	5.19E-04	3.61	0.07	3.62	0.19	2.539	0.104	17.71	3.19	wings
48501	SO (8_9-7_8)	346528.48	78.78	5.38E-04	3.71	0.07	3.66	0.18	4.665	0.179	32.93	5.93	wings
50501	^{34}SO (2_2-1_1)	84410.69	19.23	4.95E-06	3.91	0.17	5.14	0.42	0.038	0.003	0.25	0.04	
50501	^{34}SO (3_4-2_3)	135775.73	15.61	3.00E-05	4.16	0.05	2.83	0.13	0.321	0.012	1.28	0.22	
50501	^{34}SO (4_3-3_2)	155506.80	28.37	3.96E-05	3.86	0.08	3.68	0.18	0.201	0.009	1.09	0.19	
50501	^{34}SO (4_4-3_3)	168815.14	33.41	5.50E-05	4.29	0.15	5.17	0.36	0.212	0.017	1.49	0.26	
50501	^{34}SO (5_4-4_3)	201846.48	38.06	9.47E-05	3.52	0.18	5.07	0.44	0.217	0.015	1.83	0.31	
50501	^{34}SO (5_5-4_4)	211013.03	43.54	1.12E-04	3.99	0.12	5.42	0.28	0.199	0.010	1.85	0.32	
50501	^{34}SO (5_6-4_5)	215839.92	34.38	1.26E-04	3.67	0.17	4.24	0.41	0.426	0.035	3.13	0.53	
50501	^{34}SO (6_5-5_4)	246663.47	49.89	1.81E-04	3.93	0.18	4.99	0.43	0.124	0.009	1.19	0.21	
50501	^{34}SO (6_6-5_5)	253207.02	55.69	2.00E-04	3.73	0.15	6.08	0.38	0.114	0.006	1.38	0.24	
50501	^{34}SO (6_7-5_6)	256877.81	46.71	2.15E-04	3.91	0.12	5.05	0.31	0.464	0.023	4.73	0.80	
50501	^{34}SO (8_7-7_6)	333900.98	79.86	4.69E-04	3.56	0.16	4.91	0.42	0.288	0.019	2.68	0.48	wings
50501	^{34}SO (8_8-7_7)	337580.15	86.07	4.89E-04	3.30	0.10	5.40	0.25	0.302	0.012	3.12	0.56	wings
50501	^{34}SO (8_9-7_8)	339857.27	77.34	5.08E-04	3.68	0.12	5.36	0.29	0.383	0.017	3.93	0.71	wings
30591	o-H_2CO ($6_{1,5}$-$6_{1,6}$)	101332.99	72.40	1.57E-06	3.14	0.18	4.43	0.42	0.111	0.009	0.65	0.07	

Table 4. continued.

TAG	Species & Transition	Frequency (MHz)	E_{up} (K)	A_{ij} s^{-1}	V_o (km s^{-1})	δ_{V_o}	*FWHM* (km s^{-1})	δ_{FWHM}	Int (K)	δ_{Int}	Flux (K km s^{-1})	δ_{Flux}	Comments
30591	o-H_2CO ($7_{1,6}$-$7_{1,7}$)	135030.44	97.63	2.79E-06	2.63	0.13	3.26	0.30	0.154	0.012	0.71	0.12	
30591	o-H_2CO ($2_{1,2}$-$1_{1,1}$)	140839.50	6.76	5.29E-05	4.00	0.24	4.34	0.57	3.051	0.343	18.88	3.21	self abs, wings
30591	o-H_2CO ($2_{1,1}$-$1_{1,0}$)	150498.33	7.45	6.46E-05	3.89	0.19	4.49	0.46	2.975	0.232	19.47	3.31	self abs, wings
30591	o-H_2CO ($8_{1,7}$-$8_{1,8}$)	173461.70	126.44	4.61E-06	2.40	0.18	4.01	0.44	0.137	0.013	0.85	0.15	
30591	o-H_2CO ($3_{1,3}$-$2_{1,2}$)	211211.47	16.90	2.27E-04	4.19	0.04	4.80	0.09	3.771	0.060	30.93	5.26	
30591	o-H_2CO ($3_{1,2}$-$2_{1,1}$)	225697.77	18.29	2.77E-04	3.65	0.25	4.36	0.59	4.646	0.543	36.30	6.17	
30591	o-H_2CO ($5_{1,5}$-$4_{1,4}$)	351768.65	47.29	1.20E-03	3.59	0.07	2.92	0.16	6.392	0.293	36.28	6.53	wings
30591	o-H_2CO ($5_{3,3}$-$4_{3,2}$)	364275.14	143.26	8.88E-04	3.49	0.06	4.16	0.13	1.166	0.033	9.57	1.72	
30591	o-H_2CO ($5_{3,2}$-$4_{3,1}$)	364288.88	143.26	8.88E-04	3.52	0.06	4.12	0.14	1.186	0.035	9.65	1.74	
30581	p-H_2CO ($2_{0,2}$-$1_{0,1}$)	145602.95	10.48	7.80E-05	3.52	0.21	3.26	0.50	2.428	0.324	11.40	1.94	
30581	p-H_2CO ($3_{0,3}$-$2_{0,2}$)	218222.19	20.96	2.81E-04	3.87	0.06	4.30	0.13	3.212	0.083	24.13	4.10	
30581	p-H_2CO ($3_{2,2}$-$2_{2,1}$)	218475.63	68.09	1.57E-04	3.75	0.08	4.75	0.18	1.036	0.034	8.62	1.47	
30581	p-H_2CO ($3_{2,1}$-$2_{2,0}$)	218760.07	68.11	1.57E-04	3.69	0.08	4.27	0.19	1.100	0.042	8.22	1.40	
30581	p-H_2CO ($5_{0,5}$-$4_{0,4}$)	362736.05	52.31	1.37E-03	3.56	0.07	2.87	0.15	3.320	0.153	18.74	3.37	wings
30581	p-H_2CO ($5_{2,4}$-$4_{2,3}$)	363945.89	99.54	1.16E-03	3.69	0.07	4.01	0.15	1.512	0.050	11.97	2.15	
30581	p-H_2CO ($5_{2,3}$-$4_{2,2}$)	365363.43	99.66	1.18E-03	3.62	0.06	3.98	0.15	1.337	0.044	10.51	1.89	
31501	HDCO ($6_{1,5}$-$6_{1,6}$)	112066.60	75.53	2.13E-06	2.82	0.27	3.91	0.65	0.042	0.006	0.22	0.04	
31501	HDCO ($2_{1,1}$-$1_{1,0}$)	134284.83	17.63	4.59E-05	3.86	0.11	2.82	0.26	0.366	0.029	1.45	0.25	
31501	HDCO ($7_{1,6}$-$7_{1,7}$)	149214.25	97.99	3.79E-06	2.67	0.10	2.05	0.25	0.079	0.008	0.23	0.04	
31501	HDCO ($3_{1,2}$-$2_{1,1}$)	201341.36	27.29	1.97E-04	3.82	0.15	4.47	0.36	0.557	0.039	4.12	0.70	
31501	HDCO ($4_{1,4}$-$3_{1,3}$)	246924.60	37.60	3.96E-04	3.54	0.14	3.91	0.33	0.275	0.020	2.09	0.36	
31501	HDCO ($4_{0,4}$-$3_{0,3}$)	256585.54	30.85	4.74E-04	3.92	0.13	4.13	0.31	0.842	0.054	7.02	1.19	
31501	HDCO ($4_{2,3}$-$3_{2,2}$)	257748.70	62.77	3.61E-04	3.76	0.14	4.42	0.32	0.231	0.014	2.07	0.36	
31501	HDCO ($4_{3,2}$-$3_{3,1}$)	258070.94	102.56	2.11E-04	2.27	0.43	6.12	1.21	0.105	0.015	1.30	0.24	
31501	HDCO ($4_{1,3}$-$3_{1,2}$)	268292.02	40.17	5.09E-04	3.71	0.04	4.18	0.10	0.484	0.010	4.30	0.73	
31501	HDCO ($5_{1,4}$-$4_{1,3}$)	335096.78	56.25	1.04E-03	3.55	0.16	3.85	0.39	0.532	0.044	3.90	0.70	
31503	$H_2^{13}CO$ ($2_{1,2}$-$1_{1,1}$)	137449.95	21.72	4.93E-05	3.54	0.07	3.18	0.16	0.110	0.005	0.50	0.09	
31503	$H_2^{13}CO$ ($2_{0,2}$-$1_{0,1}$)	141983.74	10.22	7.25E-05	3.38	0.11	3.32	0.26	0.130	0.009	0.62	0.11	
31503	$H_2^{13}CO$ ($2_{1,1}$-$1_{1,0}$)	146635.67	22.38	5.99E-05	3.14	0.13	3.74	0.32	0.181	0.013	0.98	0.17	
31503	$H_2^{13}CO$ ($3_{1,3}$-$2_{1,2}$)	206131.63	31.62	2.11E-04	3.36	0.12	4.28	0.29	0.257	0.015	1.85	0.32	
31503	$H_2^{13}CO$ ($3_{0,3}$-$2_{0,2}$)	212811.18	20.44	2.61E-04	3.12	0.23	3.54	0.62	0.147	0.020	0.89	0.15	
31503	$H_2^{13}CO$ ($3_{1,2}$-$2_{1,1}$)	219908.52	32.94	2.56E-04	2.85	0.19	3.03	0.44	0.330	0.042	1.76	0.30	
31503	$H_2^{13}CO$ ($4_{1,4}$-$3_{1,3}$)	274762.11	44.80	5.47E-04	3.24	0.16	5.31	0.40	0.202	0.013	2.36	0.41	
31503	$H_2^{13}CO$ ($5_{0,5}$-$4_{0,4}$)	353811.87	51.02	1.27E-03	2.56	0.09	1.45	0.21	0.300	0.038	0.85	0.15	
31503	$H_2^{13}CO$ ($5_{2,4}$-$4_{2,3}$)	354898.59	98.41	1.08E-03	2.71	0.10	1.39	0.24	0.200	0.029	0.54	0.10	
31503	$H_2^{13}CO$ ($5_{3,3}$-$4_{3,2}$)	355190.90	157.52	8.25E-04	2.55	0.05	1.23	0.12	0.190	0.016	0.46	0.08	
31503	$H_2^{13}CO$ ($5_{3,2}$-$4_{3,1}$)	355202.60	157.52	8.25E-04	2.43	0.09	1.81	0.21	0.173	0.017	0.61	0.11	
31503	$H_2^{13}CO$ ($5_{1,4}$-$4_{1,3}$)	366270.15	64.59	1.36E-03	2.63	0.07	1.99	0.17	0.337	0.025	1.33	0.24	
32592	o-D_2CO ($3_{0,3}$-$2_{0,2}$)	174413.12	16.78	1.44E-04	4.09	0.12	2.30	0.27	0.510	0.052	1.80	0.31	
32592	o-D_2CO ($4_{0,4}$-$3_{0,3}$)	231410.23	27.88	3.47E-04	4.00	0.12	4.18	0.29	0.430	0.026	3.29	0.56	
32592	o-D_2CO ($4_{2,2}$-$3_{2,1}$)	236102.09	49.80	2.77E-04	4.00	0.26	4.87	0.67	0.171	0.018	1.55	0.27	
32592	o-D_2CO ($6_{0,6}$-$5_{0,5}$)	342522.13	58.12	1.17E-03	3.40	0.15	3.80	0.40	0.268	0.021	1.96	0.35	
32592	o-D_2CO ($6_{2,5}$-$5_{2,4}$)	349630.61	80.41	1.11E-03	2.78	0.24	3.86	0.69	0.214	0.026	1.60	0.29	
32592	o-D_2CO ($6_{2,4}$-$5_{2,3}$)	357871.46	81.21	1.19E-03	2.80	0.21	3.81	0.51	0.199	0.022	1.49	0.27	
32582	p-D_2CO ($2_{1,2}$-$1_{1,1}$)	110837.83	5.32	2.58E-05	4.34	0.06	1.96	0.15	0.194	0.013	0.51	0.06	
32582	p-D_2CO ($3_{1,3}$-$2_{1,2}$)	166102.75	13.29	1.10E-04	4.19	0.15	2.66	0.36	0.280	0.032	1.12	0.19	

Table 4. continued.

TAG	Species & Transition	Frequency (MHz)	E_{up} (K)	A_{ij} s^{-1}	V_o (km s^{-1})	δ_{V_o}	$FWHM$ (km s^{-1})	δ_{FWHM}	Int (K)	δ_{Int}	Flux (K km s^{-1})	δ_{Flux}	Comments
32582	p-D_2CO ($4_{1,4}$-$3_{1,3}$)	221191.67	23.91	2.85E-04	3.89	0.14	4.22	0.36	0.182	0.012	1.35	0.23	
32582	p-D_2CO ($4_{3,2}$-$3_{3,1}$)	234293.36	68.57	1.58E-04	2.91	0.23	3.90	0.56	0.048	0.006	0.34	0.07	
32582	p-D_2CO ($4_{1,3}$-$3_{1,2}$)	245532.75	26.83	3.90E-04	3.62	0.19	4.41	0.50	0.073	0.006	0.62	0.11	
32582	p-D_2CO ($6_{1,6}$-$5_{1,5}$)	330674.35	53.03	1.02E-03	2.70	0.13	1.43	0.30	0.204	0.037	0.55	0.10	
32582	p-D_2CO ($6_{3,4}$-$5_{3,3}$)	351894.28	99.52	9.54E-04	2.73	0.07	1.92	0.16	0.157	0.011	0.58	0.11	
32582	p-D_2CO ($6_{3,3}$-$5_{3,2}$)	352243.69	99.55	9.56E-04	2.62	0.16	1.56	0.42	0.147	0.031	0.45	0.08	
32503	$H_2C^{18}O$ ($2_{1,1}$-$1_{1,0}$)	143213.07	22.18	5.58E-05	2.94	0.26	3.13	0.68	0.051	0.009	0.23	0.05	
32503	$H_2C^{18}O$ ($3_{0,3}$-$2_{0,2}$)	208006.44	19.97	2.44E-04	2.58	0.27	3.99	0.64	0.034	0.005	0.23	0.04	
32503	$H_2C^{18}O$ ($5_{1,5}$-$4_{1,4}$)	335815.93	60.23	1.05E-03	2.70	0.38	2.42	0.92	0.060	0.019	0.28	0.05	
32503	$H_2C^{18}O$ ($5_{1,4}$-$4_{1,3}$)	357741.05	63.39	1.26E-03	2.62	0.06	1.14	0.14	0.194	0.021	0.44	0.08	
64502	SO_2 ($13_{4,10}$-$14_{3,11}$)	82951.94	122.97	1.26E-06	2.82	0.44	7.67	1.32	0.028	0.003	0.27	0.04	
64502	SO_2 ($8_{1,7}$-$8_{0,8}$)	83688.09	36.72	6.82E-06	4.04	0.10	3.89	0.23	0.399	0.021	1.99	0.22	
64502	SO_2 ($8_{3,5}$-$9_{2,8}$)	86639.09	55.20	1.34E-06	3.10	0.18	4.67	0.44	0.046	0.004	0.28	0.04	
64502	SO_2 ($7_{3,5}$-$8_{2,6}$)	97702.33	47.84	1.81E-06	3.34	0.23	6.60	0.60	0.040	0.003	0.35	0.05	
64502	SO_2 ($2_{2,0}$-$3_{1,3}$)	100878.10	12.59	1.03E-06	4.43	0.18	3.29	0.42	0.040	0.005	0.17	0.02	
64502	SO_2 ($3_{1,3}$-$2_{0,2}$)	104029.42	7.74	1.01E-05	4.13	0.07	3.40	0.16	0.460	0.018	2.08	0.23	
64502	SO_2 ($16_{2,14}$-$15_{3,13}$)	104033.58	137.53	3.17E-06	3.36	0.14	4.92	0.35	0.055	0.003	0.36	0.04	
64502	SO_2 ($10_{1,9}$-$10_{0,10}$)	104239.29	54.71	1.12E-05	3.98	0.10	4.17	0.23	0.375	0.018	2.08	0.23	
64502	SO_2 ($12_{1,11}$-$11_{2,10}$)	129105.83	76.41	9.03E-06	4.14	0.18	5.23	0.43	0.209	0.015	1.52	0.26	
64502	SO_2 ($10_{2,8}$-$10_{1,9}$)	129514.81	60.93	2.50E-05	4.02	0.09	4.16	0.22	0.432	0.020	2.51	0.43	
64502	SO_2 ($12_{1,11}$-$12_{0,12}$)	131014.86	76.41	1.86E-05	3.94	0.13	5.18	0.30	0.198	0.010	1.43	0.24	
64502	SO_2 ($14_{2,12}$-$14_{1,13}$)	132744.86	108.12	2.93E-05	3.86	0.10	5.78	0.25	0.154	0.006	1.25	0.21	
64502	SO_2 ($8_{2,6}$-$8_{1,7}$)	134004.86	43.15	2.50E-05	4.02	0.12	3.88	0.28	0.347	0.022	1.89	0.32	
64502	SO_2 ($5_{1,5}$-$4_{0,4}$)	135696.02	15.66	2.21E-05	3.97	0.08	3.10	0.19	0.724	0.038	3.16	0.54	
64502	SO_2 ($5_{3,3}$-$6_{2,4}$)	139355.06	35.89	3.85E-06	3.66	0.25	4.78	0.60	0.072	0.008	0.49	0.09	
64502	SO_2 ($6_{2,4}$-$6_{1,5}$)	140306.17	29.20	2.53E-05	3.84	0.07	3.48	0.17	0.501	0.021	2.49	0.42	
64502	SO_2 ($16_{2,14}$-$16_{1,15}$)	143057.11	137.53	3.57E-05	3.88	0.09	5.81	0.23	0.299	0.010	2.49	0.42	
64502	SO_2 ($10_{4,6}$-$11_{3,9}$)	146550.08	89.84	5.90E-06	3.40	0.18	6.01	0.46	0.097	0.006	0.84	0.15	
64502	SO_2 ($4_{2,2}$-$4_{1,3}$)	146605.52	19.03	2.47E-05	3.93	0.09	4.30	0.22	0.468	0.021	2.91	0.50	
64502	SO_2 ($15_{5,11}$-$16_{4,12}$)	150381.10	171.68	6.95E-06	3.17	0.36	7.53	1.01	0.067	0.006	0.73	0.13	
64502	SO_2 ($2_{2,0}$-$2_{1,1}$)	151378.63	12.59	1.87E-05	3.96	0.10	3.94	0.24	0.247	0.013	1.42	0.24	
64502	SO_2 ($3_{2,2}$-$3_{1,3}$)	158199.74	15.34	2.53E-05	3.63	0.11	4.17	0.25	0.352	0.018	2.17	0.37	
64502	SO_2 ($18_{2,16}$-$18_{1,17}$)	160342.99	170.76	4.69E-05	3.49	0.08	7.03	0.21	0.229	0.005	2.40	0.41	
64502	SO_2 ($4_{3,1}$-$5_{2,4}$)	160543.06	31.29	4.32E-06	3.70	0.16	3.98	0.38	0.077	0.006	0.46	0.08	
64502	SO_2 ($10_{0,10}$-9_{19})	160827.88	49.71	3.95E-05	4.01	0.08	3.86	0.20	0.826	0.036	4.76	0.81	
64502	SO_2 ($18_{2,16}$-$17_{3,15}$)	163119.38	170.76	1.35E-05	3.85	0.25	7.38	0.71	0.119	0.008	1.31	0.23	
64502	SO_2 ($14_{1,13}$-$14_{0,14}$)	163605.53	101.75	3.01E-05	3.98	0.07	5.63	0.17	0.322	0.008	2.72	0.46	
64502	SO_2 ($5_{2,4}$-$5_{1,5}$)	165144.65	23.59	3.12E-05	3.97	0.12	2.36	0.27	0.466	0.047	1.66	0.28	
64502	SO_2 ($7_{1,7}$-$6_{0,6}$)	165225.45	27.08	4.13E-05	3.81	0.12	2.46	0.29	0.743	0.075	2.75	0.47	
64502	SO_2 ($16_{1,15}$-$16_{0,16}$)	200809.18	130.67	4.70E-05	3.35	0.11	5.76	0.28	0.173	0.007	1.65	0.28	
64502	SO_2 ($12_{0,12}$-$11_{1,11}$)	203391.55	70.12	8.80E-05	4.12	0.10	5.36	0.24	0.494	0.019	4.41	0.75	
64502	SO_2 ($11_{2,10}$-$11_{1,11}$)	205300.57	70.22	5.32E-05	3.84	0.11	5.74	0.29	0.351	0.013	3.38	0.58	
64502	SO_2 ($3_{2,2}$-$2_{1,1}$)	208700.34	15.34	6.72E-05	4.00	0.10	4.87	0.24	0.472	0.019	3.89	0.66	
64502	SO_2 ($16_{3,13}$-$16_{2,14}$)	214689.39	147.84	9.90E-05	3.72	0.13	6.68	0.36	0.444	0.017	5.12	0.87	
64502	SO_2 ($17_{6,12}$-$18_{5,13}$)	214728.29	228.96	1.89E-05	3.63	0.12	6.52	0.32	0.108	0.004	1.21	0.22	
64502	SO_2 ($22_{2,20}$-$22_{1,20}$)	216643.30	248.45	9.27E-05	3.42	0.10	6.87	0.30	0.202	0.006	2.41	0.41	
64502	SO_2 ($11_{1,11}$-$10_{0,10}$)	221965.22	60.36	1.14E-04	3.99	0.14	5.06	0.35	0.838	0.047	7.51	1.28	

Table 4. continued.

TAG	Species & Transition	Frequency (MHz)	E_{up} (K)	A_{ij} s^{-1}	V_o (km s^{-1})	δ_{V_o}	*FWHM* (km s^{-1})	δ_{FWHM}	Int (K)	δ_{Int}	Flux (K km s^{-1})	δ_{Flux}	Comments
64502	SO_2 ($6_{4,2}$-$7_{3,5}$)	223883.57	58.58	1.16E-05	3.65	0.15	4.62	0.36	0.080	0.005	0.66	0.12	
64502	SO_2 ($20_{2,18}$-$19_{3,17}$)	224264.81	207.76	3.94E-05	3.42	0.11	5.75	0.30	0.107	0.004	1.10	0.19	
64502	SO_2 ($13_{2,12}$-$13_{1,13}$)	225153.70	92.99	6.52E-05	3.76	0.11	5.92	0.32	0.381	0.015	4.04	0.69	
64502	SO_2 ($14_{3,11}$-$14_{2,12}$)	226300.03	118.99	1.07E-04	3.38	0.08	6.46	0.21	0.400	0.010	4.64	0.79	
64502	SO_2 (11_{57}-$12_{4,8}$)	229347.63	122.01	1.91E-05	2.72	0.18	4.49	0.44	0.105	0.009	0.85	0.15	
64502	SO_2 ($4_{2,2}$-$3_{1,3}$)	235151.72	19.03	7.69E-05	4.00	0.14	4.64	0.33	0.415	0.025	3.57	0.61	
64502	SO_2 ($16_{1,15}$-$15_{2,14}$)	236216.69	130.67	7.50E-05	3.89	0.13	6.39	0.37	0.369	0.016	4.39	0.75	
64502	SO_2 ($12_{3,9}$-$12_{2,10}$)	237068.83	93.96	1.14E-04	3.64	0.06	6.19	0.15	0.335	0.006	3.87	0.66	
64502	SO_2 ($18_{1,17}$-$18_{0,18}$)	240942.79	163.07	7.02E-05	3.68	0.12	7.82	0.36	0.361	0.011	5.35	0.91	
64502	SO_2 ($5_{2,4}$-$4_{1,3}$)	241615.80	23.59	8.45E-05	3.91	0.13	5.21	0.32	0.630	0.032	6.24	1.06	
64502	SO_2 ($14_{0,14}$-$13_{1,13}$)	244254.22	93.90	1.64E-04	4.03	0.10	6.11	0.28	0.565	0.019	6.63	1.13	
64502	SO_2 ($10_{3,7}$-$10_{2,8}$)	245563.42	72.71	1.19E-04	3.77	0.10	5.58	0.24	0.174	0.006	1.88	0.32	
64502	SO_2 ($15_{2,14}$-$15_{1,15}$)	248057.40	119.33	8.05E-05	3.52	0.35	7.73	1.02	0.063	0.006	0.94	0.17	
64502	SO_2 ($13_{1,13}$-$12_{0,12}$)	251199.67	82.18	1.76E-04	3.78	0.12	5.70	0.30	0.607	0.027	6.82	1.16	
64502	SO_2 ($8_{3,5}$-$8_{2,6}$)	251210.58	55.20	1.20E-04	3.65	0.04	6.10	0.12	0.392	0.006	4.72	0.80	
64502	SO_2 ($6_{3,3}$-$6_{2,4}$)	254280.54	41.40	1.14E-04	3.23	0.17	6.67	0.51	0.353	0.018	4.71	8.00	
64502	SO_2 ($4_{3,1}$-$4_{2,2}$)	255553.30	31.29	9.28E-05	4.17	0.28	6.75	0.70	0.060	0.005	0.81	0.14	
64502	SO_2 ($3_{3,1}$-$3_{2,2}$)	255958.04	27.62	6.62E-05	4.91	0.37	4.64	0.90	0.039	0.006	0.36	0.07	
64502	SO_2 ($5_{3,3}$-$5_{2,4}$)	256246.95	35.89	1.07E-04	3.82	0.14	5.21	0.34	0.441	0.024	4.63	7.87	
64502	SO_2 ($7_{3,5}$-$7_{2,6}$)	257099.97	47.84	1.22E-04	3.88	0.16	4.47	0.37	0.398	0.029	3.59	0.62	
64502	SO_2 ($9_{3,7}$-$9_{2,8}$)	258942.20	63.47	1.32E-04	3.79	0.11	5.88	0.27	0.371	0.014	4.44	0.76	
64502	SO_2 ($11_{3,9}$-$11_{2,10}$)	262256.91	82.80	1.41E-04	3.75	0.10	6.11	0.26	0.454	0.015	5.74	0.98	
64502	SO_2 ($7_{2,6}$-$6_{1,5}$)	271529.01	35.50	1.11E-04	3.98	0.18	5.01	0.44	0.440	0.033	4.76	0.81	
64502	SO_2 ($17_{2,16}$-$17_{1,17}$)	273752.82	149.22	9.97E-05	3.34	0.17	5.94	0.41	0.179	0.010	2.32	0.40	
64502	SO_2 ($15_{3,13}$-$15_{2,14}$)	275240.18	132.54	1.64E-04	3.72	0.15	5.85	0.39	0.329	0.017	4.23	0.72	
64502	SO_2 ($21_{2,20}$-$21_{1,21}$)	332091.43	219.53	1.51E-04	3.43	0.23	5.62	0.59	0.114	0.009	1.22	0.22	
64502	SO_2 ($4_{3,1}$-$3_{2,2}$)	332505.24	31.29	3.29E-04	3.79	0.10	3.71	0.23	0.742	0.040	5.23	0.94	
64502	SO_2 ($8_{2,6}$-$7_{1,7}$)	334673.35	43.15	1.27E-04	3.76	0.15	3.24	0.35	0.451	0.042	2.78	0.50	
64502	SO_2 ($19_{1,19}$-$18_{0,18}$)	346652.17	168.14	5.22E-04	3.69	0.07	5.40	0.17	0.442	0.011	4.61	0.83	
64502	SO_2 ($5_{3,3}$-$4_{2,2}$)	351257.22	35.89	3.36E-04	3.79	0.10	3.79	0.24	0.700	0.038	5.15	0.93	
64502	SO_2 ($14_{4,10}$-$14_{3,11}$)	351873.87	135.87	3.43E-04	3.75	0.27	7.26	0.76	0.227	0.015	3.20	0.58	
64502	SO_2 ($12_{4,8}$-$12_{3,9}$)	355045.52	111.00	3.40E-04	3.59	0.10	5.58	0.26	0.349	0.013	3.80	0.69	
64502	SO_2 ($13_{4,10}$-$13_{3,11}$)	357165.39	122.97	3.51E-04	3.73	0.09	5.49	0.23	0.329	0.011	3.54	0.64	
64502	SO_2 ($15_{4,12}$-$15_{3,13}$)	357241.19	149.68	3.62E-04	3.72	0.13	6.05	0.34	0.283	0.012	3.35	0.60	
64502	SO_2 ($11_{4,8}$-$11_{3,9}$)	357387.58	99.95	3.38E-04	3.75	0.10	5.56	0.26	0.411	0.015	4.48	0.81	
64502	SO_2 ($8_{4,4}$-$8_{3,5}$)	357581.45	72.36	3.06E-04	4.05	0.08	4.62	0.20	0.403	0.014	3.64	0.66	
64502	SO_2 ($9_{4,6}$-$9_{3,7}$)	357671.82	80.64	3.20E-04	3.93	0.19	5.57	0.51	0.338	0.023	3.68	0.66	
64502	SO_2 ($7_{4,4}$-$7_{3,5}$)	357892.44	65.01	2.87E-04	3.68	0.08	4.26	0.19	0.434	0.017	3.62	0.65	
64502	SO_2 ($6_{4,2}$-$6_{3,3}$)	357925.85	58.58	2.60E-04	3.69	0.11	4.69	0.26	0.398	0.019	3.66	0.66	
64502	SO_2 ($17_{4,14}$-$17_{3,15}$)	357962.91	180.11	3.73E-04	3.51	0.13	5.55	0.32	0.264	0.012	2.86	0.52	
64502	SO_2 ($5_{4,2}$-$5_{3,3}$)	358013.15	53.07	2.18E-04	3.89	0.11	5.00	0.25	0.313	0.014	3.06	0.55	
64502	SO_2 ($4_{4,0}$-$4_{3,1}$)	358037.89	48.48	1.45E-04	3.24	0.19	4.37	0.44	0.115	0.010	0.98	0.18	
64502	SO_2 ($20_{0,20}$-$19_{1,19}$)	358215.63	185.33	5.83E-04	3.56	0.11	5.60	0.28	0.294	0.011	3.23	0.58	
64502	SO_2 ($19_{4,16}$-$19_{3,17}$)	359770.68	214.26	3.85E-04	3.94	0.18	6.85	0.50	0.220	0.010	2.96	0.53	
64502	SO_2 ($15_{2,14}$-$14_{1,13}$)	366214.47	119.33	3.04E-04	3.66	0.09	5.26	0.23	0.334	0.012	3.48	0.63	
66002	$^{34}SO_2$($3_{1,3}$-$2_{0,2}$)	102031.88	7.64	9.50E-06	3.68	0.16	3.91	0.37	0.030	0.002	0.15	0.02	
66002	$^{34}SO_2$($5_{1,5}$-$4_{0,4}$)	133471.47	15.54	2.11E-05	4.43	0.23	1.75	0.54	0.066	0.017	0.16	0.03	

Table 4. continued.

TAG	Species & Transition	Frequency (MHz)	E_{up} (K)	A_{ij} s^{-1}	V_o (km s^{-1})	δ_{V_o}	$FWHM$ (km s^{-1})	δ_{FWHM}	Int (K)	δ_{Int}	Flux (K km s^{-1})	δ_{Flux}	Comments
66002	$^{34}SO_2(6_{2,4}$-$6_{1,5})$	134826.12	28.83	2.27E-05	2.79	0.19	5.03	0.52	0.056	0.004	0.40	0.07	
66002	$^{34}SO_2(11_{2,10}$-$11_{1,11})$	201376.42	69.74	4.96E-05	2.71	0.24	3.94	0.57	0.042	0.005	0.28	0.06	
66002	$^{34}SO_2(11_{1,11}$-$10_{0,10})$	219355.01	60.08	1.11E-04	3.05	0.40	6.39	0.95	0.057	0.007	0.64	0.11	
32504	CH_3OH ($7_{2,6}$-$8_{1,7}$ A^-)	80993.24	102.7	1.04E-06	3.59	0.44	7.43	1.01	0.032	0.004	0.30	0.05	
32504	CH_3OH ($5_{-1,5}$-$4_{+0,4,}$ E)	84521.17	40.39	1.97E-06	3.93	0.15	4.25	0.35	0.327	0.024	1.79	0.20	
32504	CH_3OH ($6_{-2,5}$-$7_{+1,7}$ E)	85568.08	74.66	1.13E-06	3.90	0.35	7.68	0.84	0.048	0.004	0.47	0.06	
32504	CH_3OH ($7_{2,6}$-$6_{3,3}$ A^-)	86615.60	102.7	6.85E-07	2.71	0.18	4.65	0.41	0.043	0.003	0.26	0.04	
32504	CH_3OH ($7_{2,5}$-$6_{3,4}$ A^+)	86902.95	102.72	6.92E-07	2.78	0.31	5.31	0.76	0.044	0.005	0.30	0.04	
32504	CH_3OH ($8_{-4,5}$-$9_{-3,7}$ E)	89505.81	171.46	7.65E-07	3.04	0.26	6.30	0.59	0.050	0.004	0.41	0.05	
32504	CH_3OH ($8_{+3,5}$-$9_{+2,7}$ E)	94541.77	131.28	1.29E-06	3.32	0.34	7.46	0.85	0.046	0.004	0.45	0.05	
32504	CH_3OH ($8_{0,8}$-$7_{1,7}$ A^+)	95169.46	83.54	4.26E-06	3.85	0.09	4.75	0.21	0.241	0.009	1.50	0.17	
32504	CH_3OH ($2_{1,2}$-$1_{1,1}$ A^+)	95914.31	21.44	2.49E-06	3.44	0.05	5.18	0.11	0.122	0.002	0.83	0.09	
32504	CH_3OH ($2_{0,2}$-$1_{0,1}$ A^+)	96741.38	6.97	3.41E-06	3.80	0.11	2.81	0.26	0.621	0.047	2.29	0.25	
32504	CH_3OH ($2_{+0,2}$-$1_{+0,1}$ E)	96744.55	20.09	3.41E-06	3.64	0.14	4.47	0.35	0.186	0.012	1.09	0.12	
32504	CH_3OH ($2_{+1,1}$-$1_{+1,0}$ E)	96755.51	28.01	2.62E-06	3.53	0.10	5.00	0.23	0.109	0.004	0.72	0.08	
32504	CH_3OH ($2_{1,1}$-$1_{1,0}$ A^-)	97582.80	21.56	2.63E-06	3.71	0.06	5.32	0.15	0.114	0.003	0.80	0.09	
32504	CH_3OH ($13_{2,11}$- $12_{3,9}$ A^+)	100638.90	233.61	1.69E-06	2.55	0.11	6.13	0.28	0.064	0.002	0.52	0.06	
32504	CH_3OH ($7_{-2,6}$-$7_{+1,6}$ E)	101293.34	90.91	3.73E-08	2.11	0.39	4.07	0.99	0.020	0.004	0.11	0.02	
32504	CH_3OH ($9_{-2,8}$-$9_{+1,8}$ E)	101737.17	130.4	1.08E-07	2.65	0.23	4.20	0.61	0.041	0.004	0.23	0.03	
32504	CH_3OH ($11_{-2,10}$-$11_{+1,10}$ E)	102658.05	179.19	2.65E-07	2.56	0.25	4.98	0.61	0.046	0.004	0.30	0.04	
32504	CH_3OH ($12_{-2,11}$-$12_{+1,11}$ E)	103381.15	207.08	3.98E-07	2.81	0.28	6.01	0.66	0.041	0.004	0.33	0.04	
32504	CH_3OH ($11_{-1,11}$-$10_{-2,9}$ E)	104300.41	158.64	1.96E-06	3.32	0.18	6.74	0.42	0.079	0.004	0.71	0.08	
32504	CH_3OH ($10_{4,7}$-$11_{3,8}$ A^-)	104354.82	207.99	1.57E-06	3.63	0.45	7.78	1.15	0.047	0.006	0.49	0.06	
32504	CH_3OH ($3_{1,3}$-$4_{0,4}$ A^+)	107013.80	28.35	6.13E-06	3.36	0.12	5.52	0.30	0.068	0.003	0.50	0.06	
32504	CH_3OH ($0_{+0,0}$-$1_{-1,1}$ E)	108893.96	13.13	1.47E-05	3.44	0.12	5.70	0.30	0.043	0.002	0.33	0.05	
32504	CH_3OH ($12_{1,1}$-$11_{2,10}$ A^-)	129433.41	197.08	4.69E-06	2.82	0.22	5.88	0.52	0.112	0.009	0.92	0.16	
32504	CH_3OH ($6_{2,5}$-$7_{1,6}$ A^+)	132621.94	86.46	4.26E-06	2.14	0.26	4.31	0.69	0.071	0.008	0.43	0.08	
32504	CH_3OH ($6_{-1,6}$-$5_{+0,5}$ E)	132890.69	54.31	7.75E-06	3.56	0.09	3.70	0.21	0.279	0.014	1.45	0.25	
32504	CH_3OH ($5_{-2,4}$-$6_{-1,6}$ E)	133605.50	60.73	4.01E-06	4.15	0.18	6.67	0.47	0.095	0.005	0.89	0.16	
32504	CH_3OH ($8_{2,7}$-$7_{3,4}$ A^-)	134896.96	121.27	3.00E-06	4.35	0.31	7.81	0.89	0.122	0.010	1.35	0.23	
32504	CH_3OH ($7_{+3,4}$-$8_{+2,6}$ E)	143169.50	112.71	4.13E-06	3.08	0.27	7.10	0.83	0.121	0.009	1.24	0.21	
32504	CH_3OH ($3_{1,3}$-$2_{1,2}$ A^+)	143865.80	28.35	1.07E-05	3.80	0.09	6.12	0.22	0.307	0.009	2.70	0.46	
32504	CH_3OH ($3_{+0,3}$-$2_{+0,2}$ E)	145093.71	27.05	1.23E-05	3.53	0.10	3.46	0.26	0.358	0.020	1.79	0.30	
32504	CH_3OH ($3_{-1,3}$-$2_{-1,2}$ E)	145097.37	19.51	1.10E-05	3.68	0.12	3.36	0.27	0.655	0.046	3.17	0.54	
32504	CH_3OH ($3_{0,3}$-$2_{0,2}$ A^+)	145103.15	13.93	1.23E-05	3.64	0.08	2.90	0.19	0.856	0.050	3.57	0.61	
32504	CH_3OH ($3_{1,2}$-$2_{1,1}$ A^-)	146368.34	28.59	1.13E-05	3.79	0.09	5.43	0.22	0.310	0.011	2.43	0.41	
32504	CH_3OH ($12_{-1,12}$-$11_{-2,10}$ E)	150884.58	186.43	5.86E-06	3.60	0.21	7.65	0.52	0.146	0.008	1.62	0.28	
32504	CH_3OH ($13_{+0,13}$-$13_{-1,13}$ E)	151860.32	223.82	1.15E-05	3.52	0.19	7.82	0.49	0.077	0.004	0.88	0.15	
32504	CH_3OH ($12_{+0,12}$-$12_{-1,12}$ E)	153281.24	193.79	1.29E-05	2.65	0.30	7.08	0.80	0.120	0.010	1.25	0.21	
32504	CH_3OH ($11_{+0,11}$-$11_{-1,11}$ E)	154425.78	166.05	1.42E-05	2.96	0.17	7.34	0.44	0.124	0.006	1.33	0.23	
32504	CH_3OH ($10_{+0,10}$-$10_{-1,10}$ E)	155320.92	140.6	1.55E-05	3.55	0.13	6.89	0.32	0.143	0.005	1.45	0.25	
32504	CH_3OH ($9_{+0,9}$-$9_{-1,9}$ E)	155997.52	117.46	1.67E-05	3.99	0.13	8.07	0.34	0.166	0.005	1.98	0.34	
32504	CH_3OH ($6_{2,4}$-$7_{1,7}$ A^+)	156127.70	86.47	6.54E-06	3.19	0.34	7.82	1.04	0.110	0.010	1.27	0.22	
32504	CH_3OH ($8_{+0,8}$-$8_{-1,8}$ E)	156488.87	96.61	1.78E-05	3.45	0.13	6.46	0.30	0.205	0.007	1.96	0.33	
32504	CH_3OH ($2_{1,2}$-$3_{0,3}$ A^+)	156602.41	21.44	1.78E-05	3.73	0.10	5.46	0.24	0.278	0.011	2.24	0.38	
32504	CH_3OH ($7_{+0,7}$-$7_{-1,7}$ E)	156828.53	78.08	1.88E-05	3.78	0.08	6.40	0.19	0.270	0.007	2.56	0.44	
32504	CH_3OH ($6_{+0,6}$-$6_{-1,6}$ E)	157048.62	61.85	1.96E-05	3.33	0.14	5.44	0.34	0.232	0.012	1.87	0.32	

Table 4. continued.

TAG	Species & Transition	Frequency (MHz)	E_{up} (K)	A_{ij} s^{-1}	V_o (km s^{-1})	δ_{V_o}	*FWHM* (km s^{-1})	δ_{FWHM}	Int (K)	δ_{Int}	Flux (K km s^{-1})	δ_{Flux}	Comments
32504	CH_3OH ($5_{+0,5}$-$5_{-1,5}$ E)	157179.02	47.93	2.04E-05	3.62	0.13	5.24	0.32	0.260	0.013	2.01	0.34	
32504	CH_3OH ($4_{+0,4}$-$4_{-1,4}$ E)	157246.06	36.34	2.10E-05	3.74	0.09	4.34	0.22	0.290	0.013	1.86	0.32	
32504	CH_3OH ($2_{+0,2}$-$2_{-1,2}$ E)	157276.06	20.09	2.18E-05	3.86	0.17	4.90	0.42	0.332	0.023	2.41	0.41	
32504	CH_3OH ($1_{+1,0}$-$1_{+0,1}$ E)	165050.20	23.37	2.35E-05	3.14	0.27	8.18	0.71	0.112	0.008	1.38	0.24	
32504	CH_3OH ($2_{+1,1}$-$2_{+0,2}$ E)	165061.16	28.01	2.34E-05	3.20	0.22	7.24	0.58	0.142	0.008	1.54	0.26	
32504	CH_3OH ($3_{+1,2}$-$3_{+0,3}$ E)	165099.27	34.98	2.33E-05	3.09	0.34	8.41	0.88	0.125	0.010	1.59	0.27	
32504	CH_3OH ($4_{+1,3}$-$4_{+0,4}$ E)	165190.53	44.26	2.32E-05	3.37	0.39	7.85	1.11	0.130	0.013	1.54	0.26	
32504	CH_3OH ($4_{+1,3}$-$4_{+0,4}$ E)	165190.53	44.26	2.32E-05	3.42	0.40	7.84	1.20	0.130	0.012	1.54	0.26	
32504	CH_3OH ($6_{+1,5}$-$6_{+0,6}$ E)	165678.77	69.8	2.30E-05	4.18	0.11	6.51	0.27	0.294	0.010	2.89	0.49	
32504	CH_3OH ($7_{+1,6}$-$7_{+0,7}$ E)	166169.21	86.05	2.28E-05	3.84	0.09	6.82	0.22	0.274	0.007	2.82	0.48	
32504	CH_3OH ($8_{+1,7}$-$8_{+0,8}$ E)	166898.65	104.62	2.28E-05	3.78	0.08	7.22	0.19	0.228	0.005	2.49	0.43	
32504	CH_3OH ($9_{+1,8}$-$9_{+0,9}$ E)	167931.13	125.52	2.27E-05	3.70	0.17	7.63	0.44	0.237	0.011	2.75	0.47	
32504	CH_3OH ($10_{+1,9}$-$10_{+0,10}$ E)	169335.34	148.73	2.28E-05	3.45	0.27	6.79	0.83	0.162	0.013	1.68	0.29	
32504	CH_3OH ($3_{+2,1}$-$2_{+1,1}$ E)	170060.58	36.17	2.55E-05	3.78	0.10	3.97	0.23	0.494	0.025	2.99	0.51	
32504	CH_3OH ($11_{+1,10}$-$11_{+0,11}$ E)	171182.58	174.27	2.30E-05	3.86	0.19	7.19	0.48	0.169	0.009	1.86	0.32	
32504	CH_3OH ($7_{+0,7}$-$6_{+1,5}$ E)	172445.95	78.08	1.16E-05	3.60	0.11	6.28	0.27	0.195	0.007	1.87	0.32	
32504	CH_3OH ($10_{0,10}$-$9_{1,9}$ A^+)	198403.22	127.6	4.10E-05	3.53	0.12	6.28	0.31	0.131	0.005	1.35	0.23	
32504	CH_3OH ($8_{4,4}$-$9_{3,7}$ A^+)	201088.98	163.9	9.13E-06	3.07	0.54	6.84	1.34	0.086	0.014	0.97	0.17	
32504	CH_3OH ($5_{2,3}$-$6_{1,6}$ A^+)	201445.59	72.53	1.30E-05	3.29	0.11	8.52	0.28	0.139	0.004	1.97	0.34	
32504	CH_3OH ($1_{1,1}$-$2_{0,2}$ A^+)	205791.27	16.84	3.36E-05	3.52	0.09	5.74	0.21	0.227	0.007	2.19	0.37	
32504	CH_3OH ($1_{+1,0}$-$0_{+0,0}$ E)	213427.12	23.37	3.37E-05	3.50	0.10	5.46	0.25	0.208	0.008	1.96	0.33	
32504	CH_3OH ($5_{+1,4}$-$4_{+2,2}$ E)	216945.60	55.87	1.21E-05	3.31	0.16	6.82	0.52	0.150	0.007	1.78	0.31	
32504	CH_3OH ($4_{+2,2}$-$3_{+1,2}$ E)	218440.05	45.46	4.69E-05	3.81	0.11	5.07	0.28	0.614	0.028	5.45	0.93	
32504	CH_3OH ($8_{-1,8}$-$7_{+0,7}$ E)	229758.76	89.1	4.19E-05	3.38	0.16	5.60	0.40	0.385	0.022	3.92	0.67	
32504	CH_3OH ($3_{-2,2}$-$4_{-1,4}$ E)	230027.06	39.83	1.49E-05	3.27	0.16	6.42	0.41	0.121	0.006	1.41	0.24	
32504	CH_3OH ($10_{-3,8}$-$11_{-2,10}$ E)	232945.83	190.37	2.13E-05	2.73	0.28	6.67	0.70	0.128	0.011	1.57	0.27	
32504	CH_3OH ($5_{1,5}$-$4_{1,4}$ A^+)	239746.25	49.06	5.66E-05	3.27	0.18	4.40	0.42	0.293	0.024	2.43	0.42	
32504	CH_3OH ($5_{+3,2}$-$6_{+2,4}$ E)	240241.50	82.53	1.44E-05	3.34	0.24	7.03	0.61	0.146	0.010	1.94	0.33	
32504	CH_3OH ($5_{+0,5}$-$4_{+0,4}$) E	241700.22	47.94	6.04E-05	3.76	0.10	5.19	0.25	0.641	0.023	6.37	1.08	
32504	CH_3OH ($5_{-1,5}$-$4_{-1,4}$ E)	241767.22	40.39	5.81E-05	3.85	0.16	4.56	0.39	1.088	0.077	9.44	1.61	
32504	CH_3OH ($5_{0,5}$-$4_{0,4}$ A^+)	241791.43	34.82	6.05E-05	4.08	0.12	4.22	0.30	1.248	0.075	10.0	1.70	
32504	CH_3OH ($5_{+1,4}$-$4_{+1,3}$ E)	241879.07	55.87	5.96E-05	3.77	0.15	5.82	0.42	0.496	0.026	5.49	0.93	
32504	CH_3OH ($5_{2,3}$-$4_{2,2}$ A^+)	241887.70	72.53	5.11E-05	3.51	0.16	7.04	0.46	0.299	0.013	4.01	0.68	
32504	CH_3OH ($5_{1,4}$-$4_{1,3}$ A^-)	243915.83	49.66	5.97E-05	3.68	0.10	5.35	0.24	0.499	0.019	5.12	0.87	
32504	CH_3OH ($4_{2,2}$-$5_{1,5}$ A^+)	247228.69	60.93	2.12E-05	3.36	0.36	7.58	0.95	0.061	0.006	0.90	0.16	
32504	CH_3OH ($8_{3,5}$-$8_{2,6}$ $A^\mp$)	251517.26	133.36	7.96E-05	3.04	0.07	6.27	0.19	0.271	0.006	3.36	0.57	
32504	CH_3OH ($6_{3,3}$-$6_{2,4}$ $A^\mp$)	251738.52	98.55	7.46E-05	3.24	0.10	6.40	0.27	0.301	0.010	3.80	0.65	
32504	CH_3OH ($8_{3,6}$-$8_{2,7}$ $A^\pm$)	251984.70	133.36	7.99E-05	3.00	0.19	5.56	0.44	0.244	0.018	2.68	0.46	
32504	CH_3OH ($2_{+1,1}$-$1_{+0,1}$ E)	261805.71	28.01	5.57E-05	3.87	0.13	6.04	0.31	0.349	0.015	4.36	0.74	
32504	CH_3OH ($6_{+1,5}$-$5_{+2,3}$ E)	265289.65	69.8	2.58E-05	3.01	0.09	5.92	0.22	0.173	0.006	2.15	0.38	
32504	CH_3OH ($5_{+2,3}$-$4_{+1,3}$ E)	266838.13	57.07	7.74E-05	3.35	0.09	3.69	0.22	0.359	0.019	2.80	0.48	
32504	CH_3OH ($2_{-2,1}$-$3_{-1,3}$ E)	278342.26	32.86	1.65E-05	3.59	0.28	7.87	0.89	0.077	0.005	1.35	0.24	
32504	CH_3OH ($11_{1,10}$-$11_{0,11}$ $A^\mp$)	331502.37	169.01	3.93E-04	3.37	0.14	5.18	0.35	0.319	0.018	3.14	0.57	
32504	CH_3OH ($2_{2,1}$-$3_{1,2}$ A^-)	335133.69	44.67	2.69E-05	3.32	0.22	5.05	0.52	0.122	0.009	1.17	0.21	
32504	CH_3OH ($7_{1,7}$-$6_{1,6}$ A^+)	335582.01	78.97	1.63E-04	3.32	0.08	4.26	0.19	0.238	0.009	1.93	0.35	
32504	CH_3OH ($7_{+0,7}$-$6_{+0,6}$ E)	338124.50	78.08	1.70E-04	3.42	0.14	4.14	0.33	0.319	0.021	2.53	0.46	
32504	CH_3OH ($7_{-3,5}$-$6_{-3,4}$ E)	338559.93	127.71	1.40E-04	2.87	0.24	6.19	0.60	0.151	0.012	1.78	0.32	

Table 4. continued.

TAG	Species & Transition	Frequency (MHz)	E_{up} (K)	A_{ij} s^{-1}	V_o (km s^{-1})	δ_{V_o}	$FWHM$ (km s^{-1})	δ_{FWHM}	Int (K)	δ_{Int}	Flux (K km s^{-1})	δ_{Flux}	Comments
32504	CH_3OH ($7_{+3,4}$-$6_{+3,3}$ E)	338583.20	112.71	1.39E-04	3.22	0.14	6.19	0.35	0.209	0.010	2.47	0.45	
32504	CH_3OH ($7_{1,6}$-$6_{1,5}$ A^-)	341415.64	80.09	1.71E-04	3.75	0.09	4.44	0.21	0.525	0.021	4.48	0.81	
32504	CH_3OH ($4_{+0,4}$-$3_{-1,3}$ E)	350687.73	36.33	8.67E-05	3.16	0.12	6.55	0.29	0.498	0.019	6.33	1.14	
32504	CH_3OH ($1_{1,1}$-$0_{0,0}$ A^+)	350905.12	16.84	3.31E-04	3.85	0.14	4.54	0.33	0.599	0.037	5.27	0.95	
32504	CH_3OH ($13_{0,13}$-$12_{1,12}$ A^+)	355603.11	211.03	2.53E-04	3.18	0.11	5.77	0.27	0.270	0.010	3.04	0.55	
32504	CH_3OH ($4_{+1,3}$-$3_{+0,3}$ E)	358605.80	44.26	1.32E-04	3.55	0.16	4.79	0.39	0.352	0.024	3.30	0.59	
32504	CH_3OH ($11_{+0,11}$-$10_{+1,9}$ E)	360848.86	166.05	1.21E-04	3.15	0.17	5.91	0.45	0.194	0.011	2.25	0.41	
32504	CH_3OH ($7_{+2,5}$-$6_{+1,5}$ E)	363739.82	87.26	1.71E-04	3.70	0.08	4.72	0.20	0.516	0.019	4.80	0.86	
33502	$^{13}CH_3OH$ ($2_{1,2}$-$1_{1,1}$ A^+)	93619.46	21.30	2.32E-06	3.47	0.23	1.78	0.45	0.028	0.007	0.07	0.01	
33502	$^{13}CH_3OH$ ($2_{-1,2}$-$1_{-1,1}$ E)	94405.16	12.40	2.38E-06	2.65	0.26	2.14	0.62	0.027	0.006	0.08	0.01	
33502	$^{13}CH_3OH$ ($2_{0,2}$-$1_{0,1}$ A^+)	94407.13	6.80	3.17E-06	3.08	0.47	5.53	1.59	0.022	0.003	0.16	0.03	
33502	$^{13}CH_3OH$ ($2_{0,2}$-$1_{0,1}$ A^+)	94411.02	19.91	3.17E-06	3.66	0.54	3.52	1.30	0.019	0.006	0.09	0.02	
33502	$^{13}CH_3OH$ ($2_{1,1}$-$1_{1,0}$ A^-)	95208.66	21.41	2.44E-06	2.65	0.19	6.21	0.47	0.050	0.003	0.41	0.05	
33502	$^{13}CH_3OH$ ($3_{0,3}$-$2_{0,2}$ A^+)	141602.53	13.59	1.15E-05	2.72	0.21	3.89	0.54	0.066	0.007	0.36	0.07	
33502	$^{13}CH_3OH$ ($8_{+0,8}$-$8_{-1,8}$ E)	155695.81	94.59	1.77E-05	2.12	0.15	2.96	0.39	0.070	0.007	0.30	0.06	
33502	$^{13}CH_3OH$ ($5_{0,5}$-$4_{0,4}$ A^+)	235881.17	47.08	5.61E-05	2.90	0.09	3.31	0.23	0.088	0.005	0.54	0.10	
33502	$^{13}CH_3OH$ ($5_{1,4}$-$4_{1,3}$ A^-)	237983.38	48.82	5.54E-05	3.15	0.26	5.95	0.67	0.073	0.007	0.82	0.15	
(*)	CH_2DOH ($2_{0,2}$-$1_{0,1}$ o1)	89251.20	17.20		3.50	0.29	5.86	0.78	0.029	0.030	0.23	0.02	
(*)	CH_2DOH ($2_{0,2}$-$1_{0,1}$ e1)	89275.40	13.80		3.16	0.40	5.15	1.02	0.028	0.003	0.19	0.03	
(*)	CH_2DOH ($2_{0,2}$-$1_{0,1}$ e0)	89407.90	4.50		3.09	0.15	5.26	0.36	0.038	0.003	0.26	0.02	
(*)	CH_2DOH ($3_{0,3}$-$2_{0,2}$ e1)	133847.30	18.30		2.23	0.50	6.71	0.50	0.078	0.014	0.56	0.10	
(*)	CH_2DOH ($3_{0,3}$-$2_{0,2}$ o1)	133872.90	21.70		2.91	0.50	4.47	0.50	0.085	0.014	0.39	0.08	
(*)	CH_2DOH ($3_{2,2}$-$2_{2,1}$ o1)	133881.80	33.60		1.83	0.81	6.16	2.34	0.053	0.016	0.35	0.12	
(*)	CH_2DOH ($3_{2,2}$-$2_{2,1}$ e0)	134112.40	20.20		1.97	0.50	6.69	0.50	0.057	0.009	0.41	0.07	
(*)	CH_2DOH ($3_{2,1}$-$2_{2,0}$ e0)	134185.40	20.20		3.00	0.66	5.70	2.14	0.072	0.010	0.31	0.10	
(*)	CH_2DOH ($2_{1,2}$-$3_{0,3}$ e0)	207780.80	15.90		2.17	0.60	6.65	2.13	0.085	0.013	0.60	0.19	
(*)	CH_2DOH ($5_{2,3}$-$4_{1,4}$ e1)	223071.30	33.60		2.89	1.02	5.75	2.25	0.081	0.020	0.99	0.30	
(*)	CH_2DOH ($5_{2,3}$-$4_{2,2}$ e1)	223315.40	40.80		2.23	0.30	4.70	0.50	0.083	0.009	0.83	0.08	
(*)	CH_2DOH ($5_{2,4}$-$4_{2,3}$ e0)	223422.30	33.60		3.87	0.35	7.54	0.80	0.095	0.025	1.26	0.12	
(*)	CHD_2OH (2_0-1_0 e1)	83129.20	16.98		3.71	0.64	3.40	0.50	0.017	0.006	0.10	0.02	
(*)	CHD_2OH (2_0-1_0 e0)	83289.50	4.17		3.28	0.74	7.74	2.05	0.020	0.006	0.20	0.04	
(*)	CHD_2OH (4_{2-}-3_{2-} e1)	166271.00	35.65		3.78	0.67	4.15	0.50	0.057	0.010	0.43	0.09	
(*)	CHD_2OH (4_{3+}-3_{3-} e1)	166297.00	46.54		2.55	0.44	3.60	0.50	0.080	0.009	0.52	0.07	
(*)	CHD_2OH (4_{2+}-3_{2+} e1)	166304.00	35.65		2.00	0.49	3.64	0.50	0.070	0.009	0.42	0.07	
(*)	CHD_2OH (5_0-4_0 e1)	207771.00	33.63		1.90	1.26	5.85	0.50	0.051	0.013	0.51	0.13	
(*)	CHD_2OH (5_{3-}-4_{3-} e1)	207868.00	53.48		1.69	1.02	4.94	0.50	0.048	0.013	0.43	0.11	
(*)	CH_3OD (3_1-3_0)	110475.80	15.40		2.36	0.45	2.33	0.93	0.016	0.005	0.06	0.02	
(*)	CH_3OD (1_{1-}-1_{1+})	133925.40	6.00		2.56	0.53	4.00	0.50	0.046	0.009	0.32	0.06	
(*)	CH_3OD (5_{1+}-4_{1+})	223308.60	26.80		1.63	0.42	4.00	0.50	0.052	0.009	0.83	0.14	
(*)	CH_3OD (5_{0+}-4_{0+})	226538.70	22.70		3.67	0.53	5.49	1.36	0.110	0.015	1.05	0.20	
(*)	CD_3OH (4_1-3_1 E2)	156237.02	21.50		2.48	0.44	2.48	0.50	0.054	0.007	0.21	0.04	
(*)	CD_3OH (4_2-3_2 A-)	156239.30	42.00		2.20	0.38	2.12	0.50	0.051	0.007	0.17	0.04	
(*)	CD_3OH (1_0-1_1 E2)	160753.93	12.20		2.62	0.25	1.50	0.50	0.047	0.011	0.10	0.03	
29507	HCO^+ (1-0)	89188.53	4.28	4.19E-05	3.41	0.26	3.63	0.62	3.211	0.477	15.11	1.66	self-abs
29507	HCO^+ (3-2)	267557.63	25.68	1.45E-03	3.35	0.09	3.71	0.21	8.559	0.430	69.33	11.79	

Table 4. continued.

TAG	Species & Transition	Frequency (MHz)	E_{up} (K)	A_{ij} s^{-1}	V_o (km s^{-1})	δ_{V_o}	$FWHM$ (km s^{-1})	δ_{FWHM}	Int (K)	δ_{Int}	Flux (K km s^{-1})	δ_{Flux}	Comments
29507	HCO^+ (4-3)	356734.22	42.80	3.57E-03	3.10	0.05	1.27	0.12	24.109	1.904	59.73	10.75	self-abs
30504	$H^{13}CO^+$ (1-0)	86754.29	4.16	3.85E-05	4.17	0.04	2.13	0.08	1.581	0.055	4.36	0.48	
30504	$H^{13}CO^+$ (2-1)	173506.70	12.49	3.70E-04	4.48	0.07	2.14	0.15	2.347	0.146	7.71	1.31	
30504	$H^{13}CO^+$ (3-2)	260255.34	24.98	1.34E-03	3.60	0.03	3.07	0.08	1.662	0.035	10.48	1.78	
30504	$H^{13}CO^+$ (4-3)	346998.34	41.63	3.29E-03	3.52	0.05	2.39	0.11	1.943	0.079	8.97	1.61	
30510	DCO^+ (2-1)	144077.29	10.37	2.12E-04	4.32	0.01	1.44	0.03	2.638	0.052	5.44	0.92	
30510	DCO^+ (3-2)	216112.58	20.74	7.66E-04	4.39	0.03	3.08	0.09	1.082	0.023	5.78	0.98	
30510	DCO^+ (5-4)	360169.78	51.86	3.76E-03	3.86	0.09	2.51	0.22	0.616	0.046	3.04	0.55	
31506	$HC^{18}O^+$ (1-0)	85162.22	4.09	3.64E-05	4.18	0.03	1.93	0.08	0.176	0.006	0.44	0.05	
31506	$HC^{18}O^+$ (2-1)	170322.63	12.26	3.50E-04	4.33	0.06	1.78	0.15	0.293	0.021	0.80	0.14	
31506	$HC^{18}O^+$ (3-2)	255479.39	24.52	1.27E-03	3.62	0.16	2.73	0.39	0.067	0.008	0.37	0.07	
31508	$D^{13}CO^+$ (2-1)	141465.13	10.18	2.00E-04	4.40	0.07	1.38	0.16	0.163	0.016	0.32	0.06	
31508	$D^{13}CO^+$ (3-2)	212194.49	20.37	7.25E-04	4.63	0.26	3.30	0.56	0.049	0.007	0.28	0.05	
30505	$HC^{17}O^+$ (2-1)	174113.17	12.53	3.74E-04	3.94	0.22	4.03	0.71	0.056	0.006	0.35	0.07	
44501	CS (2-1)	97980.95	7.05	1.68E-05	3.88	0.08	3.54	0.18	3.393	0.150	15.80	1.74	small wings
44501	CS (3-2)	146969.03	14.11	6.07E-05	3.66	0.14	3.69	0.33	5.353	0.414	28.54	4.85	self-abs
44501	CS (5-4)	244935.56	35.27	2.98E-04	3.65	0.10	4.02	0.25	5.689	0.300	44.06	7.49	
44501	CS (7-6)	342882.85	65.83	8.40E-04	3.62	0.06	2.98	0.14	6.638	0.270	38.06	6.85	small wings
46501	$C^{34}S$ (2-1)	96412.95	6.94	1.60E-05	3.83	0.05	2.80	0.13	0.548	0.021	2.01	0.22	
46501	$C^{34}S$ (3-2)	144617.10	13.88	5.78E-05	3.68	0.07	3.40	0.17	0.834	0.036	4.08	0.69	
46501	$C^{34}S$ (5-4)	241016.09	34.70	2.84E-04	3.58	0.06	4.44	0.15	1.102	0.031	9.27	1.58	
46501	$C^{34}S$ (7-6)	337396.46	64.77	8.00E-04	3.44	0.06	3.74	0.13	0.808	0.025	5.77	1.04	
45501	^{13}CS (2-1)	92494.31	6.66	1.41E-05	3.86	0.08	3.00	0.19	0.213	0.012	0.83	0.09	
45501	^{13}CS (3-2)	138739.33	13.32	5.11E-05	3.80	0.12	3.59	0.27	0.331	0.022	1.69	0.29	
45501	^{13}CS (5-4)	231220.68	33.29	2.51E-04	3.38	0.12	5.18	0.29	0.459	0.022	4.35	0.74	
45501	^{13}CS (6-5)	277455.41	46.61	4.40E-04	3.73	0.12	4.48	0.29	0.215	0.012	2.14	0.37	
45502	$C^{33}S$ (2-1)	97172.06	7.00	1.64E-05	4.64	0.09	2.63	0.20	0.093	0.006	0.32	0.04	
45502	$C^{33}S$ (3-2)	145755.73	13.99	5.92E-05	3.39	0.14	6.46	0.32	0.124	0.005	1.16	0.20	hf structure
45502	$C^{33}S$ (5-4)	242913.61	34.98	2.91E-04	3.15	0.09	5.61	0.21	0.318	0.010	3.41	0.58	
45502	$C^{33}S$ (7-6)	340052.58	65.28	8.19E-04	3.54	0.11	5.51	0.26	0.217	0.009	2.29	0.41	
27501	HCN (1-0)	88631.60	4.25	2.41E-05	4.46	0.33	9.50	0.79	1.765	0.127	21.71	2.39	hf structure
27501	HCN (3-2)	265886.43	25.52	8.36E-04	3.00	0.22	5.94	0.51	2.812	0.209	35.12	5.97	
27501	HCN (4-3)	354505.48	42.54	2.05E-03	3.25	0.26	5.73	0.60	3.637	0.331	40.65	7.32	self abs
28002	$H^{13}CN$ (1_2-0_1)	86340.18	4.14	2.22E-05	3.88	0.09	2.91	0.25	0.284	0.009	1.04	0.12	hf structure
28002	$H^{13}CN$ (1_1-0_1)	86338.77	4.14	2.22E-05	3.84	0.06	2.87	0.17	0.191	0.005	0.75	0.09	hf structure
28002	$H^{13}CN$ (1_0-0_1)	86342.27	4.14	2.22E-05	3.81	0.13	2.46	0.33	0.079	0.008	0.25	0.03	hf structure
28002	$H^{13}CN$ (3-2)	259011.82	24.86	6.48E-04	3.32	0.58	6.63	2.62	0.600	0.080	8.16	1.39	
28002	$H^{13}CN$ (4-3)	345339.76	41.44	1.90E-03	4.00	0.09	5.39	0.23	0.664	0.022	6.90	1.24	
28509	DCN (2-1)	144828.00	10.43	1.27E-04	4.16	0.21	4.24	0.56	0.635	0.062	3.88	0.66	
28509	DCN (3-2)	217238.54	20.85	4.57E-04	3.36	0.07	4.54	0.19	0.440	0.013	3.49	0.59	
28509	DCN (5-4)	362045.75	52.13	2.25E-03	3.38	0.06	3.48	0.24	0.570	0.015	3.90	0.70	odd profile
28003	$HC^{15}N$ (1-0)	86054.96	4.13	2.20E-05	4.03	0.18	3.51	0.43	0.114	0.012	0.51	0.06	
28003	$HC^{15}N$ (2-1)	172107.96	12.39	2.11E-04	3.29	0.16	5.37	0.41	0.228	0.014	1.88	0.32	
28003	$HC^{15}N$ (3-2)	258157.10	24.78	7.65E-04	3.70	0.07	6.81	0.21	0.186	0.003	2.57	0.45	

Table 4. continued.

TAG	Species & Transition	Frequency (MHz)	E_{up} (K)	A_{ij} s^{-1}	V_o (km s^{-1})	δ_{V_o}	$FWHM$ (km s^{-1})	δ_{FWHM}	Int (K)	δ_{Int}	Flux (K km s^{-1})	δ_{Flux}	Comments
28003	$HC^{15}N$ (4-3)	344200.32	41.30	1.88E-03	3.39	0.36	6.38	0.99	0.122	0.012	1.49	0.27	
44003	CH_3CHO ($5_{1,5}$-$4_{1,4}$ A)	93580.86	15.75	2.53E-05	3.15	0.23	2.52	0.56	0.041	0.008	0.13	0.02	
44003	CH_3CHO ($5_{1,5}$-$4_{1,4}$ E)	93595.28	15.82	2.53E-05	3.14	0.17	2.70	0.40	0.046	0.006	0.16	0.02	
44003	CH_3CHO ($5_{0,5}$-$4_{0,4}$ E)	95947.34	13.93	2.84E-05	2.88	0.13	2.60	0.32	0.053	0.006	0.18	0.02	
44003	CH_3CHO ($5_{0,5}$-$4_{0,4}$ A)	95963.38	13.84	2.84E-05	2.82	0.11	2.93	0.25	0.061	0.005	0.24	0.03	
44003	CH_3CHO ($5_{2,4}$-$4_{2,3}$ A)	96274.20	22.93	2.41E-05	2.66	0.05	2.26	0.11	0.055	0.002	0.16	0.02	
44003	CH_3CHO ($5_{4,1}$-$4_{4,0}$ E)	96353.16	49.99	1.04E-05	2.40	0.12	2.43	0.28	0.035	0.004	0.11	0.02	
44003	CH_3CHO ($5_{4,2}$-$4_{4,1}$ E)	96360.78	49.95	1.04E-05	2.67	0.15	2.19	0.34	0.028	0.004	0.08	0.01	
44003	CH_3CHO ($5_{3,2}$-$4_{3,1}$ E)	96368.35	34.26	1.85E-05	3.35	0.19	3.58	0.52	0.048	0.005	0.22	0.03	
44003	CH_3CHO ($5_{3,2}$-$4_{3,1}$ A)	96371.75	34.26	1.85E-05	2.59	0.16	2.31	0.39	0.033	0.005	0.10	0.02	
44003	CH_3CHO ($5_{3,3}$-$4_{3,2}$ E)	96384.40	34.16	1.85E-05	3.27	0.43	3.53	1.13	0.033	0.008	0.16	0.02	
44003	CH_3CHO ($5_{2,4}$-$4_{2,3}$ E)	96425.62	22.91	2.41E-05	2.83	0.09	1.88	0.21	0.055	0.005	0.13	0.02	
44003	CH_3CHO ($5_{2,3}$-$4_{2,2}$ E)	96475.54	23.03	2.42E-05	3.03	0.13	2.15	0.29	0.048	0.006	0.13	0.02	
44003	CH_3CHO ($5_{2,3}$-$4_{2,2}$ A)	96632.63	22.96	2.44E-05	2.84	0.16	2.20	0.37	0.041	0.006	0.12	0.02	
44003	CH_3CHO ($5_{1,4}$-$4_{1,3}$ E)	98863.33	16.59	2.99E-05	3.15	0.05	2.35	0.11	0.064	0.003	0.20	0.02	
44003	CH_3CHO ($5_{1,4}$-$4_{1,3}$ A)	98900.95	16.51	2.99E-05	3.10	0.11	2.46	0.25	0.057	0.005	0.19	0.02	
44003	CH_3CHO ($6_{1,6}$-$5_{1,5}$ A)	112248.73	21.13	4.50E-05	3.08	0.18	3.06	0.46	0.062	0.007	0.26	0.04	
44003	CH_3CHO ($6_{1,6}$-$5_{1,5}$ E)	112254.52	21.21	4.50E-05	2.91	0.10	2.70	0.23	0.083	0.006	0.30	0.04	
44003	CH_3CHO ($6_{0,6}$-$5_{0,5}$ E)	114940.19	19.45	4.96E-05	3.23	0.16	4.02	0.45	0.068	0.005	0.37	0.04	
44003	CH_3CHO ($6_{0,6}$-$5_{0,5}$ A)	114959.91	19.35	4.96E-05	3.31	0.12	3.16	0.29	0.067	0.005	0.29	0.03	
44003	CH_3CHO ($6_{2,5}$-$5_{2,4}$ A)	115493.94	28.48	4.48E-05	3.21	0.19	4.10	0.54	0.049	0.005	0.27	0.04	
44003	CH_3CHO ($7_{0,7}$-$6_{0,6}$ E)	133830.49	25.87	7.92E-05	2.93	0.06	2.36	0.14	0.119	0.006	0.39	0.07	
44003	CH_3CHO ($7_{0,7}$-$6_{0,6}$ A)	133854.10	25.78	7.92E-05	3.69	0.30	3.74	0.79	0.114	0.014	0.60	0.11	
44003	CH_3CHO ($7_{2,6}$-$6_{2,5}$ A)	134694.45	34.94	7.42E-05	3.34	0.19	3.11	0.50	0.078	0.010	0.34	0.06	
44003	CH_3CHO ($7_{6,1}$-$6_{6,0}$ E)	134877.32	107.11	2.15E-05	3.18	0.20	2.15	0.47	0.040	0.008	0.12	0.02	
44003	CH_3CHO ($7_{5,2}$-$6_{5,1}$ E)	134900.24	82.29	3.98E-05	2.50	0.13	1.54	0.31	0.068	0.012	0.15	0.03	
44003	CH_3CHO ($7_{5,3}$-$6_{5,2}$ E)	134905.47	82.25	3.98E-05	2.66	0.10	1.63	0.22	0.095	0.011	0.22	0.04	
44003	CH_3CHO ($7_{4,3}$-$6_{4,2}$ E)	134922.26	62.02	5.47E-05	2.57	0.17	3.65	0.47	0.072	0.007	0.37	0.06	
44003	CH_3CHO ($7_{4,4}$-$6_{4,3}$ E)	134933.40	61.97	5.47E-05	2.74	0.17	1.64	0.39	0.075	0.015	0.17	0.03	
44003	CH_3CHO ($7_{3,5}$-$6_{3,4}$ A)	134963.33	46.28	6.64E-05	2.90	0.16	2.02	0.38	0.056	0.009	0.16	0.03	
44003	CH_3CHO ($7_{3,4}$-$6_{3,3}$ E)	134973.05	46.29	6.64E-05	2.45	0.13	2.87	0.32	0.065	0.006	0.26	0.04	
44003	CH_3CHO ($7_{3,4}$-$6_{3,3}$ A)	134987.26	46.29	6.64E-05	2.56	0.12	2.72	0.26	0.082	0.007	0.33	0.06	
44003	CH_3CHO ($19_{2,17}$-$19_{1,18}$ A)	135272.97	187.63	1.23E-05	2.60	0.23	1.99	0.55	0.064	0.015	0.18	0.03	
44003	CH_3CHO ($7_{2,5}$-$6_{2,4}$ E)	135476.68	35.09	7.40E-05	2.96	0.11	2.85	0.27	0.089	0.007	0.36	0.06	
44003	CH_3CHO ($7_{1,6}$-$6_{1,5}$ E)	138284.88	28.92	8.57E-05	2.99	0.21	2.56	0.50	0.069	0.012	0.25	0.04	
44003	CH_3CHO ($7_{1,6}$-$6_{1,5}$ A)	138319.75	28.85	8.57E-05	3.30	0.12	4.11	0.33	0.072	0.004	0.42	0.07	
44003	CH_3CHO ($8_{1,8}$-$7_{1,7}$ A)	149507.55	34.59	1.10E-04	3.37	0.20	3.80	0.56	0.109	0.012	0.60	0.11	
44003	CH_3CHO ($6_{1,6}$-$5_{0,5}$ A)	152048.58	21.13	1.28E-05	2.90	0.33	4.00	0.88	0.054	0.009	0.31	0.06	
44003	CH_3CHO ($8_{0,8}$-$7_{0,7}$ A)	152635.07	33.10	1.18E-04	2.72	0.29	3.95	0.78	0.072	0.011	0.42	0.08	
44003	CH_3CHO ($6_{2,5}$-$6_{1,6}$ A)	153004.35	28.48	1.04E-05	2.71	0.12	2.50	0.29	0.035	0.004	0.13	0.03	
44003	CH_3CHO ($8_{7,1}$-$7_{7,0}$ E)	154131.38	143.81	2.86E-05	2.76	0.11	1.59	0.25	0.060	0.008	0.14	0.03	
44003	CH_3CHO ($8_{7,1}$-$7_{7,0}$ A)	154145.47	143.74	2.86E-05	2.03	0.23	1.94	0.54	0.077	0.018	0.22	0.04	
44003	CH_3CHO ($8_{7,2}$-$7_{7,1}$ A)	154145.47	143.74	2.86E-05	2.03	0.23	1.94	0.54	0.077	0.018	0.22	0.04	
44003	CH_3CHO ($8_{6,2}$-$7_{6,1}$ E)	154151.99	114.50	5.35E-05	2.97	0.14	1.80	0.33	0.049	0.008	0.13	0.03	
44003	CH_3CHO ($8_{6,3}$-$7_{6,2}$ E)	154173.84	114.41	5.35E-05	2.32	0.10	1.56	0.24	0.073	0.010	0.17	0.03	
44003	CH_3CHO ($8_{5,3}$-$7_{5,2}$ E)	154182.91	89.69	7.45E-05	2.93	0.28	3.74	0.74	0.046	0.007	0.25	0.05	
44003	CH_3CHO ($8_{5,4}$-$7_{5,3}$ E)	154188.54	89.65	7.45E-05	2.68	0.17	2.02	0.40	0.075	0.013	0.22	0.04	

Table 4. continued.

TAG	Species & Transition	Frequency (MHz)	E_{up} (K)	A_{ij} s^{-1}	V_o (km s^{-1})	δ_{V_o}	*FWHM* (km s^{-1})	δ_{FWHM}	Int (K)	δ_{Int}	Flux (K km s^{-1})	δ_{Flux}	Comments
44003	CH_3CHO ($8_{4,4}$-$7_{4,3}$ A)	154201.47	69.49	9.18E-05	2.75	0.07	2.82	0.17	0.115	0.006	0.48	0.08	
44003	CH_3CHO ($8_{3,6}$-$7_{3,5}$ A)	154274.72	53.69	1.05E-04	3.01	0.08	3.36	0.20	0.077	0.004	0.38	0.07	
44003	CH_3CHO ($8_{3,5}$-$7_{3,4}$ E)	154296.57	53.69	1.05E-04	2.51	0.10	1.90	0.24	0.092	0.010	0.26	0.05	
44003	CH_3CHO ($8_{2,6}$-$7_{2,5}$ E)	155179.64	42.54	1.15E-04	3.07	0.17	2.83	0.43	0.103	0.013	0.43	0.08	
44003	CH_3CHO ($8_{2,6}$-$7_{2,5}$ A)	155342.11	42.50	1.17E-04	3.07	0.16	3.17	0.41	0.086	0.009	0.40	0.07	
44003	CH_3CHO ($8_{1,7}$-$7_{1,6}$ E)	157937.75	36.50	1.29E-04	3.27	0.14	2.60	0.35	0.112	0.013	0.43	0.08	
44003	CH_3CHO ($8_{1,7}$-$7_{1,6}$ A)	157974.71	36.43	1.29E-04	3.14	0.19	2.86	0.45	0.097	0.013	0.41	0.07	
44003	CH_3CHO ($8_{2,7}$-$8_{1,8}$ E)	159691.61	42.33	1.08E-05	2.74	0.32	3.47	0.81	0.031	0.006	0.16	0.03	
44003	CH_3CHO ($10_{0,10}$-$9_{1,9}$ A)	162043.81	50.44	1.57E-05	2.68	0.08	2.46	0.19	0.054	0.004	0.20	0.04	
44003	CH_3CHO ($10_{0,10}$-$9_{1,9}$ E)	162371.09	50.53	1.57E-05	2.72	0.21	1.41	0.50	0.046	0.014	0.10	0.02	
44003	CH_3CHO ($9_{2,8}$-$9_{1,9}$ E)	164727.07	50.64	1.21E-05	2.29	0.07	2.36	0.17	0.066	0.004	0.24	0.05	
44003	CH_3CHO ($7_{1,7}$-$6_{0,6}$ A)	167980.42	27.42	1.75E-05	2.73	0.16	3.90	0.44	0.070	0.006	0.41	0.08	
44003	CH_3CHO ($9_{1,9}$-$8_{1,8}$ E)	168088.65	42.73	1.57E-04	4.28	0.32	3.81	0.81	0.111	0.014	0.64	0.12	
44003	CH_3CHO ($9_{1,9}$-$8_{1,8}$ A)	168093.48	42.66	1.57E-04	3.18	0.17	3.08	0.42	0.115	0.013	0.54	0.10	
44003	CH_3CHO ($9_{0,9}$-$8_{0,8}$ A)	171296.97	41.32	1.68E-04	2.53	0.20	2.10	0.48	0.102	0.020	0.33	0.06	
44003	CH_3CHO ($9_{8,1}$-$8_{8,0}$ E)	173388.23	185.90	3.67E-05	2.43	0.17	2.22	0.39	0.040	0.006	0.14	0.04	
44003	CH_3CHO ($9_{6,4}$-$8_{6,3}$ E)	173453.47	122.74	9.73E-05	2.65	0.19	2.29	0.45	0.067	0.011	0.24	0.05	
44003	CH_3CHO ($9_{3,7}$-$8_{3,6}$ A)	173594.97	62.02	1.56E-04	2.74	0.15	4.29	0.44	0.077	0.005	0.51	0.10	
44003	CH_3CHO ($9_{2,7}$-$8_{2,6}$ E)	174982.61	50.94	1.70E-04	3.61	0.17	2.85	0.43	0.090	0.011	0.40	0.08	
44003	CH_3CHO ($10_{1,9}$-$9_{1,8}$ E)	197094.46	54.48	2.56E-04	3.26	0.50	3.43	1.10	0.077	0.021	0.43	0.08	
44003	CH_3CHO ($14_{2,13}$-$14_{1,14}$ E)	198062.33	105.90	1.88E-05	3.56	0.25	3.36	0.49	0.027	0.002	0.09	0.03	
44003	CH_3CHO ($9_{1,9}$-$8_{0,8}$ E)	198698.17	42.73	3.03E-05	3.50	0.36	3.36	0.84	0.015	0.003	0.08	0.03	
44003	CH_3CHO ($18_{3,15}$-$18_{2,16}$ A)	199332.25	179.21	3.23E-05	2.90	0.44	2.80	1.13	0.036	0.012	0.16	0.04	
44003	CH_3CHO ($11_{1,11}$-$10_{1,10}$ E)	205161.94	61.54	2.90E-04	2.81	0.31	4.40	0.81	0.080	0.011	0.59	0.10	
44003	CH_3CHO ($11_{1,11}$-$10_{1,10}$ A)	205170.70	61.46	2.90E-04	3.01	0.11	4.13	0.29	0.065	0.004	0.45	0.08	
44003	CH_3CHO ($11_{0,11}$-$10_{0,10}$ A)	208267.03	60.43	3.05E-04	3.22	0.19	3.95	0.49	0.065	0.061	0.43	0.08	
44003	CH_3CHO ($16_{3,13}$-$16_{2,14}$ A)	208730.58	146.56	3.46E-05	3.07	0.24	2.28	0.59	0.052	0.011	0.20	0.04	
44003	CH_3CHO ($11_{2,10}$-$10_{2,9}$ A)	211243.10	69.99	3.09E-04	3.68	0.29	4.14	0.72	0.070	0.010	0.50	0.09	
44003	CH_3CHO ($11_{2,10}$-$10_{2,9}$ E)	211273.76	70.00	3.09E-04	3.57	0.28	3.82	0.69	0.064	0.010	0.41	0.07	
44003	CH_3CHO ($11_{6,6}$-$10_{6,5}$ E)	212021.55	142.16	2.27E-04	2.77	0.21	3.49	0.47	0.049	0.006	0.29	0.05	
44003	CH_3CHO ($11_{5,6}$-$10_{5,5}$ E)	212059.55	117.44	2.56E-04	2.63	0.20	3.93	0.50	0.060	0.006	0.40	0.07	
44003	CH_3CHO ($11_{5,7}$-$10_{5,6}$ E)	212066.05	117.41	2.56E-04	2.29	0.39	3.59	0.92	0.059	0.013	0.36	0.07	
44003	CH_3CHO ($11_{4,8}$-$10_{4,7}$ A)	212128.40	97.25	2.81E-04	3.55	0.15	3.58	0.37	0.061	0.005	0.38	0.07	
44003	CH_3CHO ($11_{4,7}$-$10_{4,6}$ A)	212134.15	97.25	2.81E-04	2.28	0.20	3.96	0.47	0.056	0.006	0.38	0.07	
44003	CH_3CHO ($11_{4,7}$-$10_{4,6}$ E)	212151.90	97.18	2.81E-04	2.46	0.34	4.30	0.82	0.056	0.009	0.41	0.07	
44003	CH_3CHO ($11_{4,8}$-$10_{4,7}$ E)	212171.48	97.14	2.81E-04	2.77	0.27	4.46	0.64	0.053	0.007	0.41	0.07	
44003	CH_3CHO ($11_{3,9}$-$10_{3,8}$ A)	212257.12	81.47	3.00E-04	2.82	0.10	4.39	0.27	0.081	0.004	0.61	0.11	
44003	CH_3CHO ($11_{3,9}$-$10_{3,8}$ E)	212384.72	81.39	2.99E-04	2.95	0.17	4.35	0.43	0.064	0.005	0.48	0.08	
44003	CH_3CHO ($11_{3,8}$-$10_{3,7}$ E)	212400.95	81.48	3.00E-04	2.99	0.11	4.85	0.32	0.079	0.004	0.66	0.11	
44003	CH_3CHO ($10_{1,1}$-$9_{0,9}$ A)	214443.39	51.62	3.93E-05	2.39	0.67	3.57	1.70	0.034	0.013	0.21	0.05	
44003	CH_3CHO ($11_{2,9}$-$10_{2,8}$ E)	214800.80	70.60	3.24E-04	3.01	0.28	3.35	0.67	0.130	0.022	0.75	0.13	
44003	CH_3CHO ($11_{2,9}$-$10_{2,8}$ A)	214845.02	70.57	3.25E-04	3.79	0.33	3.48	0.81	0.112	0.022	0.67	0.12	
44003	CH_3CHO ($4_{2,2}$-$3_{1,2}$ E)	215604.58	18.40	1.48E-05	2.55	0.40	2.86	0.89	0.032	0.009	0.16	0.04	
44003	CH_3CHO ($16_{2,15}$-$16_{1,16}$ A)	216435.02	134.36	2.31E-05	2.35	0.21	2.48	0.48	0.035	0.006	0.15	0.04	
44003	CH_3CHO ($14_{3,11}$-$14_{2,12}$ E)	216534.44	117.68	3.32E-05	2.84	0.26	2.24	0.53	0.041	0.008	0.16	0.04	
44003	CH_3CHO ($11_{1,10}$-$10_{1,9}$ E)	216581.94	64.87	3.41E-04	3.36	0.21	4.11	0.53	0.084	0.009	0.60	0.11	
44003	CH_3CHO ($11_{1,10}$-$10_{1,9}$ A)	216630.22	64.81	3.41E-04	3.03	0.13	3.62	0.34	0.069	0.005	0.43	0.08	

Table 4. continued.

TAG	Species & Transition	Frequency (MHz)	E_{up} (K)	A_{ij} s^{-1}	V_o (km s^{-1})	δ_{V_o}	$FWHM$ (km s^{-1})	δ_{FWHM}	Int (K)	δ_{Int}	Flux (K km s^{-1})	δ_{Flux}	Comments
44003	CH_3CHO ($12_{1,12}$-$11_{1,11}$ E)	223649.88	72.27	3.78E-04	3.03	0.31	3.61	0.75	0.089	0.016	0.57	0.10	
44003	CH_3CHO ($12_{1,12}$-$11_{1,11}$ A)	223660.42	72.20	3.78E-04	2.63	0.32	3.66	0.79	0.103	0.018	0.67	0.12	
44003	CH_3CHO ($12_{3,9}$-$12_{2,10}$ E)	223909.92	92.61	2.95E-05	2.47	0.20	2.08	0.74	0.039	0.011	0.14	0.03	
44003	CH_3CHO ($13_{0,13}$-$12_{1,12}$ A)	226256.31	83.06	4.91E-05	2.72	0.10	2.25	0.46	0.070	0.012	0.29	0.05	
44003	CH_3CHO ($13_{0,13}$-$12_{1,12}$ E)	226487.69	83.14	4.90E-05	2.75	0.47	4.00	1.12	0.057	0.013	0.41	0.08	
44003	CH_3CHO ($12_{0,12}$-$11_{0,11}$ E)	226551.59	71.39	3.94E-04	2.55	0.21	2.36	0.42	0.196	0.032	0.83	0.14	
44003	CH_3CHO ($12_{0,12}$-$11_{0,11}$ A)	226592.71	71.31	3.94E-04	2.68	0.12	2.37	0.25	0.155	0.015	0.66	0.11	
44003	CH_3CHO ($11_{3,8}$-$11_{2,9}$ E)	226857.71	81.48	2.78E-05	2.95	0.33	3.08	0.77	0.086	0.019	0.48	0.08	
44003	CH_3CHO ($11_{3,8}$-$11_{2,9}$ A)	227514.36	81.49	3.90E-05	2.43	0.12	1.55	0.16	0.072	0.006	0.20	0.04	
44003	CH_3CHO ($12_{2,11}$-$11_{2,10}$ A)	230301.88	81.04	4.04E-04	2.79	0.21	3.93	0.55	0.063	0.007	0.45	0.08	
44003	CH_3CHO ($12_{6,7}$-$11_{6,6}$ E)	231310.46	153.26	3.16E-04	2.12	0.26	3.79	0.66	0.068	0.010	0.47	0.09	
44003	CH_3CHO ($12_{5,7}$-$11_{5,6}$ E)	231363.29	128.54	3.48E-04	2.55	0.34	2.51	0.92	0.067	0.020	0.31	0.06	
44003	CH_3CHO ($12_{5,8}$-$11_{5,7}$ E)	231369.74	128.51	3.48E-04	2.42	0.09	2.30	0.46	0.083	0.013	0.35	0.07	
44003	CH_3CHO ($12_{4,9}$-$11_{4,8}$ A)	231456.80	108.35	3.75E-04	2.93	0.29	2.67	0.57	0.085	0.016	0.42	0.08	
44003	CH_3CHO ($12_{4,8}$-$11_{4,7}$ A)	231467.49	108.36	3.75E-04	2.72	0.08	3.49	0.20	0.083	0.004	0.53	0.10	
44003	CH_3CHO ($12_{4,8}$-$11_{4,7}$ E)	231484.29	108.29	3.75E-04	2.63	0.19	3.56	0.46	0.078	0.008	0.51	0.09	
44003	CH_3CHO ($12_{3,1}$-$11_{3,9}$ A)	231595.18	92.58	3.96E-04	2.33	0.18	1.60	0.33	0.117	0.019	0.34	0.06	
44003	CH_3CHO ($12_{3,1}$-$11_{3,9}$ E)	231748.89	92.51	3.94E-04	2.88	0.40	2.62	0.90	0.112	0.034	0.54	0.10	
44003	CH_3CHO ($12_{3,9}$-$11_{3,8}$ E)	231847.62	92.61	3.94E-04	2.65	0.04	1.94	0.07	0.107	0.003	0.38	0.07	
44003	CH_3CHO ($12_{3,9}$-$11_{3,8}$ A)	231968.42	92.63	3.98E-04	2.79	0.29	5.27	0.81	0.153	0.016	1.48	0.26	
44003	CH_3CHO ($5_{2,4}$-$4_{1,3}$ A)	232691.37	22.93	3.10E-05	2.48	0.25	1.89	0.42	0.041	0.008	0.14	0.03	
44003	CH_3CHO ($5_{2,3}$-$4_{1,3}$ E)	232981.31	23.03	1.34E-05	3.69	0.34	3.70	0.82	0.031	0.006	0.21	0.05	
44003	CH_3CHO ($6_{3,3}$-$6_{2,4}$ E)	233845.39	39.81	3.38E-05	2.64	0.24	4.04	0.66	0.065	0.006	0.48	0.09	
44003	CH_3CHO ($12_{2,10}$-$11_{2,9}$ E)	234795.46	81.87	4.28E-04	3.42	0.31	3.82	0.82	0.062	0.010	0.44	0.08	
44003	CH_3CHO ($12_{2,10}$-$11_{2,9}$ A)	234825.83	81.84	4.28E-04	3.11	0.10	2.27	0.21	0.053	0.005	0.22	0.05	
44003	CH_3CHO ($10_{3,8}$-$10_{2,9}$ A)	238092.28	71.28	4.26E-05	3.36	0.42	3.29	1.00	0.052	0.013	0.32	0.06	
44003	CH_3CHO ($12_{3,10}$-$1_{2,11}$ E)	238677.10	92.51	3.41E-05	2.36	0.27	3.25	0.64	0.046	0.008	0.28	0.05	
44003	CH_3CHO ($11_{3,9}$-$11_{2,10}$ A)	239106.30	81.47	4.37E-05	2.79	0.24	2.54	0.79	0.039	0.010	0.19	0.05	
44003	CH_3CHO ($13_{3,1}$-$13_{2,12}$ A)	242010.29	104.62	4.61E-05	2.40	0.44	1.56	0.59	0.039	0.007	0.12	0.03	
44003	CH_3CHO ($13_{1,1}$-$12_{1,12}$ E)	242106.02	83.89	4.81E-04	3.33	0.25	3.58	0.64	0.089	0.012	0.61	0.11	
44003	CH_3CHO ($13_{1,1}$-$12_{1,12}$ A)	242118.14	83.82	4.81E-04	3.09	0.27	4.63	0.68	0.087	0.010	0.77	0.14	
44003	CH_3CHO ($13_{0,1}$-$12_{0,12}$ E)	244789.26	83.14	4.99E-04	2.96	0.27	3.20	0.67	0.070	0.012	0.43	0.08	
44003	CH_3CHO ($13_{0,1}$-$12_{0,12}$ A)	244832.18	83.06	4.99E-04	3.20	0.68	4.12	1.88	0.062	0.019	0.49	0.09	
44003	CH_3CHO ($12_{1,1}$-$11_{0,11}$ E)	244853.65	72.27	6.20E-05	2.82	0.20	2.09	0.40	0.051	0.009	0.21	0.04	
44003	CH_3CHO ($14_{0,14}$-$13_{1,13}$ E)	247341.32	95.76	6.63E-05	2.82	0.35	3.44	0.97	0.042	0.008	0.28	0.05	
44003	CH_3CHO ($6_{2,5}$-$5_{1,4}$ A)	249284.54	28.48	3.62E-05	3.19	0.16	2.54	0.30	0.034	0.004	0.17	0.04	
44003	CH_3CHO ($13_{4,10}$-$12_{4,9}$ A)	250795.66	120.39	4.87E-04	3.35	0.28	3.06	0.67	0.080	0.015	0.48	0.09	
44003	CH_3CHO ($13_{3,11}$-$12_{3,10}$ A)	250934.55	104.62	5.10E-04	2.95	0.21	2.28	0.44	0.034	0.006	0.15	0.04	
44003	CH_3CHO ($13_{3,11}$-$12_{3,10}$ E)	251095.44	104.56	5.05E-04	2.70	0.12	2.69	0.25	0.082	0.007	0.43	0.08	
44003	CH_3CHO ($13_{3,10}$-$12_{3,9}$ A)	251489.29	104.70	5.14E-04	2.67	0.13	3.59	0.30	0.068	0.005	0.48	0.09	
44003	CH_3CHO ($13_{2,11}$-$12_{2,10}$ E)	254827.18	94.10	5.51E-04	2.58	0.15	2.25	0.37	0.083	0.012	0.37	0.06	
44003	CH_3CHO ($13_{2,11}$-$12_{2,10}$ A)	254850.50	94.08	5.51E-04	2.70	0.32	3.85	0.77	0.070	0.012	0.54	0.09	
44003	CH_3CHO ($13_{1,12}$-$12_{1,11}$ E)	255326.98	88.45	5.64E-04	2.07	0.23	3.99	0.56	0.029	0.003	0.23	0.05	
44003	CH_3CHO ($13_{1,13}$-$12_{0,12}$ A)	260694.05	83.82	7.73E-05	2.61	0.08	1.81	0.28	0.081	0.010	0.30	0.05	
44003	CH_3CHO ($15_{0,15}$-$14_{1,14}$ E)	267893.38	109.25	8.70E-05	2.08	0.10	2.88	0.23	0.076	0.005	0.46	0.08	
44003	CH_3CHO ($14_{6,8}$-$13_{6,7}$ E)	269864.17	178.33	5.49E-04	2.27	0.21	2.24	0.76	0.074	0.020	0.36	0.08	
44003	CH_3CHO ($14_{6,9}$-$13_{6,8}$ E)	269899.81	178.24	5.49E-04	2.74	0.22	3.54	0.54	0.079	0.010	0.60	0.12	

Table 4. continued.

TAG	Species & Transition	Frequency (MHz)	E_{up} (K)	A_{ij} s^{-1}	V_o (km s^{-1})	δ_{V_o}	$FWHM$ (km s^{-1})	δ_{FWHM}	Int (K)	δ_{Int}	Flux (K km s^{-1})	δ_{Flux}	Comments
44003	CH_3CHO ($14_{5,9}$-$13_{5,8}$ E)	269991.32	153.53	5.88E-04	2.37	0.31	3.56	0.72	0.087	0.015	0.66	0.13	
44003	CH_3CHO ($14_{5,10}$-$13_{5,9}$ E)	269997.52	153.50	5.87E-04	2.57	0.13	2.90	0.28	0.104	0.009	0.65	0.12	
44003	CH_3CHO ($14_{4,11}$-$13_{4,10}$ A)	270145.42	133.36	6.20E-04	2.44	0.32	2.71	0.83	0.122	0.031	0.71	0.13	
44003	CH_3CHO ($14_{4,11}$-$13_{4,10}$ E)	270212.78	133.26	6.19E-04	3.00	0.37	3.96	0.91	0.112	0.022	0.95	0.18	
44003	CH_3CHO ($14_{3,12}$-$13_{3,11}$ A)	270271.70	117.60	6.44E-04	2.18	0.38	4.16	0.91	0.112	0.021	1.00	0.18	
44003	CH_3CHO ($14_{3,12}$-$13_{3,11}$ E)	270415.84	117.54	6.37E-04	2.95	0.30	3.89	0.78	0.102	0.016	0.86	0.16	
44003	CH_3CHO ($14_{3,11}$-$13_{3,10}$ E)	270963.26	117.68	6.41E-04	2.46	0.10	2.41	0.25	0.100	0.009	0.52	0.10	
44003	CH_3CHO ($15_{1,15}$-$14_{1,14}$ E)	278924.43	109.78	7.40E-04	3.02	0.17	2.87	0.41	0.065	0.008	0.41	0.09	
44003	CH_3CHO ($15_{1,15}$-$14_{1,14}$ A)	278939.44	109.71	7.40E-04	2.34	0.14	3.22	0.34	0.075	0.007	0.54	0.11	
44003	CH_3CHO ($17_{3,15}$-$16_{3,14}$ A)	328231.53	162.07	1.18E-03	2.92	0.11	1.56	0.26	0.162	0.023	0.48	0.09	
44003	CH_3CHO ($11_{4,8}$-$11_{3,9}$ E)	328237.67	97.14	1.05E-04	2.66	0.15	0.98	0.31	0.129	0.036	0.24	0.05	
44003	CH_3CHO ($11_{4,7}$-$11_{3,8}$ A)	328242.99	97.25	1.07E-04	2.89	0.14	1.61	0.38	0.085	0.015	0.26	0.05	
44003	CH_3CHO ($17_{4,14}$-$16_{4,13}$ A)	328259.00	177.83	1.15E-03	2.21	0.09	1.22	0.22	0.110	0.017	0.25	0.05	
44003	CH_3CHO ($17_{4,14}$-$16_{4,13}$ E)	328361.96	177.75	1.14E-03	2.62	0.09	0.97	0.18	0.164	0.028	0.30	0.06	
44003	CH_3CHO ($17_{4,13}$-$16_{4,12}$ A)	328385.99	177.84	1.15E-03	2.49	0.23	1.30	0.54	0.097	0.035	0.24	0.05	
44003	CH_3CHO ($13_{4,10}$-$13_{3,11}$ A)	328520.34	120.39	1.11E-04	1.98	0.06	1.13	0.13	0.069	0.007	0.15	0.03	
44003	CH_3CHO ($11_{4,8}$-$11_{3,9}$ A)	328797.19	97.25	1.07E-04	1.84	0.06	1.14	0.13	0.083	0.008	0.18	0.03	
44003	CH_3CHO ($10_{4,7}$-$10_{3,8}$ A)	328927.15	87.07	1.05E-04	2.69	0.18	1.54	0.45	0.077	0.018	0.23	0.04	
44003	CH_3CHO ($5_{4,2}$-$5_{3,3}$ E)	328946.84	49.95	6.93E-05	2.36	0.07	0.91	0.22	0.082	0.016	0.14	0.03	
44003	CH_3CHO ($4_{4,1}$-$4_{3,2}$ E)	328970.47	45.32	4.61E-05	2.64	0.07	1.46	0.20	0.069	0.007	0.19	0.04	
44003	CH_3CHO ($9_{4,6}$-$9_{3,7}$ A)	329040.02	77.81	1.02E-04	2.33	0.06	0.91	0.10	0.118	0.012	0.20	0.04	
44003	CH_3CHO ($8_{4,4}$-$8_{3,5}$ A)	329046.77	69.49	9.72E-05	2.99	0.19	1.14	0.47	0.120	0.042	0.26	0.05	
44003	CH_3CHO ($17_{1,16}$-$16_{1,15}$ E)	331602.53	146.65	1.25E-03	3.03	0.09	1.13	0.21	0.117	0.018	0.25	0.05	
44003	CH_3CHO ($17_{1,16}$-$16_{1,15}$ A)	331680.47	146.60	1.25E-03	2.62	0.17	1.28	0.47	0.129	0.032	0.32	0.06	
44003	CH_3CHO ($5_{3,3}$-$4_{2,2}$ A)	331916.57	34.26	1.17E-04	2.71	0.14	1.02	0.35	0.116	0.034	0.22	0.04	
44003	CH_3CHO ($18_{1,18}$-$17_{1,17}$ E)	333941.28	155.22	1.28E-03	2.51	0.05	1.36	0.12	0.144	0.011	0.37	0.07	
44003	CH_3CHO ($18_{1,18}$-$17_{1,17}$ A)	333959.74	155.15	1.28E-03	2.28	0.22	2.32	0.52	0.111	0.021	0.49	0.09	
44003	CH_3CHO ($17_{2,15}$-$16_{2,14}$ E)	334904.64	152.63	1.28E-03	2.74	0.24	1.92	0.62	0.149	0.026	0.55	0.10	
44003	CH_3CHO ($17_{2,15}$-$16_{2,14}$ A)	334931.81	152.61	1.28E-03	2.46	0.12	1.89	0.28	0.124	0.016	0.45	0.08	
44003	CH_3CHO ($18_{0,18}$-$17_{0,17}$ E)	335317.99	154.93	1.30E-03	2.43	0.05	1.48	0.13	0.143	0.011	0.40	0.07	
44003	CH_3CHO ($18_{0,18}$-$17_{0,17}$ A)	335358.84	154.85	1.29E-03	2.62	0.06	1.26	0.15	0.154	0.015	0.37	0.07	
44003	CH_3CHO ($9_{2,7}$-$8_{1,8}$ A)	339976.01	50.91	5.43E-05	2.90	0.20	1.59	0.46	0.065	0.017	0.20	0.04	
44003	CH_3CHO ($18_{1,18}$-$17_{0,17}$ E)	341464.93	155.22	1.95E-04	2.52	0.14	1.95	0.34	0.120	0.017	0.45	0.08	
44003	CH_3CHO ($18_{2,17}$-$17_{2,16}$ E)	343780.08	166.47	1.38E-03	3.20	0.10	1.45	0.25	0.077	0.011	0.22	0.04	
44003	CH_3CHO ($18_{2,17}$-$17_{2,16}$ A)	343803.08	166.46	1.38E-03	2.78	0.08	1.18	0.20	0.108	0.016	0.24	0.05	
44003	CH_3CHO ($18_{3,16}$-$17_{3,15}$ E)	347563.58	178.71	1.41E-03	2.55	0.12	1.88	0.28	0.121	0.016	0.44	0.08	
44003	CH_3CHO ($18_{4,15}$-$17_{4,14}$ A)	347650.37	194.51	1.38E-03	2.34	0.25	1.59	0.61	0.109	0.035	0.34	0.06	
44003	CH_3CHO ($18_{4,15}$-$17_{4,14}$ E)	347756.85	194.44	1.36E-03	2.71	0.11	1.55	0.27	0.131	0.020	0.39	0.07	
44003	CH_3CHO ($18_{4,14}$-$17_{4,13}$ E)	347830.95	194.47	1.36E-03	2.48	0.16	1.85	0.39	0.127	0.023	0.45	0.08	
44003	CH_3CHO ($18_{4,14}$-$17_{4,13}$ A)	347838.99	194.54	1.38E-03	2.24	0.14	1.73	0.35	0.143	0.024	0.48	0.09	
44003	CH_3CHO ($18_{3,15}$-$17_{3,14}$ E)	350134.53	179.18	1.44E-03	2.98	0.12	2.74	0.31	0.177	0.015	0.94	0.17	
44003	CH_3CHO ($18_{3,15}$-$17_{3,14}$ A)	350134.53	179.21	1.44E-03	3.13	0.18	3.10	0.46	0.168	0.019	1.01	0.18	
44003	CH_3CHO ($18_{1,17}$-$17_{1,16}$ E)	350362.91	163.46	1.47E-03	2.33	0.13	1.37	0.30	0.137	0.026	0.37	0.07	
44003	CH_3CHO ($18_{1,17}$-$17_{1,16}$ A)	350445.94	163.42	1.47E-03	2.55	0.04	1.89	0.09	0.192	0.008	0.70	0.13	
44003	CH_3CHO ($13_{2,12}$-$12_{1,11}$ E)	350572.18	93.02	9.70E-05	2.71	0.24	1.74	0.63	0.088	0.021	0.30	0.06	
44003	CH_3CHO ($13_{2,12}$-$12_{1,11}$ A)	351574.51	93.01	9.83E-05	2.80	0.10	1.44	0.25	0.114	0.015	0.32	0.06	
44003	CH_3CHO ($6_{3,3}$-$5_{2,4}$ A)	351588.98	39.81	1.25E-04	2.50	0.14	1.00	0.30	0.123	0.033	0.24	0.05	

Table 4. continued.

TAG	Species & Transition	Frequency (MHz)	E_{up} (K)	A_{ij} s^{-1}	V_o (km s^{-1})	δ_{V_o}	*FWHM* (km s^{-1})	δ_{FWHM}	Int (K)	δ_{Int}	Flux (K km s^{-1})	δ_{Flux}	Comments
44003	CH_3CHO ($19_{0,19}$-$18_{0,18}$ A)	353425.95	171.82	1.52E-03	2.35	0.10	1.18	0.24	0.152	0.026	0.35	0.06	
44003	CH_3CHO ($18_{2,16}$-$17_{2,15}$ E)	354813.01	169.66	1.52E-03	2.65	0.18	1.97	0.43	0.124	0.024	0.47	0.09	
44003	CH_3CHO ($18_{2,16}$-$17_{2,15}$ A)	354845.88	169.64	1.52E-03	3.61	0.11	1.19	0.26	0.149	0.028	0.35	0.06	
44003	CH_3CHO ($19_{1,19}$-$18_{0,18}$ A)	358507.80	172.06	2.31E-04	2.62	0.12	1.40	0.28	0.105	0.018	0.29	0.05	
44003	CH_3CHO ($19_{2,18}$-$18_{2,17}$ A)	362561.10	183.86	1.62E-03	2.60	0.12	1.31	0.30	0.123	0.023	0.32	0.06	
46509	H_2CS ($3_{1,3}$-$2_{1,2}$)	101477.81	22.91	1.26E-05	3.79	0.06	2.59	0.14	0.248	0.012	0.85	0.09	
46509	H_2CS ($3_{0,3}$-$2_{0,2}$)	103040.45	9.89	1.48E-05	3.88	0.10	2.96	0.24	0.154	0.011	0.61	0.07	
46509	H_2CS ($3_{1,2}$-$2_{1,1}$)	104617.04	23.21	1.38E-05	3.81	0.10	2.71	0.23	0.229	0.017	0.83	0.09	
46509	H_2CS ($4_{1,4}$-$3_{1,3}$)	135298.26	29.40	3.27E-05	3.59	0.11	3.03	0.25	0.320	0.023	1.37	0.23	
46509	H_2CS ($4_{0,4}$-$3_{0,3}$)	137371.21	16.48	3.65E-05	3.94	0.14	2.63	0.32	0.177	0.019	0.66	0.11	
46509	H_2CS ($4_{1,3}$-$3_{1,2}$)	139483.68	29.91	3.58E-05	3.85	0.11	3.30	0.27	0.324	0.023	1.52	0.26	
46509	H_2CS ($5_{1,5}$-$4_{1,4}$)	169114.08	37.52	6.68E-05	3.68	0.09	4.10	0.22	0.421	0.020	2.62	0.45	
46509	H_2CS ($5_{0,5}$-$4_{0,4}$)	171688.12	24.72	7.28E-05	3.94	0.13	4.31	0.31	0.221	0.014	1.46	0.25	
46509	H_2CS ($5_{1,4}$-$4_{1,3}$)	174345.22	38.27	7.32E-05	3.32	0.10	3.34	0.24	0.367	0.023	1.89	0.32	
46509	H_2CS ($6_{1,6}$-$5_{1,5}$)	202924.05	47.26	1.19E-04	3.30	0.15	4.08	0.36	0.357	0.027	2.43	0.41	
46509	H_2CS ($6_{0,6}$-$5_{0,5}$)	205987.86	34.61	1.28E-04	3.34	0.13	4.32	0.29	0.215	0.012	1.55	0.27	
46509	H_2CS ($6_{2,5}$-$5_{2,4}$)	206054.17	87.28	1.14E-04	4.55	0.08	5.79	0.22	0.152	0.003	1.48	0.25	
46509	H_2CS ($6_{1,5}$-$5_{1,4}$)	209200.62	48.31	1.30E-04	3.32	0.09	4.80	0.22	0.354	0.014	2.89	0.49	
46509	H_2CS ($7_{1,7}$-$6_{1,6}$)	236727.02	58.62	1.92E-04	3.66	0.06	4.73	0.15	0.494	0.014	4.36	0.74	
46509	H_2CS ($7_{0,7}$-$6_{0,6}$)	240266.87	46.14	2.05E-04	3.51	0.15	5.19	0.35	0.287	0.017	2.82	0.48	
46509	H_2CS ($7_{2,6}$-$6_{2,5}$)	240382.05	98.82	1.88E-04	3.01	0.18	6.73	0.46	0.108	0.006	1.38	0.24	
46509	H_2CS ($7_{2,5}$-$6_{2,4}$)	240549.07	98.84	1.89E-04	3.75	0.29	6.84	0.75	0.092	0.008	1.19	0.21	
46509	H_2CS ($7_{1,6}$-$6_{1,5}$)	244048.50	60.03	2.10E-04	3.42	0.06	4.73	0.15	0.380	0.010	3.45	0.59	
46509	H_2CS ($8_{1,8}$-$7_{1,7}$)	270521.93	71.60	2.90E-04	3.05	0.12	4.78	0.28	0.421	0.021	4.33	0.74	
46509	H_2CS ($8_{2,7}$-$7_{2,6}$)	274703.35	112.00	2.89E-04	3.68	0.13	5.89	0.34	0.083	0.004	1.07	0.20	
46509	H_2CS ($8_{2,6}$-$7_{2,5}$)	274953.74	112.03	2.90E-04	4.00	0.14	7.43	0.40	0.094	0.004	1.53	0.27	
46509	H_2CS ($8_{1,7}$-$7_{1,6}$)	278887.66	73.41	3.18E-04	3.62	0.06	4.20	0.15	0.271	0.008	2.54	0.44	
46509	H_2CS ($10_{1,10}$-$9_{1,9}$)	338083.20	102.43	5.77E-04	3.21	0.14	3.70	0.34	0.237	0.018	1.68	0.30	
46509	H_2CS ($10_{0,10}$-$9_{0,9}$)	342946.42	90.59	6.08E-04	3.12	0.19	4.33	0.48	0.154	0.014	1.28	0.23	
46509	H_2CS ($10_{2,8}$-$9_{2,7}$)	343813.17	143.38	5.88E-04	3.70	0.32	5.77	0.83	0.086	0.009	0.96	0.18	
46509	H_2CS ($10_{1,9}$-$9_{1,8}$)	348534.36	105.19	6.32E-04	3.76	0.14	5.37	0.35	0.430	0.022	4.47	0.80	
47505	$H_2^{13}CS$ ($3_{1,3}$-$2_{1,2}$)	97632.20	22.54	1.12E-05	4.97	0.35	3.23	0.83	0.013	0.003	0.06	0.02	
47505	$H_2^{13}CS$ ($5_{1,4}$-$4_{1,3}$)	167543.38	37.29	6.49E-05	4.54	0.15	3.27	0.36	0.075	0.007	0.37	0.07	
47505	$H_2^{13}CS$ ($7_{1,7}$-$6_{1,6}$)	227760.42	56.90	1.71E-04	3.32	0.31	3.93	0.74	0.025	0.004	0.17	0.04	
47505	$H_2^{13}CS$ ($7_{2,5}$-$6_{2,4}$)	231280.89	97.06	1.68E-04	3.53	0.40	8.01	1.19	0.155	0.013	2.28	0.39	
47504	HDCS ($3_{1,3}$-$2_{1,2}$)	91171.07	17.74	9.12E-06	3.87	0.19	4.00	0.53	0.032	0.002	0.17	0.02	
47504	HDCS ($3_{0,3}$-$2_{0,2}$)	92981.60	8.93	1.09E-05	3.90	0.08	1.99	0.27	0.057	0.004	0.15	0.02	
47504	HDCS ($3_{1,2}$-$2_{1,1}$)	94828.49	18.09	1.03E-05	3.67	0.24	1.88	0.60	0.028	0.008	0.07	0.01	
47504	HDCS ($5_{1,5}$-$4_{1,4}$)	151927.54	30.86	4.83E-05	3.62	0.20	2.97	0.55	0.044	0.006	0.19	0.04	
47504	HDCS ($5_{0,5}$-$4_{0,4}$)	154885.03	22.31	5.33E-05	3.81	0.12	3.19	0.35	0.050	0.004	0.23	0.05	
60503	OCS (7-6)	85139.10	16.34	1.71E-06	3.22	0.10	5.09	0.25	0.222	0.009	1.46	0.16	
60503	OCS (8-7)	97301.21	21.01	2.58E-06	3.11	0.14	4.59	0.33	0.277	0.017	1.67	0.19	
60503	OCS (9-8)	109463.06	26.27	3.70E-06	3.08	0.11	4.61	0.26	0.139	0.007	0.86	0.10	
60503	OCS (11-10)	133785.90	38.53	6.82E-06	3.20	0.15	4.75	0.34	0.456	0.028	3.04	0.52	
60503	OCS (12-11)	145946.81	45.53	8.88E-06	2.91	0.14	4.59	0.34	0.423	0.027	2.80	0.48	
60503	OCS (13-12)	158107.36	53.12	1.13E-05	2.84	0.15	4.04	0.36	0.477	0.036	2.86	0.49	wings

Table 4. continued.

TAG	Species & Transition	Frequency (MHz)	E_{up} (K)	A_{ij} s^{-1}	V_o (km s^{-1})	δ_{V_o}	$FWHM$ (km s^{-1})	δ_{FWHM}	Int (K)	δ_{Int}	Flux (K km s^{-1})	δ_{Flux}	Comments
60503	OCS (14-13)	170267.49	61.29	1.42E-05	3.20	0.19	5.02	0.47	0.385	0.030	2.95	0.50	wings
60503	OCS (17-16)	206745.16	89.31	2.56E-05	2.94	0.18	5.21	0.43	0.580	0.040	5.09	0.87	
60503	OCS (18-17)	218903.36	99.81	3.04E-05	2.90	0.20	5.34	0.49	0.615	0.048	5.76	0.98	
60503	OCS (19-18)	231060.99	110.90	3.58E-05	3.07	0.15	5.22	0.36	0.606	0.035	5.78	0.98	
60503	OCS (20-19)	243218.04	122.57	4.18E-05	3.00	0.12	5.94	0.29	0.503	0.020	5.71	0.97	
60503	OCS (21-20)	255374.46	134.83	4.84E-05	4.10	0.50	7.05	1.38	0.047	0.006	0.66	0.12	
62505	$OC^{34}S$ (7-6)	83057.97	15.94	1.59E-06	2.64	0.17	3.93	0.48	0.062	0.005	0.31	0.04	
62505	$OC^{34}S$ (8-7)	94922.80	20.50	2.40E-06	2.24	0.21	3.05	0.51	0.066	0.009	0.26	0.03	
62505	$OC^{34}S$ (11-10)	130515.73	37.58	6.33E-06	2.55	0.15	3.57	0.37	0.112	0.009	0.56	0.10	
62505	$OC^{34}S$ (13-12)	154242.78	51.82	1.05E-05	2.34	0.19	3.87	0.52	0.137	0.013	0.78	0.14	
62505	$OC^{34}S$ (17-16)	201691.98	87.12	2.37E-05	2.34	0.10	4.92	0.33	0.144	0.006	1.17	0.20	
62505	$OC^{34}S$ (18-17)	213553.06	97.37	2.82E-05	2.35	0.08	3.78	0.21	0.177	0.008	1.15	0.20	
62505	$OC^{34}S$ (19-18)	225413.64	108.19	3.32E-05	2.51	0.13	4.43	0.35	0.163	0.010	1.29	0.23	
62505	$OC^{34}S$ (20-19)	237273.64	119.58	3.88E-05	3.11	0.18	4.90	0.56	0.141	0.010	1.29	0.22	
62505	$OC^{34}S$ (23-22)	272849.96	157.16	5.92E-05	2.48	0.15	3.41	0.35	0.133	0.012	0.99	0.18	
61502	$O^{13}CS$ (8-7)	96988.12	20.95	2.56E-06	2.07	0.29	4.38	0.79	0.033	0.004	0.19	0.03	
61502	$O^{13}CS$ (9-8)	109110.85	26.18	3.66E-06	2.41	0.30	3.05	0.71	0.034	0.007	0.14	0.03	
61502	$O^{13}CS$ (11-10)	133355.42	38.40	6.76E-06	2.65	0.15	2.49	0.36	0.090	0.011	0.31	0.06	
61502	$O^{13}CS$ (12-11)	145477.20	45.38	8.80E-06	2.26	0.19	4.18	0.48	0.082	0.007	0.49	0.09	
61502	$O^{13}CS$ (13-12)	157598.62	52.95	1.12E-05	2.45	0.22	3.85	0.54	0.101	0.011	0.58	0.10	
61502	$O^{13}CS$ (14-13)	169719.65	61.09	1.41E-05	2.99	0.29	5.23	0.85	0.072	0.008	0.57	0.11	
61502	$O^{13}CS$ (18-17)	218199.00	99.49	3.01E-05	2.77	0.19	6.42	0.48	0.098	0.006	1.10	0.19	
61502	$O^{13}CS$ (19-18)	230317.53	110.54	3.54E-05	3.78	0.08	6.20	0.21	0.098	0.002	1.11	0.19	
61502	$O^{13}CS$ (21-20)	254552.73	134.40	4.80E-05	2.26	0.30	4.12	0.85	0.076	0.011	0.63	0.11	
61502	$O^{13}CS$ (22-21)	266669.38	147.19	5.52E-05	2.20	0.43	4.94	1.10	0.048	0.009	0.50	0.10	
60003	$HCOOCH_3$ ($7_{2,6}$-$6_{2,5}$ E)	84449.17	19.00	7.96E-06	2.75	0.25	2.30	0.58	0.017	0.004	0.05	0.02	
60003	$HCOOCH_3$ ($7_{2,6}$-$6_{2,5}$ A)	84454.75	18.98	7.96E-06	2.66	0.24	3.31	0.59	0.025	0.004	0.11	0.02	
60003	$HCOOCH_3$ ($7_{4,4}$-$6_{4,3}$ A)	86210.06	27.15	6.24E-06	2.93	0.43	4.18	1.16	0.024	0.005	0.13	0.03	
60003	$HCOOCH_3$ ($7_{4,3}$-$6_{4,2}$ A)	86250.55	27.15	6.25E-06	2.82	0.20	2.63	0.48	0.023	0.004	0.08	0.02	
60003	$HCOOCH_3$ ($7_{3,5}$-$6_{3,4}$ E)	86268.74	22.53	7.50E-06	3.25	0.27	2.45	0.69	0.028	0.006	0.09	0.02	
60003	$HCOOCH_3$ ($7_{3,4}$-$6_{3,3}$ A)	87161.29	22.58	7.81E-06	2.72	0.33	3.01	0.82	0.040	0.009	0.15	0.02	
60003	$HCOOCH_3$ ($7_{1,6}$-$6_{1,5}$ E)	88843.19	17.96	9.82E-06	3.09	0.36	2.85	1.00	0.035	0.009	0.13	0.02	
60003	$HCOOCH_3$ ($7_{1,6}$-$6_{1,5}$ A)	88851.61	17.94	9.82E-06	2.71	0.15	2.77	0.35	0.033	0.004	0.12	0.02	
60003	$HCOOCH_3$ ($8_{1,8}$-$7_{1,7}$ E)	89314.66	20.15	1.02E-05	2.37	0.38	3.00	1.08	0.034	0.009	0.13	0.02	
60003	$HCOOCH_3$ ($7_{2,5}$-$6_{2,4}$ E)	90145.72	19.68	9.74E-06	2.49	0.17	2.01	0.38	0.045	0.007	0.12	0.02	
60003	$HCOOCH_3$ ($7_{2,5}$-$6_{2,4}$ A)	90156.47	19.67	9.75E-06	1.99	0.20	1.61	0.38	0.028	0.006	0.06	0.02	
60003	$HCOOCH_3$ ($8_{0,8}$-$7_{0,7}$ E)	90227.66	20.08	1.05E-05	3.35	0.28	2.55	0.69	0.033	0.008	0.11	0.02	
60003	$HCOOCH_3$ ($8_{2,7}$-$7_{2,6}$ E)	96070.73	23.61	1.20E-05	2.84	0.13	3.22	0.31	0.043	0.004	0.18	0.02	
60003	$HCOOCH_3$ ($8_{6,2}$-$7_{6,1}$ E)	98270.50	45.15	6.05E-06	2.76	0.34	3.08	0.85	0.017	0.004	0.07	0.02	
60003	$HCOOCH_3$ ($8_{5,3}$-$7_{5,2}$ E)	98424.21	37.86	8.47E-06	2.75	0.14	2.39	0.32	0.034	0.004	0.11	0.02	
60003	$HCOOCH_3$ ($8_{5,3}$-$7_{5,2}$ A)	98435.80	37.84	8.47E-06	2.61	0.20	3.04	0.54	0.040	0.005	0.16	0.02	
60003	$HCOOCH_3$ ($8_{3,6}$-$7_{3,5}$ E)	98606.86	27.26	1.20E-05	2.49	0.15	3.56	0.40	0.031	0.003	0.15	0.02	
60003	$HCOOCH_3$ ($8_{3,6}$-$7_{3,5}$ A)	98611.16	27.24	1.20E-05	2.67	0.24	3.00	0.65	0.045	0.007	0.18	0.02	
60003	$HCOOCH_3$ ($8_{4,5}$-$7_{4,4}$ A)	98682.62	31.89	1.05E-05	2.63	0.14	3.36	0.35	0.047	0.004	0.21	0.03	
60003	$HCOOCH_3$ ($8_{4,5}$-$7_{4,4}$ E)	98712.00	31.90	1.02E-05	2.52	0.14	1.96	0.31	0.040	0.006	0.10	0.02	
60003	$HCOOCH_3$ ($8_{4,4}$-$7_{4,3}$ E)	98747.91	31.91	1.02E-05	2.58	0.10	2.40	0.27	0.030	0.002	0.09	0.02	

Table 4. continued.

TAG	Species & Transition	Frequency (MHz)	E_{up} (K)	A_{ij} s^{-1}	V_o (km s^{-1})	δ_{V_o}	*FWHM* (km s^{-1})	δ_{FWHM}	Int (K)	δ_{Int}	Flux (K km s^{-1})	δ_{Flux}	Comments
60003	$HCOOCH_3$ ($8_{4,4}$-$7_{4,3}$ A)	98792.29	31.89	1.05E-05	2.34	0.40	3.20	1.33	0.035	0.008	0.15	0.02	
60003	$HCOOCH_3$ ($8_{3,5}$-$7_{3,4}$ E)	100294.60	27.41	1.26E-05	2.37	0.09	2.62	0.21	0.035	0.002	0.12	0.02	
60003	$HCOOCH_3$ ($8_{3,5}$-$7_{3,4}$ A)	100308.18	27.40	1.26E-05	2.62	0.13	2.81	0.33	0.034	0.003	0.13	0.02	
60003	$HCOOCH_3$ ($8_{1,7}$-$7_{1,6}$ E)	100482.24	22.78	1.43E-05	2.47	0.20	3.36	0.51	0.034	0.004	0.15	0.02	
60003	$HCOOCH_3$ ($8_{2,6}$-$7_{2,5}$ E)	103466.57	24.65	1.52E-05	2.16	0.14	3.57	0.36	0.041	0.003	0.20	0.03	
60003	$HCOOCH_3$ ($8_{2,6}$-$7_{2,5}$ A)	103478.66	24.63	1.52E-05	2.47	0.16	2.90	0.37	0.039	0.004	0.15	0.02	
60003	$HCOOCH_3$ ($9_{6,3}$-$8_{6,2}$ E)	110652.81	50.46	1.10E-05	2.38	0.19	2.04	0.45	0.036	0.007	0.10	0.01	
60003	$HCOOCH_3$ ($10_{1,10}$-$9_{1,9}$ E)	110788.66	30.27	1.97E-05	2.31	0.23	2.50	0.57	0.053	0.010	0.18	0.02	
60003	$HCOOCH_3$ ($10_{1,10}$-$9_{1,9}$ A)	110790.53	30.26	1.97E-05	2.20	0.30	3.49	0.79	0.038	0.004	0.18	0.02	
60003	$HCOOCH_3$ ($9_{5,4}$-$8_{5,3}$ E)	110873.96	43.18	1.38E-05	2.39	0.15	2.60	0.45	0.036	0.004	0.12	0.01	
60003	$HCOOCH_3$ ($9_{5,5}$-$8_{5,4}$ E)	110882.33	43.16	1.38E-05	2.82	0.19	2.39	0.53	0.029	0.004	0.09	0.01	
60003	$HCOOCH_3$ ($9_{5,4}$-$8_{5,3}$ A)	110890.26	43.16	1.38E-05	2.59	0.25	1.87	0.63	0.023	0.006	0.06	0.01	
60003	$HCOOCH_3$ ($10_{0,10}$-$9_{0,9}$ E)	111169.90	30.25	1.99E-05	2.35	0.14	3.57	0.47	0.058	0.004	0.28	0.04	
60003	$HCOOCH_3$ ($10_{0,10}$-$9_{0,9}$ A)	111171.63	30.23	1.99E-05	2.72	0.41	3.25	1.06	0.047	0.008	0.20	0.04	
60003	$HCOOCH_3$ ($9_{4,6}$-$8_{4,5}$ A)	111195.96	37.22	1.62E-05	2.54	0.20	2.49	0.56	0.047	0.007	0.16	0.03	
60003	$HCOOCH_3$ ($9_{4,6}$-$8_{4,5}$ E)	111223.49	37.23	1.53E-05	2.56	0.20	2.00	0.46	0.037	0.007	0.10	0.02	
60003	$HCOOCH_3$ ($9_{4,5}$-$8_{4,4}$ A)	111453.30	37.24	1.63E-05	2.74	0.14	2.18	0.37	0.043	0.006	0.13	0.03	
60003	$HCOOCH_3$ ($9_{1,8}$-$8_{1,7}$ A)	111682.19	28.12	1.98E-05	2.74	0.29	2.00	0.67	0.027	0.008	0.07	0.02	
60003	$HCOOCH_3$ ($9_{3,6}$-$8_{3,5}$ E)	113743.11	32.87	1.92E-05	2.66	0.19	2.53	0.47	0.060	0.009	0.21	0.02	
60003	$HCOOCH_3$ ($9_{3,6}$-$8_{3,5}$ A)	113756.61	32.86	1.92E-05	2.70	0.23	2.50	0.69	0.050	0.009	0.17	0.02	
60003	$HCOOCH_3$ ($10_{2,8}$-$9_{2,7}$ E)	129296.36	36.45	3.06E-05	2.55	0.09	2.31	0.20	0.081	0.006	0.26	0.05	
60003	$HCOOCH_3$ ($10_{2,8}$-$9_{2,7}$ A)	129310.17	36.43	3.06E-05	2.74	0.14	1.67	0.38	0.054	0.007	0.12	0.02	
60003	$HCOOCH_3$ ($12_{0,12}$-$11_{1,11}$ E)	131914.52	42.44	5.10E-06	3.08	0.12	1.76	0.29	0.049	0.007	0.12	0.02	
60003	$HCOOCH_3$ ($12_{1,12}$-$11_{1,11}$ E)	132105.51	42.44	3.38E-05	2.47	0.25	3.00	0.94	0.061	0.008	0.25	0.05	
60003	$HCOOCH_3$ ($12_{1,12}$-$11_{1,11}$ A)	132107.20	42.43	3.38E-05	2.46	0.34	2.00	0.86	0.056	0.012	0.16	0.03	
60003	$HCOOCH_3$ ($12_{0,12}$-$11_{0,11}$ E)	132245.13	42.44	3.39E-05	2.37	0.23	3.26	0.68	0.067	0.009	0.31	0.06	
60003	$HCOOCH_3$ ($12_{0,12}$-$11_{0,11}$ A)	132246.73	42.42	3.39E-05	2.70	0.22	2.78	0.49	0.050	0.004	0.19	0.04	
60003	$HCOOCH_3$ ($12_{1,12}$-$11_{0,11}$ E)	132436.11	42.44	5.16E-06	2.25	0.19	2.49	0.47	0.033	0.005	0.11	0.02	
60003	$HCOOCH_3$ ($12_{1,12}$-$11_{0,11}$ A)	132437.49	42.43	5.16E-06	2.33	0.57	2.69	1.31	0.022	0.005	0.08	0.02	
60003	$HCOOCH_3$ ($11_{1,10}$-$10_{1,9}$ A)	132928.74	40.38	3.36E-05	2.70	0.28	2.00	0.81	0.052	0.014	0.15	0.03	
60003	$HCOOCH_3$ ($11_{3,9}$-$10_{3,8}$ A)	135101.63	44.96	3.37E-05	2.46	0.18	2.23	0.43	0.053	0.009	0.17	0.03	
60003	$HCOOCH_3$ ($11_{8,3}$-$10_{8,2}$ E)	135143.06	81.42	1.72E-05	1.86	0.04	2.08	0.10	0.045	0.002	0.13	0.02	
60003	$HCOOCH_3$ ($11_{8,4}$-$10_{8,3}$ E)	135156.25	81.40	1.72E-05	2.70	0.35	2.00	0.87	0.043	0.016	0.12	0.02	
60003	$HCOOCH_3$ ($11_{6,5}$-$10_{6,4}$ A)	135541.48	62.86	2.59E-05	3.18	0.21	2.50	0.50	0.052	0.009	0.19	0.03	
60003	$HCOOCH_3$ ($11_{5,7}$-$10_{5,6}$ A)	135921.95	55.60	2.95E-05	2.21	0.19	2.32	0.47	0.063	0.010	0.21	0.04	
60003	$HCOOCH_3$ ($11_{5,7}$-$10_{5,6}$ E)	135942.98	55.61	2.92E-05	1.89	0.12	2.68	0.29	0.052	0.005	0.20	0.03	
60003	$HCOOCH_3$ ($11_{4,8}$-$10_{4,7}$ A)	136282.60	49.70	3.25E-05	2.69	0.07	3.83	0.19	0.072	0.003	0.39	0.07	
60003	$HCOOCH_3$ ($11_{4,7}$-$10_{4,6}$ E)	137293.18	49.81	3.31E-05	2.83	0.06	3.06	0.16	0.054	0.002	0.23	0.04	
60003	$HCOOCH_3$ ($11_{4,7}$-$10_{4,6}$ A)	137313.33	49.80	3.33E-05	2.52	0.07	1.49	0.16	0.050	0.005	0.10	0.02	
60003	$HCOOCH_3$ ($11_{3,8}$-$10_{3,7}$ A)	141260.42	45.75	3.87E-05	2.89	0.11	2.59	0.27	0.079	0.007	0.29	0.06	
60003	$HCOOCH_3$ ($11_{2,9}$-$10_{2,8}$ E)	141652.99	43.25	4.06E-05	2.34	0.24	2.00	0.56	0.126	0.030	0.36	0.06	
60003	$HCOOCH_3$ ($13_{0,13}$-$12_{0,12}$ E)	142815.48	49.29	4.29E-05	2.60	0.07	2.68	0.21	0.106	0.005	0.41	0.07	
60003	$HCOOCH_3$ ($13_{0,13}$-$12_{0,12}$ A)	142817.02	49.27	4.29E-05	2.66	0.36	2.00	0.94	0.095	0.026	0.27	0.05	
60003	$HCOOCH_3$ ($13_{1,13}$-$12_{0,12}$ E)	142924.51	49.29	6.59E-06	2.90	0.21	2.00	0.64	0.089	0.019	0.25	0.05	
60003	$HCOOCH_3$ ($13_{1,13}$-$12_{0,12}$ A)	142925.91	49.28	6.59E-06	2.98	0.20	2.50	0.49	0.088	0.008	0.31	0.06	
60003	$HCOOCH_3$ ($12_{1,11}$-$11_{1,10}$ E)	143234.20	47.27	4.22E-05	2.43	0.12	2.96	0.32	0.085	0.007	0.36	0.07	
60003	$HCOOCH_3$ ($12_{1,11}$-$11_{1,10}$ A)	143240.51	47.25	4.23E-05	2.44	0.19	2.60	0.51	0.078	0.009	0.29	0.05	

Table 4. continued.

TAG	Species & Transition	Frequency (MHz)	E_{up} (K)	A_{ij} s^{-1}	V_o (km s^{-1})	δ_{V_o}	*FWHM* (km s^{-1})	δ_{FWHM}	Int (K)	δ_{Int}	Flux (K km s^{-1})	δ_{Flux}	Comments
60003	$HCOOCH_3$ ($12_{10,3}$-$11_{10,2}$ E)	147325.39	112.37	1.45E-05	2.64	0.17	2.21	0.40	0.050	0.008	0.16	0.03	
60003	$HCOOCH_3$ ($12_{9,3}$-$11_{9,2}$ E)	147397.07	99.78	2.09E-05	2.29	0.09	4.28	0.24	0.100	0.004	0.62	0.11	
60003	$HCOOCH_3$ ($12_{8,4}$-$11_{8,3}$ E)	147524.31	88.50	2.65E-05	2.38	0.11	2.46	0.28	0.064	0.006	0.23	0.05	
60003	$HCOOCH_3$ ($12_{8,5}$-$11_{8,4}$ E)	147538.64	88.49	2.65E-05	2.54	0.12	2.25	0.31	0.056	0.006	0.18	0.04	
60003	$HCOOCH_3$ ($12_{6,6}$-$11_{6,5}$ A)	148045.82	69.96	3.62E-05	2.47	0.33	2.00	0.72	0.067	0.009	0.19	0.04	
60003	$HCOOCH_3$ ($12_{5,8}$-$11_{5,7}$ A)	148516.04	62.73	4.03E-05	2.34	0.07	1.67	0.16	0.079	0.007	0.19	0.04	
60003	$HCOOCH_3$ ($12_{5,8}$-$11_{5,7}$ E)	148545.01	62.74	3.87E-05	2.58	0.22	2.07	0.60	0.076	0.015	0.23	0.04	
60003	$HCOOCH_3$ ($12_{5,7}$-$11_{5,6}$ E)	148614.84	62.76	3.88E-05	2.27	0.18	2.00	0.44	0.085	0.016	0.25	0.05	
60003	$HCOOCH_3$ ($12_{5,7}$-$11_{5,6}$ A)	148664.52	62.74	4.04E-05	2.27	0.15	2.50	0.39	0.072	0.009	0.26	0.05	
60003	$HCOOCH_3$ ($12_{4,9}$-$11_{4,8}$ E)	148797.79	56.86	4.35E-05	2.23	0.21	3.07	0.80	0.077	0.010	0.34	0.06	
60003	$HCOOCH_3$ ($12_{4,9}$-$11_{4,8}$ A)	148805.94	56.84	4.35E-05	2.37	0.12	2.48	0.30	0.085	0.009	0.31	0.06	
60003	$HCOOCH_3$ ($13_{1,12}$-$12_{2,11}$ E)	149065.24	54.64	5.23E-06	2.53	0.04	1.41	0.09	0.046	0.002	0.09	0.02	
60003	$HCOOCH_3$ ($13_{1,12}$-$12_{2,11}$ A)	149074.31	54.62	5.23E-06	3.37	0.15	1.38	0.36	0.031	0.006	0.06	0.02	
60003	$HCOOCH_3$ ($12_{4,8}$-$11_{4,7}$ A)	150618.30	57.03	4.52E-05	2.42	0.23	2.00	0.63	0.094	0.021	0.28	0.05	
60003	$HCOOCH_3$ ($13_{2,12}$-$12_{2,11}$ A)	151956.62	54.76	5.05E-05	2.77	0.07	1.96	0.17	0.052	0.004	0.15	0.03	
60003	$HCOOCH_3$ ($14_{1,14}$-$13_{0,13}$ A)	153460.91	56.64	8.26E-06	2.64	0.24	2.00	0.64	0.065	0.015	0.19	0.04	
60003	$HCOOCH_3$ ($12_{2,10}$-$11_{2,9}$ E)	153553.23	50.62	5.19E-05	2.65	0.11	2.07	0.31	0.072	0.008	0.22	0.04	
60003	$HCOOCH_3$ ($12_{2,10}$-$11_{2,9}$ A)	153566.92	50.60	5.20E-05	2.22	0.30	2.00	0.83	0.065	0.019	0.19	0.04	
60003	$HCOOCH_3$ ($12_{3,9}$-$11_{3,8}$ A)	155002.32	53.19	5.21E-05	2.47	0.08	1.78	0.18	0.074	0.006	0.19	0.04	
60003	$HCOOCH_3$ ($13_{2,12}$-$1_{1,11}$ E)	156397.53	54.78	6.11E-06	2.16	0.14	2.07	0.34	0.041	0.006	0.13	0.03	
60003	$HCOOCH_3$ ($13_{3,11}$-$1_{3,10}$ E)	158693.72	59.64	5.61E-05	2.84	0.11	2.27	0.27	0.093	0.006	0.31	0.06	
60003	$HCOOCH_3$ ($13_{3,11}$-$1_{3,10}$ A)	158704.39	59.63	5.61E-05	2.51	0.14	2.09	0.36	0.107	0.014	0.33	0.06	
60003	$HCOOCH_3$ ($13_{10,3}$-$1_{10,2}$ E)	159654.88	120.05	2.48E-05	2.79	0.11	1.78	0.26	0.044	0.005	0.12	0.02	
60003	$HCOOCH_3$ ($13_{10,4}$-$1_{10,3}$ E)	159670.85	120.03	2.48E-05	2.85	0.09	1.65	0.22	0.068	0.008	0.17	0.03	
60003	$HCOOCH_3$ ($13_{7,6}$-$12_{7,5}$ E)	160178.94	86.26	4.35E-05	2.29	0.10	2.72	0.31	0.055	0.004	0.22	0.04	
60003	$HCOOCH_3$ ($13_{6,7}$-$12_{6,6}$ E)	160578.37	77.68	4.86E-05	2.43	0.14	2.70	0.36	0.080	0.008	0.32	0.06	
60003	$HCOOCH_3$ ($13_{6,8}$-$12_{6,7}$ A)	160585.83	77.67	4.86E-05	2.26	0.11	3.67	0.34	0.079	0.004	0.43	0.08	
60003	$HCOOCH_3$ ($13_{6,8}$-$12_{6,7}$ E)	160591.25	77.67	4.86E-05	2.49	0.20	3.15	0.54	0.081	0.010	0.38	0.07	
60003	$HCOOCH_3$ ($13_{6,7}$-$12_{6,6}$ A)	160602.04	77.67	4.86E-05	2.39	0.10	3.42	0.33	0.083	0.005	0.42	0.07	
60003	$HCOOCH_3$ ($13_{5,9}$-$12_{5,8}$ E)	161171.47	70.47	5.13E-05	2.63	0.12	3.05	0.33	0.100	0.007	0.45	0.08	
60003	$HCOOCH_3$ ($13_{4,10}$-$12_{4,9}$ E)	161262.46	64.59	5.66E-05	2.10	0.26	2.00	0.73	0.093	0.023	0.28	0.05	
60003	$HCOOCH_3$ ($13_{4,10}$-$12_{4,9}$ A)	161273.36	64.58	5.66E-05	2.75	0.23	2.99	0.58	0.086	0.007	0.38	0.07	
60003	$HCOOCH_3$ ($13_{5,8}$-$12_{5,7}$ E)	161416.14	70.50	5.15E-05	2.32	0.18	2.00	0.44	0.075	0.014	0.22	0.04	
60003	$HCOOCH_3$ ($13_{5,8}$-$12_{5,7}$ A)	161458.22	70.49	5.35E-05	2.49	0.06	2.24	0.18	0.106	0.005	0.36	0.06	
60003	$HCOOCH_3$ ($14_{2,13}$-$13_{2,12}$ A)	162775.27	62.57	6.24E-05	2.51	0.11	3.33	0.29	0.121	0.008	0.60	0.10	
60003	$HCOOCH_3$ ($14_{1,13}$-$13_{1,12}$ E)	163829.68	62.50	6.37E-05	2.71	0.04	1.40	0.09	0.086	0.005	0.18	0.03	
60003	$HCOOCH_3$ ($15_{0,15}$-$14_{1,14}$ E)	163925.85	64.52	1.02E-05	2.75	0.07	1.72	0.19	0.061	0.005	0.16	0.03	
60003	$HCOOCH_3$ ($15_{0,15}$-$14_{1,14}$ A)	163927.37	64.50	1.02E-05	2.72	0.21	2.00	0.55	0.035	0.008	0.10	0.02	
60003	$HCOOCH_3$ ($15_{1,15}$-$14_{1,14}$ E)	163960.39	64.52	6.53E-05	2.59	0.03	2.06	0.07	0.126	0.003	0.39	0.07	
60003	$HCOOCH_3$ ($15_{1,15}$-$14_{1,14}$ A)	163961.88	64.50	6.54E-05	2.83	0.46	2.00	0.99	0.141	0.024	0.42	0.07	
60003	$HCOOCH_3$ ($15_{0,15}$-$14_{0,14}$ E)	163987.45	64.52	6.54E-05	2.57	0.07	1.68	0.21	0.110	0.009	0.28	0.05	
60003	$HCOOCH_3$ ($15_{0,15}$-$14_{0,14}$ A)	163988.91	64.50	6.54E-05	2.66	0.24	2.00	0.64	0.105	0.021	0.32	0.06	
60003	$HCOOCH_3$ ($15_{1,15}$-$14_{0,14}$ A)	164023.42	64.50	1.02E-05	2.94	0.06	2.75	0.14	0.067	0.003	0.28	0.05	
60003	$HCOOCH_3$ ($13_{4,9}$-$12_{4,8}$ E)	164205.98	64.92	5.98E-05	2.14	0.14	3.16	0.36	0.071	0.006	0.34	0.06	
60003	$HCOOCH_3$ ($13_{4,9}$-$12_{4,8}$ A)	164223.82	64.91	5.98E-05	2.58	0.07	1.81	0.17	0.063	0.005	0.17	0.03	
60003	$HCOOCH_3$ ($13_{2,11}$-$12_{2,1}$ E)	164955.70	58.53	6.46E-05	2.02	0.25	2.50	0.67	0.036	0.007	0.13	0.03	
60003	$HCOOCH_3$ ($13_{3,10}$-$12_{3,9}$ E)	168495.07	61.29	6.78E-05	2.44	0.17	2.55	0.42	0.087	0.012	0.34	0.07	

Table 4. continued.

TAG	Species & Transition	Frequency (MHz)	E_{up} (K)	A_{ij} s^{-1}	V_o (km s^{-1})	δ_{V_o}	$FWHM$ (km s^{-1})	δ_{FWHM}	Int (K)	δ_{Int}	Flux (K km s^{-1})	δ_{Flux}	Comments
60003	$HCOOCH_3$ ($13_{3,10}$-$12_{3,9}$ A)	168513.75	61.28	6.78E-05	2.14	0.25	3.00	0.67	0.091	0.011	0.41	0.08	
60003	$HCOOCH_3$ ($14_{3,12}$-$13_{3,11}$ E)	170233.27	67.81	6.99E-05	2.39	0.06	1.64	0.14	0.087	0.006	0.22	0.05	
60003	$HCOOCH_3$ ($14_{3,12}$-$13_{3,11}$ A)	170244.09	67.80	6.99E-05	2.81	0.12	2.00	0.33	0.081	0.009	0.25	0.05	
60003	$HCOOCH_3$ ($6_{4,3}$-$5_{3,3}$ E)	170458.42	23.02	6.05E-06	2.74	0.17	1.25	0.41	0.055	0.015	0.10	0.03	
60003	$HCOOCH_3$ ($14_{10,5}$-$13_{10,4}$ E)	172032.76	128.29	3.73E-05	2.20	0.09	3.10	0.22	0.083	0.005	0.39	0.08	
60003	$HCOOCH_3$ ($14_{9,5}$-$13_{9,4}$ E)	172157.64	115.71	4.48E-05	3.16	0.05	2.17	0.14	0.068	0.003	0.23	0.05	
60003	$HCOOCH_3$ ($14_{8,6}$-$13_{8,5}$ E)	172364.37	104.45	5.16E-05	2.63	0.19	2.30	0.52	0.080	0.012	0.28	0.06	
60003	$HCOOCH_3$ ($14_{8,7}$-$13_{8,6}$ E)	172380.95	104.44	5.16E-05	2.37	0.16	2.64	0.41	0.080	0.010	0.32	0.06	
60003	$HCOOCH_3$ ($15_{1,14}$-$14_{2,13}$ A)	172393.49	70.85	8.93E-06	2.93	0.15	2.50	0.40	0.058	0.005	0.22	0.05	
60003	$HCOOCH_3$ ($14_{6,8}$-$13_{6,7}$ E)	173185.19	86.00	6.32E-05	2.62	0.05	1.60	0.12	0.096	0.006	0.24	0.05	
60003	$HCOOCH_3$ ($14_{6,9}$-$13_{6,8}$ E)	173194.27	85.98	6.32E-05	2.56	0.18	3.29	0.53	0.075	0.007	0.38	0.07	
60003	$HCOOCH_3$ ($14_{6,8}$-$13_{6,7}$ A)	173218.68	85.98	6.35E-05	2.44	0.12	2.15	0.29	0.079	0.009	0.26	0.05	
60003	$HCOOCH_3$ ($15_{1,14}$-$14_{1,13}$ E)	174209.80	70.86	7.69E-05	2.85	0.09	2.75	0.26	0.078	0.005	0.33	0.07	
60003	$HCOOCH_3$ ($15_{1,14}$-$14_{1,13}$ A)	174215.56	70.85	7.70E-05	2.59	0.10	2.37	0.26	0.108	0.009	0.40	0.07	
60003	$HCOOCH_3$ ($14_{5,9}$-$13_{5,8}$ E)	174377.41	78.87	6.83E-05	2.78	0.07	1.72	0.22	0.102	0.008	0.27	0.05	
60003	$HCOOCH_3$ ($18_{7,12}$-$18_{6,13}$ E)	174995.67	133.72	5.36E-06	3.33	0.12	1.60	0.29	0.061	0.009	0.15	0.04	
60003	$HCOOCH_3$ ($16_{7,9}$-$16_{6,10}$ A)	176525.62	112.91	7.10E-06	3.39	0.15	1.51	0.35	0.077	0.016	0.18	0.04	
60003	$HCOOCH_3$ ($16_{6,10}$-$15_{6,9}$ E)	198636.78	104.45	9.73E-05	2.86	0.47	2.77	0.99	0.026	0.008	0.12	0.03	
60003	$HCOOCH_3$ ($16_{5,11}$-$15_{5,10}$ E)	200936.16	97.52	1.10E-04	2.46	0.32	3.00	0.83	0.063	0.014	0.31	0.06	
60003	$HCOOCH_3$ ($16_{5,11}$-$15_{5,10}$ A)	200956.37	97.51	1.10E-04	2.40	0.21	2.42	0.45	0.063	0.010	0.25	0.05	
60003	$HCOOCH_3$ ($17_{3,15}$-$16_{3,14}$ A)	203864.21	95.55	1.22E-04	3.33	0.40	3.00	0.94	0.144	0.014	0.72	0.13	
60003	$HCOOCH_3$ ($18_{2,17}$-$17_{2,16}$ A)	205501.70	98.96	1.28E-04	2.50	0.19	3.42	0.43	0.077	0.007	0.44	0.08	
60003	$HCOOCH_3$ ($18_{1,17}$-$17_{1,16}$ E)	205663.74	98.96	1.28E-04	2.24	0.52	3.00	1.30	0.081	0.030	0.41	0.08	
60003	$HCOOCH_3$ ($18_{1,17}$-$17_{1,16}$ A)	205669.41	98.94	1.28E-04	2.41	0.19	2.88	0.44	0.075	0.010	0.36	0.07	
60003	$HCOOCH_3$ ($16_{4,12}$-$15_{4,11}$ E)	206247.92	92.59	1.24E-04	2.24	0.19	3.78	0.47	0.059	0.006	0.37	0.07	
60003	$HCOOCH_3$ ($16_{3,13}$-$15_{3,12}$ A)	206619.48	89.25	1.28E-04	2.37	0.11	2.24	0.20	0.081	0.007	0.31	0.06	
60003	$HCOOCH_3$ ($17_{2,15}$-$16_{2,14}$ A)	206719.92	95.26	1.28E-04	2.87	0.09	3.90	0.25	0.075	0.004	0.50	0.09	
60003	$HCOOCH_3$ ($17_{4,14}$-$16_{4,13}$ E)	209918.52	101.43	1.31E-04	1.94	0.49	3.73	1.32	0.078	0.021	0.49	0.09	
60003	$HCOOCH_3$ ($17_{7,10}$-$16_{7,9}$ E)	210434.51	123.02	1.16E-04	2.85	0.34	2.74	0.57	0.047	0.009	0.22	0.04	
60003	$HCOOCH_3$ ($17_{7,11}$-$16_{7,10}$ A)	210442.75	123.01	1.17E-04	2.58	0.14	4.08	0.33	0.056	0.004	0.39	0.07	
60003	$HCOOCH_3$ ($17_{7,11}$-$16_{7,10}$ E)	210451.40	123.01	1.16E-04	2.12	0.14	4.11	0.33	0.052	0.004	0.37	0.07	
60003	$HCOOCH_3$ ($17_{7,10}$-$16_{7,9}$ A)	210463.20	123.01	1.17E-04	2.56	0.25	3.83	0.61	0.049	0.006	0.32	0.06	
60003	$HCOOCH_3$ ($17_{6,12}$-$16_{6,11}$ E)	211266.10	114.57	1.21E-04	2.31	0.19	4.09	0.46	0.048	0.005	0.33	0.06	
60003	$HCOOCH_3$ ($17_{6,11}$-$16_{6,10}$ A)	211575.13	114.59	1.25E-04	1.95	0.55	3.00	1.34	0.078	0.029	0.40	0.07	
60003	$HCOOCH_3$ ($17_{5,13}$-$16_{5,12}$ E)	211771.08	107.49	1.30E-04	1.97	0.39	3.50	1.03	0.076	0.016	0.45	0.08	
60003	$HCOOCH_3$ ($17_{5,13}$-$16_{5,12}$ A)	211784.86	107.48	1.31E-04	2.84	0.59	3.43	1.29	0.062	0.008	0.37	0.07	
60003	$HCOOCH_3$ ($17_{5,12}$-$16_{5,11}$ A)	214652.63	107.81	1.36E-04	2.05	0.33	4.06	0.86	0.085	0.014	0.60	0.11	
60003	$HCOOCH_3$ ($18_{3,16}$-$17_{3,15}$ A)	214792.55	105.86	1.44E-04	2.20	0.44	3.00	1.08	0.138	0.041	0.72	0.13	
60003	$HCOOCH_3$ ($18_{2,16}$-$17_{2,15}$ E)	216830.20	105.68	1.48E-04	2.13	0.51	4.26	1.46	0.057	0.011	0.42	0.08	
60003	$HCOOCH_3$ ($18_{2,16}$-$17_{2,15}$ A)	216838.89	105.67	1.48E-04	2.57	0.25	3.37	0.59	0.066	0.010	0.39	0.07	
60003	$HCOOCH_3$ ($17_{3,14}$-$16_{3,13}$ E)	218280.90	99.73	1.51E-04	2.66	0.13	4.47	0.36	0.086	0.005	0.67	0.12	
60003	$HCOOCH_3$ ($17_{3,14}$-$16_{3,13}$ A)	218297.89	99.72	1.51E-04	2.46	0.09	4.18	0.23	0.091	0.004	0.67	0.12	
60003	$HCOOCH_3$ ($17_{4,13}$-$16_{4,12}$ E)	220166.89	103.15	1.52E-04	3.00	0.22	3.31	0.52	0.058	0.008	0.34	0.07	
60003	$HCOOCH_3$ ($17_{4,13}$-$16_{4,12}$ A)	220190.29	103.15	1.52E-04	1.54	0.23	3.39	0.60	0.065	0.010	0.39	0.08	
60003	$HCOOCH_3$ ($18_{4,15}$-$17_{4,14}$ E)	221660.48	112.06	1.55E-04	1.89	0.15	4.67	0.43	0.096	0.006	0.80	0.14	
60003	$HCOOCH_3$ ($8_{5,3}$-$7_{4,3}$ E)	222657.32	37.86	1.58E-05	2.31	0.41	3.00	0.95	0.032	0.009	0.17	0.04	
60003	$HCOOCH_3$ ($18_{6,12}$-$17_{6,11}$ A)	224609.38	125.37	1.52E-04	2.18	0.18	2.93	0.45	0.071	0.009	0.37	0.07	

Table 4. continued.

TAG	Species & Transition	Frequency (MHz)	E_{up} (K)	A_{ij} s^{-1}	V_o (km s^{-1})	δ_{V_o}	$FWHM$ (km s^{-1})	δ_{FWHM}	Int (K)	δ_{Int}	Flux (K km s^{-1})	δ_{Flux}	Comments
60003	$HCOOCH_3$ ($19_{3,17}$-$18_{3,16}$ E)	225608.82	116.70	1.67E-04	2.69	0.22	3.38	0.58	0.088	0.011	0.53	0.10	
60003	$HCOOCH_3$ ($20_{2,19}$-$19_{2,18}$ E)	226713.06	120.22	1.72E-04	2.45	0.37	4.00	0.96	0.147	0.027	1.06	0.18	
60003	$HCOOCH_3$ ($20_{2,19}$-$19_{2,18}$ A)	226718.69	120.21	1.72E-04	2.23	0.21	3.07	0.53	0.130	0.019	0.72	0.12	
60003	$HCOOCH_3$ ($18_{5,13}$-$17_{5,12}$ E)	228628.88	118.79	1.66E-04	2.60	0.30	2.86	0.79	0.093	0.011	0.48	0.08	
60003	$HCOOCH_3$ ($18_{5,13}$-$17_{5,12}$ A)	228651.40	118.78	1.66E-04	2.33	0.22	2.57	0.50	0.111	0.019	0.52	0.09	
60003	$HCOOCH_3$ ($18_{3,15}$-$17_{3,14}$ E)	229405.02	110.74	1.75E-04	1.96	0.22	3.11	0.47	0.083	0.011	0.47	0.09	
60003	$HCOOCH_3$ ($19_{7,13}$-$18_{7,12}$ A)	235844.54	145.04	1.71E-04	2.25	0.11	2.28	0.28	0.076	0.008	0.32	0.06	
60003	$HCOOCH_3$ ($19_{7,13}$-$18_{7,12}$ E)	235865.97	145.04	1.67E-04	2.24	0.42	3.00	1.17	0.049	0.012	0.27	0.06	
60003	$HCOOCH_3$ ($21_{1,20}$-$20_{1,19}$ E)	237344.87	131.61	1.98E-04	2.25	0.19	4.44	0.53	0.093	0.007	0.77	0.14	
60003	$HCOOCH_3$ ($21_{1,20}$-$20_{1,19}$ A)	237350.39	131.60	1.98E-04	2.23	0.60	3.89	1.33	0.085	0.010	0.62	0.11	
60003	$HCOOCH_3$ ($21_{2,20}$-$20_{1,19}$ E)	237393.21	131.61	2.69E-05	2.53	0.27	3.81	0.69	0.052	0.008	0.37	0.08	
60003	$HCOOCH_3$ ($19_{3,16}$-$18_{3,15}$ A)	240034.67	122.25	2.01E-04	2.11	0.19	3.54	0.52	0.097	0.010	0.65	0.12	
60003	$HCOOCH_3$ ($20_{5,16}$-$19_{5,15}$ E)	249031.00	141.57	2.18E-04	1.86	0.15	3.83	0.40	0.051	0.004	0.38	0.07	
60003	$HCOOCH_3$ ($20_{3,17}$-$19_{3,16}$ A)	250258.38	134.26	2.28E-04	1.97	0.57	4.00	1.58	0.060	0.016	0.47	0.09	
60003	$HCOOCH_3$ ($20_{5,15}$-$19_{5,14}$ E)	257226.61	142.79	2.42E-04	2.67	0.34	3.50	0.92	0.055	0.011	0.39	0.08	
60003	$HCOOCH_3$ ($20_{4,16}$-$19_{4,15}$ E)	259499.90	138.67	2.54E-04	2.30	0.14	4.68	0.37	0.105	0.004	1.00	0.18	
60003	$HCOOCH_3$ ($20_{4,16}$-$19_{4,15}$ A)	259521.81	138.67	2.54E-04	2.07	0.14	3.56	0.38	0.084	0.006	0.61	0.12	
60003	$HCOOCH_3$ ($8_{7,1}$-$7_{6,1}$ E)	278094.52	53.78	4.39E-05	2.21	0.17	3.28	0.45	0.048	0.005	0.35	0.09	
60003	$HCOOCH_3$ ($13_{7,6}$-$12_{6,6}$ E)	339152.69	86.26	5.21E-05	2.66	0.13	1.37	0.30	0.052	0.010	0.14	0.03	
60003	$HCOOCH_3$ ($13_{7,7}$-$12_{6,6}$ A)	339185.91	86.24	5.22E-05	2.64	0.31	1.81	0.80	0.030	0.010	0.10	0.02	
44505	SiO (2-1)	86846.96	6.25	2.93E-05	4.87	0.14	4.57	0.32	0.358	0.021	2.07	0.23	small wings
44505	SiO (3-2)	130268.61	12.50	1.06E-04	4.34	0.08	4.62	0.19	0.224	0.009	5.38	0.86	
44505	SiO (4-3)	173688.31	20.84	2.60E-04	4.97	0.13	6.05	0.32	0.623	0.035	5.98	1.02	wings
44505	SiO (5-4)	217104.98	31.26	5.20E-04	4.39	0.11	5.99	0.27	0.810	0.030	8.49	1.44	small wings
44505	SiO (6-5)	260518.02	43.76	9.12E-04	4.06	0.10	6.38	0.23	0.813	0.017	18.60	3.16	wings
44505	SiO (8-7)	347330.58	75.02	2.20E-03	3.79	0.10	5.79	0.23	0.825	0.025	9.23	1.66	
27002	HNC (1-0)	90663.59	4.35	2.69E-05	4.30	0.30	3.54	0.74	1.624	0.277	7.47	0.82	
27002	HNC (3-2)	271981.14	26.11	9.34E-04	3.90	0.07	3.31	0.17	2.262	0.099	16.19	2.75	
27002	HNC (4-3)	362630.30	43.51	2.30E-03	3.20	0.12	1.57	0.27	2.741	0.413	8.48	1.53	self abs
28508	DNC (2-1)	152609.77	10.99	1.54E-04	4.30	0.03	1.63	0.09	1.233	0.050	2.94	0.50	
28508	DNC (3-2)	228910.49	21.97	5.57E-04	4.32	0.04	3.31	0.10	0.333	0.006	2.00	0.34	
28005	$HN^{13}C$ (1-0)	87090.85	4.18	1.87E-05	4.41	0.09	1.83	0.22	0.443	0.045	1.05	0.12	
28005	$HN^{13}C$ (2-1)	174179.41	12.54	1.79E-04	4.10	0.18	2.26	0.50	0.339	0.053	1.18	0.20	
28005	$HN^{13}C$ (3-2)	261263.31	25.08	6.48E-04	3.27	0.40	5.69	1.39	0.158	0.017	1.85	0.32	Blend?
28005	$HN^{13}C$ (4-3)	348340.27	41.80	1.59E-03	3.19	0.45	3.96	1.50	0.099	0.019	0.76	0.14	
51501	HC_3N (9-8)	81881.47	19.65	4.21E-05	3.94	0.02	2.16	0.04	0.889	0.015	2.46	0.27	
51501	HC_3N (10-9)	90979.02	24.02	5.81E-05	3.95	0.02	2.11	0.04	0.845	0.015	2.31	0.25	
51501	HC_3N (11-10)	100076.39	28.82	7.77E-05	3.95	0.02	2.21	0.06	0.751	0.017	2.19	0.24	
51501	HC_3N (12-11)	109173.63	34.06	1.01E-04	3.87	0.03	2.35	0.06	0.296	0.006	0.93	0.11	
51501	HC_3N (15-14)	136464.41	52.40	1.99E-04	3.94	0.07	3.01	0.17	0.464	0.022	1.97	0.34	
51501	HC_3N (16-15)	145560.96	59.38	2.42E-04	3.62	0.06	2.87	0.13	0.415	0.017	1.72	0.29	
51501	HC_3N (17-16)	154657.28	66.80	2.91E-04	3.88	0.10	3.43	0.24	0.329	0.020	1.66	0.28	
51501	HC_3N (18-17)	163753.39	74.66	3.46E-04	3.86	0.11	3.80	0.25	0.377	0.022	2.15	0.37	
51501	HC_3N (19-18)	172849.30	82.96	4.08E-04	3.59	0.20	5.41	0.47	0.284	0.021	2.36	0.40	
51501	HC_3N (22-21)	200135.39	110.46	6.35E-04	3.21	0.14	6.15	0.34	0.161	0.008	1.64	0.28	
51501	HC_3N (23-22)	209230.23	120.51	7.26E-04	3.43	0.18	6.84	0.42	0.186	0.010	2.16	0.37	

Table 4. continued.

TAG	Species & Transition	Frequency (MHz)	E_{up} (K)	A_{ij} s^{-1}	V_o (km s^{-1})	δ_{V_o}	$FWHM$ (km s^{-1})	δ_{FWHM}	Int (K)	δ_{Int}	Flux (K km s^{-1})	δ_{Flux}	Comments
51501	HC_3N (24-23)	218324.72	130.98	8.26E-04	3.30	0.20	6.29	0.48	0.207	0.014	2.28	0.39	
51501	HC_3N (25-24)	227418.90	141.90	9.35E-04	3.36	0.07	6.20	0.17	0.206	0.005	2.30	0.39	
51501	HC_3N (26-25)	236512.79	153.25	1.05E-03	3.42	0.10	6.18	0.23	0.198	0.006	2.29	0.39	
51501	HC_3N (27-26)	245606.32	165.04	1.18E-03	2.64	0.27	6.27	0.63	0.068	0.006	0.82	0.14	
51501	HC_3N (29-28)	263792.31	189.92	1.46E-03	2.51	0.14	7.57	0.33	0.297	0.011	4.69	0.80	
51501	HC_3N (30-29)	272884.75	203.02	1.62E-03	3.54	0.42	6.58	1.00	0.100	0.013	1.43	0.26	
52005	DC_3N (10_{11}-9_{10})	84429.83	22.29	4.63E-05	4.08	0.27	2.68	0.73	0.052	0.009	0.18	0.03	
52005	DC_3N (11_{12}-10_{11})	92872.39	26.74	6.19E-05	4.55	0.15	2.04	0.37	0.053	0.008	0.14	0.02	
52005	DC_3N (12_{13}-11_{12})	101314.83	31.61	8.06E-05	4.27	0.14	2.43	0.39	0.041	0.005	0.13	0.02	
52005	DC_3N (13_{14}-12_{13})	109757.14	36.87	1.03E-04	4.02	0.43	2.60	1.16	0.071	0.022	0.25	0.04	
52005	DC_3N (17_{18}-16_{17})	143524.87	62.00	2.32E-04	4.24	0.28	2.60	0.66	0.061	0.013	0.23	0.04	
52005	DC_3N (19_{20}-18_{19})	160407.68	76.99	3.25E-04	4.57	0.27	3.29	0.76	0.024	0.004	0.12	0.03	
34502	H_2S ($1_{1,0}$-$1_{0,1}$)	168762.76	27.88	2.68E-05	3.92	0.19	4.84	0.45	2.420	0.194	17.80	3.03	
34502	H_2S ($2_{2,0}$-$2_{1,1}$)	216710.44	83.98	4.87E-05	3.18	0.06	4.95	0.15	0.862	0.023	7.41	1.26	
35001	HDS($1_{0,1}$-$0_{0,0}$)	244555.58	11.74	1.25E-05	3.44	0.44	3.89	1.19	0.058	0.013	0.44	0.08	
35001	HDS($2_{0,2}$-$1_{1,1}$)	333278.71	34.67	6.00E-05	2.66	0.13	0.93	0.36	0.146	0.045	0.26	0.05	
38082	o-c-C_3H_2 ($3_{1,2}$-$3_{0,3}$)	82966.20	13.70	1.09E-05	4.16	0.06	2.01	0.13	0.184	0.011	0.47	0.05	
38082	o-c-C_3H_2 ($2_{1,2}$-$1_{0,1}$)	85338.89	4.10	2.55E-05	4.21	0.02	1.98	0.04	0.625	0.012	1.59	0.18	
38082	o-c-C_3H_2 ($4_{3,2}$-$4_{2,3}$)	85656.43	26.72	1.67E-05	4.28	0.10	2.21	0.23	0.079	0.007	0.22	0.03	
38082	o-c-C_3H_2 ($3_{1,2}$-$2_{2,1}$)	145089.60	13.70	7.43E-05	4.10	0.04	1.66	0.10	0.566	0.030	1.35	0.23	
38082	o-c-C_3H_2 ($4_{1,4}$-$3_{0,3}$)	150851.91	16.96	1.80E-04	4.38	0.04	1.92	0.09	0.956	0.040	2.67	0.45	
38082	o-c-C_3H_2 ($3_{3,0}$-$2_{2,1}$)	216278.76	17.12	2.81E-04	4.36	0.11	2.86	0.41	0.183	0.019	0.91	0.16	
38082	o-c-C_3H_2 ($5_{1,4}$-$4_{2,3}$)	217940.05	33.07	4.42E-04	4.12	0.08	2.47	0.21	0.223	0.016	0.96	0.16	
38082	o-c-C_3H_2 ($4_{3,2}$-$3_{2,1}$)	227169.13	26.72	3.42E-04	4.24	0.19	3.33	0.46	0.180	0.020	1.08	0.18	
38082	o-c-C_3H_2 ($3_{2,1}$-$2_{1,2}$)	244222.13	15.82	6.48E-05	4.49	0.12	3.25	0.30	0.088	0.007	0.55	0.10	
38082	o-c-C_3H_2 ($5_{2,3}$-$4_{3,2}$)	249054.37	38.67	4.57E-04	3.49	0.35	4.10	0.86	0.052	0.009	0.42	0.08	
38082	o-c-C_3H_2 ($7_{0,7}$-$6_{1,6}$)	251314.34	48.32	9.34E-04	3.92	0.09	3.24	0.21	0.289	0.016	1.85	0.32	
38082	o-c-C_3H_2 ($6_{2,5}$-$5_{1,4}$)	251527.30	45.14	7.41E-04	3.95	0.18	2.99	0.45	0.154	0.019	0.91	0.16	
38082	o-c-C_3H_2 ($4_{4,1}$-$3_{3,0}$)	265759.44	29.87	7.98E-04	3.90	0.17	3.02	0.43	0.126	0.015	0.80	0.15	
38082	o-c-C_3H_2 ($5_{5,0}$-$4_{4,1}$)	349263.98	46.63	1.81E-03	3.75	0.27	3.15	0.68	0.113	0.019	0.69	0.13	
38092	p-c-C_3H_2 ($4_{2,2}$-$4_{1,3}$)	80723.17	28.82	1.46E-05	4.01	0.27	3.98	0.67	0.032	0.004	0.16	0.04	
38092	p-c-C_3H_2 ($2_{0,2}$-$1_{1,1}$)	82093.56	6.43	2.07E-05	4.30	0.02	1.82	0.08	0.287	0.009	0.67	0.07	
38092	p-c-C_3H_2 ($3_{2,2}$-$3_{1,3}$)	84727.70	16.14	1.14E-05	4.31	0.06	1.93	0.15	0.074	0.005	0.18	0.02	
38092	p-c-C_3H_2 ($2_{2,0}$-$1_{1,1}$)	150436.55	9.71	5.88E-05	4.23	0.05	1.37	0.12	0.193	0.015	0.39	0.07	
38092	p-c-C_3H_2 ($4_{0,4}$-$3_{1,3}$)	150820.67	19.31	1.80E-04	4.38	0.03	1.64	0.08	0.407	0.017	0.97	0.17	
38092	p-c-C_3H_2 ($3_{2,2}$-$2_{1,1}$)	155518.30	16.14	1.22E-04	4.28	0.06	1.63	0.14	0.282	0.020	0.68	0.12	
38092	p-c-C_3H_2 ($4_{2,2}$-$3_{3,1}$)	204788.93	28.82	1.36E-04	4.84	0.10	2.06	0.18	0.077	0.006	0.26	0.05	
38092	p-c-C_3H_2 ($5_{2,4}$-$4_{1,3}$)	218160.44	35.42	4.44E-04	4.13	0.30	4.96	0.87	0.094	0.011	0.81	0.14	
38092	p-c-C_3H_2 ($6_{1,5}$-$5_{2,4}$)	251508.69	47.49	7.41E-04	3.91	0.16	3.70	0.40	0.055	0.005	0.40	0.08	
39003	c-C_3HD (4_{04}-3_{13})	135640.90	17.39	1.09E-04	4.26	0.09	1.48	0.21	0.144	0.018	0.30	0.05	
39003	c-C_3HD (4_{14}-3_{03})	136370.91	17.39	1.11E-04	4.39	0.06	1.18	0.16	0.172	0.019	0.29	0.05	
39003	c-C_3HD (5_{05}-4_{14})	166112.36	25.37	2.13E-04	4.56	0.15	1.18	0.34	0.088	0.022	0.16	0.03	
39003	c-C_3HD (5_{15}-4_{04})	166250.12	25.37	2.13E-04	4.10	0.08	2.66	0.19	0.084	0.005	0.34	0.06	
39003	c-C_3HD (4_{23}-3_{12})	173911.59	22.49	1.52E-04	4.90	0.18	3.03	0.44	0.087	0.010	0.40	0.08	
46008	CH_3OCH_3 ($11_{1,10}$-$11_{0,11}$ AA)	82460.38	62.92	2.16E-06	1.76	0.29	3.55	0.77	0.022	0.004	0.10	0.02	
46008	CH_3OCH_3 ($4_{2,2}$-$4_{1,3}$ EE)	82688.77	14.74	2.31E-06	2.92	0.25	2.10	0.59	0.021	0.005	0.06	0.02	

Table 4. continued.

TAG	Species & Transition	Frequency (MHz)	E_{up} (K)	A_{ij} s^{-1}	V_o (km s^{-1})	δ_{V_o}	*FWHM* (km s^{-1})	δ_{FWHM}	Int (K)	δ_{Int}	Flux (K km s^{-1})	δ_{Flux}	Comments
46008	CH_3OCH_3 ($14_{2,12}$-$14_{1,13}$ EE)	83098.92	102.85	3.50E-06	2.18	0.21	3.66	0.58	0.039	0.005	0.19	0.03	
46008	CH_3OCH_3 ($3_{2,1}$-$3_{1,2}$ EE)	84634.40	11.09	2.18E-06	2.58	0.12	2.75	0.32	0.032	0.002	0.11	0.02	
46008	CH_3OCH_3 ($15_{2,13}$-$15_{1,14}$ AA)	88709.07	116.86	4.09E-06	2.02	0.26	2.99	0.75	0.024	0.004	0.09	0.02	
46008	CH_3OCH_3 ($3_{2,2}$-$3_{1,3}$ EE)	91476.53	11.08	2.45E-06	1.86	0.28	1.97	0.64	0.020	0.007	0.06	0.01	
46008	CH_3OCH_3 ($12_{1,11}$-$12_{0,12}$ EE)	93666.43	74.02	2.84E-06	2.50	0.39	2.23	0.95	0.046	0.016	0.13	0.02	
46008	CH_3OCH_3 ($12_{1,11}$-$12_{0,12}$ AA)	93668.35	74.02	2.84E-06	2.16	0.21	2.36	0.57	0.025	0.004	0.08	0.02	
46008	CH_3OCH_3 ($16_{2,14}$-$16_{1,15}$ EE)	95731.26	131.80	4.88E-06	2.32	0.42	2.39	1.12	0.052	0.018	0.16	0.02	
46008	CH_3OCH_3 ($5_{2,4}$-$5_{1,5}$ EE)	96849.85	19.26	3.12E-06	2.13	0.17	4.12	0.48	0.039	0.003	0.21	0.03	
46008	CH_3OCH_3 ($5_{2,4}$-$5_{1,5}$ AA)	96852.46	19.26	3.12E-06	3.04	0.20	1.72	0.41	0.021	0.005	0.05	0.01	
46008	CH_3OCH_3 ($6_{2,5}$-$6_{1,6}$ EE)	100463.04	24.71	3.46E-06	2.50	0.22	3.13	0.54	0.040	0.006	0.16	0.02	
46008	CH_3OCH_3 ($6_{2,5}$-$6_{1,6}$ AA)	100465.70	24.71	3.46E-06	3.06	0.23	2.22	0.57	0.035	0.007	0.10	0.02	
46008	CH_3OCH_3 ($8_{2,7}$-$8_{1,8}$ AA)	109576.78	38.31	4.27E-06	2.39	0.31	2.35	0.75	0.045	0.012	0.14	0.03	
46008	CH_3OCH_3 ($18_{3,15}$-$18_{2,16}$ EE)	111813.67	169.80	8.41E-06	2.13	0.39	2.47	1.05	0.037	0.011	0.12	0.03	
46008	CH_3OCH_3 ($9_{2,8}$-$9_{1,9}$ EE)	115074.91	46.46	4.78E-06	2.14	0.30	3.46	0.86	0.049	0.006	0.23	0.04	
46008	CH_3OCH_3 ($16_{3,13}$-$16_{2,14}$ EE)	115293.58	137.33	8.58E-06	2.53	0.07	2.77	0.20	0.059	0.003	0.22	0.04	
46008	CH_3OCH_3 ($16_{3,13}$-$16_{2,14}$ AA)	115295.58	137.33	8.58E-06	2.31	0.14	2.45	0.42	0.027	0.003	0.09	0.03	
46008	CH_3OCH_3 ($12_{3,9}$-$12_{2,10}$ EE)	129558.98	83.88	1.00E-05	2.53	0.24	2.85	0.63	0.062	0.011	0.25	0.05	
46008	CH_3OCH_3 ($12_{3,9}$-$12_{2,10}$ AA)	129561.82	83.88	1.00E-05	2.76	0.28	2.54	0.67	0.038	0.009	0.13	0.03	
46008	CH_3OCH_3 ($15_{1,14}$-$15_{0,15}$ AA)	131912.06	112.60	6.02E-06	1.84	0.13	3.01	0.38	0.039	0.004	0.18	0.03	
46008	CH_3OCH_3 ($11_{3,8}$-$11_{2,9}$ EE)	133268.32	72.88	1.04E-05	2.74	0.20	3.08	0.68	0.051	0.006	0.22	0.04	
46008	CH_3OCH_3 ($11_{3,8}$-$11_{2,9}$ AA)	133271.31	72.88	1.04E-05	2.29	0.34	2.07	0.95	0.054	0.015	0.16	0.03	
46008	CH_3OCH_3 ($9_{3,6}$-$9_{2,7}$ EE)	139503.68	53.67	1.10E-05	2.34	0.12	3.05	0.31	0.090	0.007	0.39	0.07	
46008	CH_3OCH_3 ($8_{3,5}$-$8_{2,6}$ EE)	141832.26	45.45	1.11E-05	2.34	0.14	2.94	0.42	0.076	0.007	0.32	0.06	
46008	CH_3OCH_3 ($13_{2,12}$-$13_{1,13}$ EE)	143162.99	88.00	7.75E-06	2.55	0.39	3.13	1.10	0.095	0.014	0.42	0.08	
46008	CH_3OCH_3 ($13_{2,12}$-$13_{1,13}$ AA)	143166.02	88.00	7.74E-06	2.65	0.14	2.10	0.45	0.072	0.010	0.22	0.04	
46008	CH_3OCH_3 ($7_{3,4}$-$7_{2,5}$ EE)	143602.99	38.15	1.10E-05	2.50	0.15	2.39	0.40	0.093	0.012	0.32	0.06	
46008	CH_3OCH_3 ($6_{3,3}$-$6_{2,4}$ EE)	144858.98	31.77	1.06E-05	2.51	0.28	3.09	0.90	0.071	0.009	0.32	0.06	
46008	CH_3OCH_3 ($6_{3,3}$-$6_{2,4}$ AA)	144862.02	31.77	1.07E-05	2.60	0.06	2.24	0.16	0.063	0.004	0.20	0.04	
46008	CH_3OCH_3 ($5_{3,2}$-$5_{2,3}$ AA)	145682.64	26.31	1.01E-05	3.16	0.29	2.32	0.52	0.056	0.004	0.19	0.04	
46008	CH_3OCH_3 ($3_{3,1}$-$3_{2,1}$ EE)	146405.19	18.12	2.79E-06	2.98	0.09	1.11	0.29	0.040	0.008	0.06	0.02	
46008	CH_3OCH_3 ($3_{2,1}$-$2_{1,2}$ EE)	146704.72	11.09	1.10E-05	2.55	0.09	2.56	0.24	0.196	0.006	0.35	0.06	
46008	CH_3OCH_3 ($3_{2,1}$-$2_{1,2}$ AA)	146707.17	11.09	1.10E-05	2.54	0.17	2.18	0.42	0.079	0.013	0.25	0.05	
46008	CH_3OCH_3 ($5_{3,3}$-$5_{2,4}$ EA)	146865.98	26.31	8.65E-06	2.73	0.15	1.40	0.38	0.053	0.012	0.11	0.03	
46008	CH_3OCH_3 ($5_{3,3}$-$5_{2,4}$ EE)	146872.55	26.31	9.66E-06	2.45	0.28	2.37	0.70	0.086	0.013	0.29	0.05	
46008	CH_3OCH_3 ($5_{3,3}$-$5_{2,4}$ AA)	146877.31	26.31	1.03E-05	2.32	0.38	3.00	1.05	0.030	0.007	0.13	0.03	
46008	CH_3OCH_3 ($6_{3,4}$-$6_{2,5}$ EA)	147202.09	31.77	1.08E-05	3.01	0.09	2.03	0.24	0.067	0.006	0.20	0.04	
46008	CH_3OCH_3 ($6_{3,4}$-$6_{2,5}$ AE)	147203.76	31.77	1.11E-05	2.84	0.20	1.41	0.51	0.081	0.024	0.17	0.03	
46008	CH_3OCH_3 ($6_{3,4}$-$6_{2,5}$ EE)	147206.81	31.77	1.11E-05	2.48	0.17	3.07	0.47	0.084	0.009	0.37	0.07	
46008	CH_3OCH_3 ($7_{3,5}$-$7_{2,6}$ AA)	147734.95	38.15	1.18E-05	2.39	0.12	1.42	0.28	0.074	0.012	0.15	0.03	
46008	CH_3OCH_3 ($8_{3,6}$-$8_{2,7}$ EE)	148500.39	45.44	1.23E-05	2.14	0.20	3.09	0.51	0.083	0.011	0.37	0.07	
46008	CH_3OCH_3 ($8_{3,6}$-$8_{2,7}$ AA)	148503.83	45.44	1.24E-05	2.82	0.30	3.27	0.63	0.051	0.003	0.24	0.05	
46008	CH_3OCH_3 ($9_{3,7}$-$9_{2,8}$ EE)	149569.78	53.64	1.29E-05	2.51	0.17	2.43	0.40	0.084	0.012	0.30	0.05	
46008	CH_3OCH_3 ($9_{3,7}$-$9_{2,8}$ AA)	149573.12	53.64	1.29E-05	2.47	0.22	3.02	0.58	0.047	0.005	0.21	0.04	
46008	CH_3OCH_3 ($10_{3,8}$-$10_{2,9}$ EE)	150995.39	62.75	1.35E-05	2.47	0.15	2.53	0.40	0.095	0.011	0.35	0.06	
46008	CH_3OCH_3 ($10_{3,8}$-$10_{2,9}$ AA)	150998.65	62.75	1.35E-05	2.28	0.16	2.08	0.39	0.080	0.012	0.24	0.05	
46008	CH_3OCH_3 ($14_{2,13}$-$14_{1,14}$ EE)	151593.92	100.61	8.77E-06	2.35	0.11	1.36	0.25	0.051	0.008	0.10	0.02	
46008	CH_3OCH_3 ($11_{3,9}$-$11_{2,10}$ EE)	152831.37	72.78	1.41E-05	2.78	0.19	2.84	0.66	0.049	0.006	0.20	0.04	

Table 4. continued.

TAG	Species & Transition	Frequency (MHz)	E_{up} (K)	A_{ij} s^{-1}	V_o (km s^{-1})	δ_{V_o}	$FWHM$ (km s^{-1})	δ_{FWHM}	Int (K)	δ_{Int}	Flux (K km s^{-1})	δ_{Flux}	Comments
46008	CH_3OCH_3 ($11_{3,9}$-$11_{2,10}$ AA)	152834.55	72.78	1.41E-05	2.80	0.34	2.60	0.90	0.039	0.009	0.15	0.03	
46008	CH_3OCH_3 ($11_{1,10}$-$10_{2,9}$ AA)	154453.66	62.92	8.02E-06	2.37	0.12	1.32	0.30	0.057	0.011	0.11	0.02	
46008	CH_3OCH_3 ($11_{1,10}$-$10_{2,9}$ EE)	154455.08	62.92	8.02E-06	2.53	0.17	2.34	0.54	0.078	0.008	0.27	0.05	
46008	CH_3OCH_3 ($12_{3,10}$-$12_{2,11}$ EE)	155128.43	83.73	1.48E-05	2.40	0.07	2.84	0.19	0.097	0.005	0.41	0.07	
46008	CH_3OCH_3 ($12_{3,10}$-$12_{2,11}$ AA)	155131.54	83.73	1.48E-05	2.49	0.20	2.39	0.55	0.080	0.014	0.28	0.05	
46008	CH_3OCH_3 ($13_{3,11}$-$13_{2,12}$ EE)	157932.36	95.58	1.56E-05	2.42	0.24	2.38	0.60	0.108	0.022	0.38	0.07	
46008	CH_3OCH_3 ($17_{1,16}$-$17_{0,17}$ EE)	159320.27	142.66	9.18E-06	2.49	0.08	1.30	0.20	0.089	0.012	0.17	0.03	
46008	CH_3OCH_3 ($17_{1,16}$-$17_{0,17}$ AA)	159323.26	142.66	9.18E-06	2.62	0.05	1.17	0.10	0.040	0.003	0.07	0.02	
46008	CH_3OCH_3 ($4_{2,3}$-$3_{1,2}$ EE)	160204.08	14.72	1.34E-05	2.60	0.17	2.05	0.42	0.089	0.015	0.27	0.05	
46008	CH_3OCH_3 ($4_{2,3}$-$3_{1,2}$ AA)	160206.57	14.72	1.35E-05	2.57	0.12	1.18	0.31	0.076	0.015	0.13	0.03	
46008	CH_3OCH_3 ($15_{2,14}$-$15_{1,15}$ EE)	160521.55	114.10	9.92E-06	2.19	0.30	2.42	0.77	0.053	0.013	0.19	0.04	
46008	CH_3OCH_3 ($14_{3,12}$-$14_{2,13}$ EE)	161282.72	108.35	1.65E-05	2.86	0.21	2.55	0.73	0.086	0.014	0.33	0.06	
46008	CH_3OCH_3 ($14_{3,12}$-$14_{2,13}$ AA)	161285.67	108.35	1.65E-05	2.68	0.14	2.14	0.34	0.070	0.009	0.23	0.04	
46008	CH_3OCH_3 ($18_{3,15}$-$17_{4,14}$ AA)	162277.21	169.80	5.05E-06	2.40	0.17	1.81	0.44	0.035	0.007	0.09	0.03	
46008	CH_3OCH_3 ($18_{3,15}$-$17_{4,14}$ EE)	162279.58	169.80	5.05E-06	2.38	0.19	1.28	0.44	0.057	0.017	0.11	0.03	
46008	CH_3OCH_3 ($4_{2,2}$-$3_{1,3}$ EE)	167743.99	14.74	1.36E-05	2.86	0.25	2.12	0.91	0.078	0.016	0.25	0.05	
46008	CH_3OCH_3 ($4_{2,2}$-$3_{1,3}$ AA)	167746.53	14.74	1.36E-05	2.55	0.07	1.16	0.16	0.083	0.010	0.15	0.03	
46008	CH_3OCH_3 ($16_{3,14}$-$16_{2,15}$ EE)	169743.49	136.61	1.88E-05	2.37	0.17	2.33	0.52	0.087	0.011	0.31	0.06	
46008	CH_3OCH_3 ($16_{2,15}$-$16_{1,16}$ AA)	169907.05	128.46	1.12E-05	2.94	0.16	1.77	0.40	0.061	0.011	0.16	0.04	
46008	CH_3OCH_3 ($18_{1,17}$-$18_{0,18}$ EE)	173084.04	158.96	1.11E-05	3.27	0.20	2.37	0.55	0.070	0.010	0.26	0.05	
46008	CH_3OCH_3 ($17_{3,15}$-$17_{2,16}$ AA)	174896.05	152.09	2.02E-05	3.05	0.21	1.71	0.56	0.064	0.015	0.17	0.04	
46008	CH_3OCH_3 ($5_{2,4}$-$4_{1,3}$ EE)	176801.27	19.26	1.67E-05	2.61	0.08	1.96	0.25	0.092	0.008	0.28	0.06	
46008	CH_3OCH_3 ($9_{4,6}$-$9_{3,7}$ EE)	204736.58	63.46	2.78E-05	2.33	0.12	2.96	0.30	0.086	0.007	0.43	0.08	
46008	CH_3OCH_3 ($8_{4,5}$-$8_{3,6}$ EA)	204832.63	55.27	1.92E-05	2.48	0.17	2.58	0.36	0.037	0.005	0.16	0.04	
46008	CH_3OCH_3 ($10_{3,8}$- $9_{2,7}$ EE)	328856.65	62.75	9.35E-05	2.43	0.25	2.08	0.69	0.155	0.031	0.61	0.11	
46008	CH_3OCH_3 ($10_{3,8}$- $9_{2,7}$ AA)	328859.97	62.75	9.35E-05	2.69	0.06	1.35	0.16	0.151	0.014	0.39	0.07	
46008	CH_3OCH_3 ($10_{3,7}$- $9_{2,8}$ EE)	340612.58	62.81	9.76E-05	2.58	0.03	1.87	0.08	0.159	0.004	0.57	0.10	
46008	CH_3OCH_3 ($10_{3,7}$- $9_{2,8}$ AA)	340615.91	62.81	9.76E-05	2.72	0.14	1.18	0.35	0.136	0.034	0.31	0.06	
46008	CH_3OCH_3 ($11_{2,9}$-$10_{1,10}$ EE)	349806.09	66.48	3.30E-05	2.49	0.05	1.14	0.11	0.093	0.008	0.20	0.04	
46008	CH_3OCH_3 ($11_{2,9}$-$10_{1,10}$ AA)	349809.18	66.48	3.30E-05	2.42	0.05	1.32	0.13	0.077	0.006	0.20	0.04	
46008	CH_3OCH_3 ($12_{3,10}$-$11_{2,9}$ EE)	359384.62	83.73	1.13E-04	2.57	0.05	1.26	0.12	0.225	0.017	0.55	0.10	
46008	CH_3OCH_3 ($12_{3,10}$-$11_{2,9}$ AA)	359387.66	83.73	1.13E-04	2.79	0.17	1.46	0.42	0.145	0.034	0.41	0.08	
46008	CH_3OCH_3 ($11_{3,8}$-$10_{2,9}$ EE)	361874.42	72.88	1.08E-04	2.68	0.18	1.28	0.49	0.196	0.056	0.49	0.09	
40502	CH_3CCH (5_2-4_2)	85450.77	41.21	1.70E-06	3.63	0.10	2.90	0.23	0.049	0.003	0.18	0.03	
40502	CH_3CCH (5_1-4_1)	85455.67	19.53	1.95E-06	3.67	0.04	2.29	0.10	0.140	0.005	0.41	0.05	
40502	CH_3CCH (5_0-4_0)	85457.30	12.30	2.03E-06	3.73	0.04	2.20	0.09	0.181	0.006	0.51	0.06	
40502	CH_3CCH (6_2-5_2)	102540.15	46.13	3.16E-06	3.96	0.05	2.62	0.11	0.087	0.003	0.30	0.04	
40502	CH_3CCH (6_1-5_1)	102546.02	24.45	3.46E-06	3.84	0.02	2.46	0.04	0.198	0.003	0.64	0.07	
40502	CH_3CCH (6_0-5_0)	102547.98	17.23	3.56E-06	3.93	0.04	2.41	0.08	0.235	0.007	0.75	0.08	
40502	CH_3CCH (8_3-7_3)	136704.50	94.56	7.39E-06	3.77	0.12	3.66	0.31	0.085	0.006	0.44	0.08	
40502	CH_3CCH (8_2-7_2)	136717.56	58.43	8.06E-06	3.93	0.16	3.70	0.45	0.100	0.009	0.52	0.09	
40502	CH_3CCH (8_1-7_1)	136725.40	36.76	8.47E-06	3.78	0.04	2.77	0.09	0.226	0.006	0.89	0.15	
40502	CH_3CCH (8_0-7_0)	136728.01	29.53	8.60E-06	3.78	0.15	2.46	0.36	0.287	0.037	1.00	0.17	
40502	CH_3CCH (9_3-8_3)	153790.77	101.94	1.10E-05	3.80	0.08	2.53	0.21	0.081	0.005	0.30	0.06	
40502	CH_3CCH (9_2-8_2)	153805.46	65.82	1.17E-05	3.53	0.10	2.27	0.25	0.110	0.010	0.37	0.07	
40502	CH_3CCH (9_1-8_1)	153814.28	44.14	1.22E-05	3.71	0.03	2.77	0.09	0.209	0.005	0.85	0.15	
40502	CH_3CCH (9_0-8_0)	153817.21	36.91	1.23E-05	3.67	0.10	2.51	0.24	0.276	0.022	1.02	0.17	

Table 4. continued.

TAG	Species & Transition	Frequency (MHz)	E_{up} (K)	A_{ij} s^{-1}	V_o (km s^{-1})	δ_{V_o}	$FWHM$ (km s^{-1})	δ_{FWHM}	Int (K)	δ_{Int}	Flux (K km s^{-1})	δ_{Flux}	Comments
40502	CH_3CCH (10_2-9_2)	170892.73	74.02	1.63E-05	3.96	0.22	3.50	0.57	0.123	0.015	0.66	0.12	
40502	CH_3CCH (10_1-9_1)	170902.52	52.34	1.68E-05	3.73	0.10	3.01	0.26	0.247	0.017	1.13	0.20	
40502	CH_3CCH (10_0-9_0)	170905.78	45.11	1.70E-05	3.94	0.05	3.23	0.12	0.301	0.009	1.48	0.25	
40502	CH_3CCH (12_1-11_1)	205076.82	71.20	2.94E-05	3.59	0.29	3.94	0.71	0.149	0.022	0.98	0.17	
40502	CH_3CCH (13_3-12_3)	222128.82	139.66	3.57E-05	3.37	0.24	4.06	0.61	0.085	0.010	0.61	0.11	
40502	CH_3CCH (13_2-12_2)	222150.01	103.54	3.69E-05	3.49	0.19	3.46	0.45	0.096	0.011	0.59	0.11	
40502	CH_3CCH (13_1-12_1)	222162.73	81.87	3.75E-05	3.20	0.23	3.31	0.59	0.121	0.018	0.71	0.12	
40502	CH_3CCH (13_0-12_0)	222166.97	74.64	3.78E-05	3.25	0.13	3.22	0.33	0.145	0.012	0.83	0.14	
40502	CH_3CCH (14_1-13_1)	239247.73	93.35	4.71E-05	3.18	0.15	3.69	0.38	0.088	0.007	0.61	0.11	
40502	CH_3CCH (14_0-13_0)	239252.29	86.12	4.73E-05	2.84	0.21	2.64	0.79	0.100	0.015	0.50	0.09	
40502	CH_3CCH (16_3-15_3)	273372.99	176.56	6.84E-05	3.97	0.28	3.87	0.72	0.081	0.012	0.69	0.13	
40502	CH_3CCH (16_2-15_2)	273399.05	140.45	6.98E-05	2.90	0.09	3.36	0.24	0.059	0.003	0.43	0.09	
41502	CH_2DCCH ($6_{1,6}$-$5_{1,5}$)	96691.59	21.70	2.90E-06	4.32	0.19	1.49	0.33	0.023	0.005	0.04	0.01	
41502	CH_2DCCH ($6_{2,5}$-$5_{2,4}$)	97077.80	38.14	2.69E-06	4.68	0.26	2.38	0.68	0.023	0.005	0.07	0.02	
41502	CH_2DCCH ($6_{0,6}$-$5_{0,5}$)	97080.73	16.31	3.02E-06	4.41	0.24	2.14	0.57	0.023	0.005	0.06	0.02	
41502	CH_2DCCH ($6_{1,5}$-$5_{1,4}$)	97472.74	21.83	2.97E-06	3.93	0.14	1.72	0.29	0.025	0.004	0.06	0.02	
25501	CCH (1 3/2 1 - 0 1/2 1)	87284.16	4.19	2.59E-07	4.00	0.04	1.83	0.11	0.168	0.008	0.40	0.05	
25501	CCH (1 3/2 2 - 0 1/2 1)	87316.93	4.19	1.53E-06	3.82	0.03	2.16	0.07	0.598	0.016	1.67	0.18	
25501	CCH (1 3/2 1 - 0 1/2 0)	87328.62	4.19	1.27E-06	3.88	0.04	1.99	0.09	0.438	0.017	1.13	0.12	
25501	CCH (1 1/2 1 - 0 1/2 1)	87402.00	4.20	1.27E-06	3.83	0.03	2.06	0.07	0.464	0.015	1.24	0.14	
25501	CCH (1 1/2 0 - 0 1/2 1)	87407.17	4.20	1.53E-06	3.80	0.01	1.82	0.04	0.287	0.005	0.68	0.08	
25501	CCH (1 1/2 1 - 0 1/2 0)	87446.51	4.20	2.61E-07	3.90	0.06	1.79	0.17	0.160	0.012	0.37	0.04	
25501	CCH (2 5/2 2 - 1 3/2 2)	174634.91	12.57	1.00E-06	3.95	0.08	2.08	0.19	0.125	0.010	0.40	0.07	
25501	CCH (2 5/2 3 - 1 3/2 2)	174663.22	12.58	1.47E-05	3.83	0.15	2.45	0.35	0.823	0.102	3.10	0.53	
25501	CCH (2 5/2 2 - 1 3/2 1)	174667.68	12.57	1.36E-05	3.82	0.11	2.20	0.25	0.620	0.062	2.11	0.36	
25501	CCH (2 3/2 2 - 1 1/2 1)	174721.78	12.58	1.16E-05	3.79	0.11	2.24	0.25	0.523	0.051	1.81	0.31	
25501	CCH (2 3/2 1 - 1 1/2 0)	174728.07	12.58	8.16E-06	3.73	0.11	2.30	0.25	0.252	0.024	0.89	0.15	
25501	CCH (2 3/2 2 - 1 3/2 2)	174806.88	12.58	2.67E-06	3.67	0.05	1.94	0.13	0.232	0.013	0.69	0.12	
25501	CCH (3 5/2 2 - 2 3/2 2)	262078.93	25.16	6.00E-06	3.73	0.11	2.12	0.19	0.520	0.040	2.30	0.60	
26501	CCD (2 5/2 3/2 - 1 3/2 3/2)	144239.71	10.38	1.91E-06	4.98	0.29	3.18	0.77	0.027	0.004	0.12	0.03	
26501	CCD (2 3/2 5/2 - 1 1/2 3/2)	144296.72	10.39	6.73E-06	3.87	0.15	2.95	0.38	0.097	0.010	0.41	0.07	
26501	CCD (2 3/2 5/2 - 1 3/2 5/2)	144376.68	10.39	1.26E-06	4.48	0.27	2.76	0.89	0.038	0.007	0.15	0.03	
26501	CCD (2 3/2 3/2 - 1 3/2 3/2)	144385.44	10.39	6.21E-07	3.93	0.17	1.28	0.44	0.042	0.011	0.08	0.02	
26504	CN (1 1/2 3/2 - 0 1/2 1/2)	113170.49	5.43	5.14E-06	4.44	0.14	1.88	0.36	0.473	0.072	1.20	0.13	
26504	CN (1 1/2 3/2 - 0 1/2 3/2)	113191.28	5.43	6.68E-06	4.52	0.11	1.76	0.27	0.515	0.066	1.23	0.14	
26504	CN (1 3/2 3/2 - 0 1/2 1/2)	113488.12	5.45	6.74E-06	4.43	0.13	1.84	0.32	0.506	0.073	1.26	0.14	
26504	CN (1 3/2 5/2 - 0 1/2 3/2)	113490.97	5.45	1.19E-05	4.59	0.16	1.87	0.41	0.880	0.157	2.22	0.24	
26504	CN (1 3/2 1/2 - 0 1/2 1/2)	113499.64	5.45	1.06E-05	4.46	0.16	1.97	0.40	0.405	0.066	1.08	0.12	
26504	CN (1 3/2 3/2 - 0 1/2 3/2)	113508.91	5.45	5.19E-06	4.48	0.12	1.92	0.27	0.427	0.052	1.11	0.12	
26504	CN (1 3/2 1/2 - 0 1/2 3/2)	113520.43	5.45	1.30E-06	4.25	0.01	1.50	0.03	0.191	0.003	0.39	0.04	
45506	HCS^+ (2-1)	85347.89	6.14	1.11E-05	4.02	0.06	2.49	0.13	0.059	0.003	0.19	0.03	
45506	HCS^+ (4-3)	170691.60	20.48	9.86E-05	3.60	0.10	2.79	0.23	0.170	0.012	0.72	0.13	
45506	HCS^+ (5-4)	213360.65	30.72	1.97E-04	3.52	0.09	4.20	0.22	0.177	0.008	1.28	0.22	
45506	HCS^+ (6-5)	256027.10	43.01	3.46E-04	3.84	0.04	3.81	0.09	0.188	0.004	1.44	0.25	
45506	HCS^+ (8-7)	341350.23	73.73	8.35E-04	3.63	0.12	3.32	0.29	0.233	0.017	1.48	0.27	
42501	H_2CCO ($4_{1,4}$-$3_{1,3}$)	80076.65	22.66	5.04E-06	3.25	0.23	2.34	0.53	0.045	0.009	0.14	0.03	

Table 4. continued.

TAG	Species & Transition	Frequency (MHz)	E_{up} (K)	A_{ij} s^{-1}	V_o (km s^{-1})	δ_{V_o}	*FWHM* (km s^{-1})	δ_{FWHM}	Int (K)	δ_{Int}	Flux (K km s^{-1})	δ_{Flux}	Comments
42501	H_2CCO ($4_{0,4}$-$3_{0,3}$)	80832.12	9.70	5.52E-06	2.84	0.16	3.04	0.43	0.037	0.004	0.14	0.03	
42501	H_2CCO ($4_{1,3}$-$3_{1,2}$)	81586.23	22.84	5.33E-06	3.56	0.22	2.78	0.54	0.057	0.009	0.20	0.03	
42501	H_2CCO ($5_{1,5}$-$4_{1,4}$)	100094.51	27.46	1.03E-05	3.29	0.05	3.09	0.13	0.076	0.003	0.31	0.04	
42501	H_2CCO ($5_{0,5}$-$4_{0,4}$)	101036.63	14.55	1.10E-05	2.92	0.08	2.11	0.19	0.050	0.004	0.14	0.02	
42501	H_2CCO ($5_{1,4}$-$4_{1,3}$)	101981.43	27.74	1.09E-05	2.96	0.20	2.99	0.50	0.076	0.010	0.30	0.04	
42501	H_2CCO ($7_{1,7}$-$6_{1,6}$)	140127.47	39.95	2.96E-05	3.13	0.16	3.08	0.38	0.128	0.014	0.56	0.10	
42501	H_2CCO ($7_{0,7}$-$6_{0,6}$)	141438.07	27.15	3.11E-05	2.63	0.11	2.07	0.32	0.120	0.012	0.36	0.06	
42501	H_2CCO ($7_{1,6}$-$6_{1,5}$)	142768.95	40.46	3.13E-05	3.15	0.16	2.95	0.40	0.143	0.016	0.61	0.11	
42501	H_2CCO ($8_{1,8}$-$7_{1,7}$)	160142.24	47.64	4.48E-05	2.81	0.19	2.19	0.44	0.159	0.028	0.52	0.09	
42501	H_2CCO ($8_{0,8}$-$7_{0,7}$)	161634.07	34.91	4.68E-05	2.83	0.18	2.04	0.42	0.133	0.024	0.41	0.07	
42501	H_2CCO ($8_{1,7}$-$7_{1,6}$)	163160.88	48.29	4.74E-05	2.90	0.13	2.06	0.31	0.167	0.022	0.51	0.09	
42501	H_2CCO ($10_{1,9}$-$9_{1,8}$)	203940.23	66.89	9.41E-05	2.76	0.31	2.78	0.83	0.137	0.034	0.63	0.11	
30008	NO ($^2\Pi_{1/2}$ $3/2^e$, 5/2 - $1/2^e$, 3/2)	150176.48	7.21	3.31E-07	4.09	0.13	1.97	0.32	0.153	0.021	0.44	0.08	
30008	NO ($^2\Pi_{1/2}$ $3/2^e$, 3/2 - $1/2^e$, 1/2)	150198.76	7.21	1.84E-07	3.95	0.10	1.41	0.23	0.092	0.013	0.19	0.04	
30008	NO ($^2\Pi_{1/2}$ $3/2^e$, 3/2 - $1/2^e$, 3/2)	150218.73	7.21	1.47E-07	3.99	0.06	1.09	0.14	0.072	0.008	0.11	0.02	
30008	NO ($^2\Pi_{1/2}$ $3/2^e$, 1/2 - $1/2^e$, 1/2)	150225.66	7.21	2.94E-07	3.91	0.08	1.83	0.21	0.073	0.006	0.19	0.04	
30008	NO ($^2\Pi_{1/2}$ $3/2^f$, 1/2 - $1/2^f$, 1/2)	150580.56	7.24	2.96E-07	4.26	0.04	1.10	0.11	0.065	0.005	0.10	0.02	
30008	NO ($^2\Pi_{1/2}$ $7/2^f$, 9/2 - $5/2^f$, 7/2)	351043.52	36.13	5.43E-06	3.95	0.37	4.90	1.35	0.152	0.018	1.44	0.26	
30008	NO ($^2\Pi_{1/2}$ $7/2^f$, 7/2 - $5/2^f$, 5/2)	351051.71	36.13	4.99E-06	3.97	0.21	3.45	0.66	0.190	0.022	1.27	0.23	
19002	HDO (2_{11}-2_{12})	241561.55	95.23	1.19E-05	2.87	0.21	6.13	0.58	0.182	0.010	2.11	0.36	
56502	CCS(6_7-5_6)	81505.17	15.39	2.43E-05	3.86	0.06	1.79	0.10	0.170	0.010	0.44	0.05	
56502	CCS(7_6-6_5)	86181.39	23.35	2.82E-05	4.31	0.22	2.59	0.57	0.055	0.005	0.18	0.03	
56502	CCS(7_7-6_6)	90686.38	26.12	3.34E-05	4.13	0.08	1.71	0.27	0.078	0.007	0.16	0.02	
56502	CCS(7_8-6_7)	93870.11	19.89	3.74E-05	4.08	0.03	1.63	0.10	0.184	0.008	0.39	0.04	
56502	CCS(8_7-7_6)	99866.52	28.14	4.46E-05	4.08	0.05	1.93	0.11	0.059	0.005	0.16	0.02	
56502	CCS(8_8-7_7)	103640.76	31.09	5.05E-05	4.02	0.07	1.88	0.18	0.075	0.004	0.18	0.02	
56502	CCS(8_9-7_8)	106347.73	25.00	5.56E-05	4.32	0.12	2.14	0.34	0.036	0.009	0.10	0.02	
56502	CCS(9_8-8_7)	113410.19	33.58	6.53E-05	4.24	0.21	3.46	0.49	0.062	0.008	0.29	0.04	
56502	CCS(10_{10}-9_9)	129548.45	42.90	9.90E-05	4.35	0.21	1.45	0.46	0.058	0.016	0.12	0.02	
56502	CCS(10_{11}-9_{10})	131551.97	37.02	1.06E-04	4.50	0.18	2.58	0.47	0.073	0.007	0.25	0.04	
56502	CCS(11_{11}-10_{10})	142501.70	49.74	1.33E-04	3.86	0.21	2.60	0.49	0.058	0.010	0.22	0.04	
56502	CCS(12_{11}-11_{10})	153449.77	53.76	1.66E-04	4.00	0.44	3.10	1.04	0.050	0.015	0.23	0.04	
37003	c-C_3H ($2_{1,2}$ 5/2 3 - $1_{1,1}$ 3/2 2)	91494.35	4.39	1.59E-05	4.16	0.07	1.81	0.14	0.038	0.003	0.09	0.01	
37003	c-C_3H ($2_{1,2}$ 5/2 2 - $1_{1,1}$ 3/2 1)	91497.61	4.39	1.38E-05	4.54	0.32	1.88	0.66	0.025	0.008	0.06	0.01	
37003	c-C_3H ($3_{1,3}$ 5/2 3 - $2_{1,2}$ 3/2 2)	133187.72	10.80	5.70E-05	4.55	0.18	1.69	0.46	0.044	0.010	0.11	0.03	
49503	C_4H (9_9-8_8)	85634.00	20.55	2.60E-06	3.94	0.16	1.75	0.39	0.062	0.012	0.14	0.02	
49503	C_4H (9_8-8_7)	85672.58	20.56	2.59E-06	3.95	0.06	1.98	0.14	0.056	0.003	0.14	0.02	
49503	C_4H (10_{10}-9_9)	95150.39	25.11	3.60E-06	3.95	0.08	1.32	0.62	0.057	0.022	0.10	0.01	
49503	C_4H (10_9-9_8)	95188.95	25.13	3.58E-06	4.11	0.20	1.26	0.53	0.061	0.021	0.10	0.01	
49503	C_4H (11_{11}-10_{10})	104666.57	30.14	4.81E-06	4.09	0.11	1.47	0.30	0.044	0.007	0.09	0.02	
49503	C_4H (11_{10}-10_9)	104705.11	30.16	4.79E-06	3.96	0.06	1.70	0.13	0.041	0.003	0.09	0.02	

Notes. All lines have been identified with the line identification package CASSIS (http://cassis.cesr.fr), except the deuterated forms of methanol. For these latter species, not yet included in the JCMT and CDMS databases, the molecular data come from Parise et al. (2002, 2004) and we derived the line parameters with the GILDAS-CLASS package (http://www.iram.fr/IRAMFR/GILDAS). * The deuterated forms of methanol, not being included in the CDMS or JPL spectroscopic databases, do not have TAG and A_{ij}. CASSIS is based on the CDMS and JPL spectroscopic databases, and the TAGs are those given by these databases to identify the molecules. CASSIS is also based on the VASTEL spectroscopic database (http://www.astro.caltech.edu/~vastel/CHIPPENDALES), in which the separation of the ortho and para forms has been performed for some molecules listed in CDMS and JPL. For this database, the TAG are adapted from those of the molecules in the original database. The columns $\delta_{\rm Int}$ and δ_{FWHM} only give respectively the statistical errors on the peak intensity and *FWHM* computed during the fit. The column $\delta_{\rm Flux}$ gives the quadratic error in the total flux in the line, taking into account the calibration error given in Sect. 3. It is computed as: $\delta_{\rm Flux} = \sqrt{({\rm Cal} \times {\rm Flux})^2 + ({\rm rms}^2 \times 2 \times FWHM \times {\rm d}v)}$, where, respectively, Cal is the calibration error, Flux is the line flux, rms is the observed rms, *FWHM* is the full width half maximum of the line, and dv the velocity resolution, at the given line frequency.